PERFORMANCE OF LIGHTWEIGHT CONCRETE CORBELS SUBJECTED TO STATIC AND REPEATED LOADS

By

CLIFFORD NII-AYI CLOTTEY

Bachelor of Science
University of Science and Technology
Kumasi, Ghana
1969

Master of Science in Civil Engineering
University of Cincinnati
Cincinnati, Ohio
1972

Submitted to the Faculty of the Graduate College
of the Oklahoma State University
in partial fulfillment of the requirements
for the Degree of
DOCTOR OF PHILOSOPHY
December, 1977

PERFORMANCE OF LIGHTWEIGHT CONCRETE CORBELS

SUBJECTED TO STATIC AND REPEATED LOADS

Thesis Approved:

John E. Lloyd
Thesis Adviser

W. M. Mawtalos

D. E. Kelly

D. E. Boyd

Norman N. Durham
Dean of the Graduate College

To my daughter,

Aldona Ann Naa-Lamiley,

for her priceless, warm and tender love

ACKNOWLEDGMENTS

The author wishes to express his sincere appreciation to the following individuals and organizations who made this study possible.

Dr. John P. Lloyd, major adviser and chairman of the author's committee, for his instruction, guidance and encouragement during this investigation; Drs. William P. Dawkins, Allen E. Kelly, and Donald E. Boyd, for their invaluable assistance and advisement while serving on the author's committee.

The African-American Institute and the University of Science and Technology, Ghana, for their financial assistance that made the author's graduate program possible; the School of Civil Engineering, Oklahoma State University, for the financial support of this research; management and staff of Thomas Concrete Products, Oklahoma City, for the supply of concrete and assistance in casting the specimens.

Messrs. Cecil K. Sharp, Preston G. Wilson, Arlin L. Harris, Jr., and George M. Cooper, for their services in the design and fabrication of special fixtures required for the investigation; Ms. Charlene Fries, for her excellent and meticulous typing, Ms. Suzanne Spears, for her flawless drafting, and both of them for their friendship and understanding; fellow graduate students, for their friendship and assistance, notably Mr. Hussam M. Ghanem, for his help in fabricating and testing of the specimens.

The author is greatly indebted to his family and friends for their sacrifices, understanding and encouragement.

TABLE OF CONTENTS

LIST OF TABLES

LIST OF FIGURES

Figure | Page

NOMENCLATURE

a	shear span; distance between the column face and the concentrated vertical load, in.
A_f	area of reinforcement necessary for flexure, sq in.
A_h	total area of stirrup reinforcement parallel to the main tension reinforcement, sq in.
A_n	area of reinforcement necessary to resist horizontal normal force N_u, sq in.
A_s	area of main tension reinforcement, sq in.
A_v	area of shear-friction reinforcement, sq in.
b	width of specimen, in.
C	resultant compression force (see Figure 5)
d	effective depth; distance from the extreme compression fiber to centroid of tension reinforcement, in.
e	exponential function
f'_c	compressive strength of concrete, ksi
f_{hy}	yield strength of horizontal stirrup, ksi
$f_{s(all)}$	allowable tensile stress in steel, ksi
f_{sy}	yield strength of main tension reinforcement, ksi
f_{vy}	yield strength of shear-friction steel, ksi
f_y	yield strength of reinforcement, ksi
F	frictional force
F_c	compressive force in concrete strut (see Figure 1)
F_t	tensile force in main tension reinforcement
h	total depth of corbel at column-corbel interface, in.

h_1	dimension of specimen (see Figure 6), in.
h_2	dimension of specimen (see Figure 6), in.
h'	dimension of specimen (see Figure 6), in.
h''	dimension of specimen (see Figure 6), in.
H	horizontal tensile force, kips
H_R	horizontal tensile force during repeated loading, kips
H_u	horizontal tensile force at failure, kips
H_1	total height of column (see Figure 6), in.
jd	distance from centroid of main tension reinforcement to center of action of resultant concrete compression force (see Figure 5), in.
$j'd$	distance from centroid of flexural tension to center of action of resultant concrete compression force, if only flexural reinforcement strength of $(A_s f_y - N_u)$ were acting in section, in.
ℓ	dimension of specimen (see Figure 6), in.
M_u	ultimate resisting moment of column-corbel interface, in.-kips
N	horizontal normal force, kips
N_u	ultimate horizontal normal force, kips
s	standard deviation
T	total tensile force
$v_u = V_u/bd$	nominal ultimate shear stress, ksi
v_{uc}	nominal ultimate shear stress of specimen with compression reinforcement, ksi
v_{uL}	nominal ultimate shear stress of larger specimen, ksi
v_{ur}	nominal ultimate shear stress of specimen subjected to repeated loading, ksi
v_{us}	nominal ultimate shear stress of specimen subjected to static loading only, ksi
$v_y = V_y/bd$	nominal shearing stress at yield, ksi

V	shear force, kips
V'	total vertical load applied to specimen, kips
$V_{(min)}$	minimum vertically repeated load, kips
$V_{(max)}$	maximum vertically repeated load, kips
V_u	ultimate shear force, kips
V'_u	ultimate total vertical load applied to specimen, kips
V_y	shear force at yield, kips
V'_y	total vertical load applied at yield, kips
w	width of bearing plate, in.
$\overline{x}$	mean value
z	internal lever arm
α	angle of internal friction
β	dimension factor as defined in Figure 2
$\gamma = 1 - \beta$	dimension factor as defined in Figure 2
λ	strength modification factor for combined loading
μ	Poisson's ratio
ρ	reinforcement ratio
ρ_h	reinforcement ratio of horizontal stirrups
ρ_s	reinforcement ratio of main tension steel
ρ_v	reinforcement ratio of shear-friction steel
$\alpha_{Nx} = N_u/bd$	externally applied normal stress angling across shear plane
ϕ	capacity reduction factor
ψ	concrete strength modification factor

CHAPTER I

INTRODUCTION

1.1 Statement of the Problem

1.1.1 General

Connections in precast concrete construction, particularly of primary members, form a critical part of the load-carrying and transfer mechanism. Hence the integrity and adequacy of a precast concrete structure depend, to a great extent, on the strength and performance of the types of connections utilized.

Ideally, connections should be so designed and detailed that the ultimate strengths of the individual members are attained before those of the connections. It is desirable therefore that the special structural members and elements which form the connections must withstand, with a known reasonable margin of safety, the various types of loading and combinations thereof imposed on the connections by the primary members during the expected life of the structure. A report on the 1964 Alaskan earthquake (1) indicated that a substantial number of precast concrete structures distressed as a result of insufficient attention to their connections.

Corbels are used extensively for beam-column connections in precast concrete construction. They are projections from faces of columns and behave like short, cantilevered, deep beams. Because of the usually low shear span-to-effective depth ratio, the loads are transferred predominantly through shear; the lower the a/d ratio, the higher the shear strength of the corbel (2) (3) (4). The precise contributions of the shear transfer mechanisms are yet to be evaluated (5).

1.1.2 Load Transfer

Under low levels of static load, the concrete remains uncracked and transfers nearly the entire load through normal and shearing stresses. As the load is increased and the principal tensile stress exceeds the tensile strength of the concrete, cracks begin to form. A redistribution of stresses occurs, and the load is then transferred in a more complex manner. The uncracked portion of the concrete continues to transfer part of the load as before; the crack region transfers some of the load by friction and mechanical interlock of the crack surfaces. The remaining portion of the load is transferred by the steel reinforcement through normal and shearing stresses and possibly dowel action (5).

During the crack formation the tensile stress in the reinforcement increases very rapidly and results in high bond stress (4). High shearing stresses may also be present in the reinforcement at the locations of the cracks as a result of dowel action. The portion of the load transferred by dowel action depends on the amount and distribution of the reinforcement (6) and the relative movement of the crack surfaces (7).

The percentage of the load transferred by friction and mechanical interlock depends on the crack width (8) (9), effectiveness of bond, and anchorage of the reinforcement (10) (11). These in turn depend on not only the amount and distribution of the reinforcement, but also the stress level in the reinforcement. Any additional load increases the tensile stress in the reinforcement and consequently increases the crack width and produces further crack propagation. This is accompanied by a reduction in the area of the uncracked portion of the concrete and an increase in the stress in the concrete in the compression zone. This increase in crack width also reduces the percentage of load transferred by friction and mechanical interlock of the crack surfaces (8) (9).

Repeated loading after the formation of cracks may cause a reduction in bond between the concrete and the reinforcement (12). The reinforcement in the anchorage zone will be subjected to high stresses and the welded portions of the reinforcement in this zone will become more susceptible to fatigue failure than under static load. In addition, the rough crack surfaces will be worn down (8) (9). This, compounded with increase in crack width, will substantially lower the effectiveness of the mechanical interlock and friction. Consequently, the load transfer capacity will be reduced (13).

1.1.3 Design Provisions

Until recent years few investigations were undertaken to study the strength and behavior of reinforced concrete corbels. Corbels were designed with equations derived for beams of normal proportions, although the assumptions for normal beams are not valid for deep beams. The current ACI Code (14) and PCI Design Handbook (15) now include special provisions for brackets and corbels. These provisions, however, are based on investigations (4) (11) of normal weight concrete specimens subjected to static loadings. Hence these provisions must be carefully interpreted when extended to other loading conditions, particularly earthquake and blast loading (5) and structural lightweight concrete. Recent design proposals (16) (17) for normal, all-lightweight and sanded-lightweight concretes were based on static tests of normal and all-lightweight concrete specimens.

1.1.4 Lightweight Concrete

In spite of the extensive applications and future prospects of structural lightweight concrete (18) (19), investigations of reinforced concrete corbels have been usually limited to normal-weight concrete. In recent investigations of reinforced deep beams of lightweight concrete (20) (21) (22), however, the results indicated that the lightweight concrete specimens exhibited not only lower cracking loads but also lower ultimate load capacities. In addition, the shear force transferred by lightweight concrete has been determined to be lower than that of normal-weight concrete (3), and all-lightweight concrete corbels also have lower shear strength than normal-weight concrete corbels (16).

The pertinent properties of structural lightweight concrete, such as the elastic modulus, tensile strength, and bond and anchorage are lower than those of normal-weight concrete (19). Furthermore, the bond strength between the mortar and the aggregate particles is usually greater than the tensile strength of the aggregate particles (23). Cracks therefore propagate through the aggregate particles instead of around them, as in normal-weight concrete. This results in less irregular crack surfaces, more relative movement between the crack surfaces, and smaller ultimate load transfer capacity (7) (24).

1.2 Purpose and Scope

The primary objective of this investigation is to determine the strength and the behavior of reinforced lightweight concrete corbels subjected to combined static and repeated loading. In this study the influence of the reinforcement ratio (ρ), the shear span-to-effective depth ratio (a/d), and the horizontal force-to-vertical force ratio (H/V) on the load transfer capacity will be determined. The effects of repeated loading on the ultimate strength and behavior will be studied. The investigation is also aimed at studying the influence of compression reinforcement as well as the size of the specimens.

The study is based on the test results of 36 reinforced, sanded-lightweight concrete corbels. Neither the influence of the concrete strength nor the yield strength of the reinforcement is investigated and only vertically repeated loading is considered.

CHAPTER II

LITERATURE REVIEW

In recent years the behavior and strength of a reinforced concrete corbel or bracket as well as its load transfer mechanism have attracted much attention. Because of the geometry of a corbel, simple flexural beam theory is not applicable to its analysis and design. After this was acknowledged, early efforts were then directed to the study of brackets.

2.1 Earlier Investigations

2.1.1 Modified Flexural Method

The difference in the design equations for long and short cantilevered beams was pointed out in 1922 by Rausch (25). In his analysis Rausch used cantilevered beams with bent bars at 45° to resist all shear forces. From flexural considerations he determined that the total tensile force resisted by the inclined bars was given by

$$T = \frac{a}{z} \left(\frac{V}{\sqrt{2}}\right) \tag{2.1}$$

where

V = vertical force acting on the cantilever;

a = shear span; and

z = internal level arm.

For short cantilevered beams with $a/z < 1.0$, the value obtained for the tensile force was too small and Equation (2.1) was no longer valid. Rausch therefore recommended that for $a/z \leq 1.0$ the design equation should be

$$T = \frac{V}{\sqrt{2}} \qquad (2.2)$$

2.1.2 Determinate Truss Analogy

In 1963 Franz and Niedenhoff (26) used photoelastic models for their study of reinforced concrete brackets. From an examination of the stress patterns, as shown in Figure 1, they found that:

1. The tensile stresses at the top of the bracket were fairly constant from the load point to the root of the bracket.

2. The stresses at the compression faces were also fairly constant.

3. The stress concentrations existed at the root of the bracket, both top (tension) and bottom (compression).

4. The shape of the bracket had little effect on the state of stress. In a rectangular bracket a "dead" area occurred in the outer bottom corner.

These tests indicated the behavior of concrete brackets under elastic conditions which exist at very low loads. From their observations Franz and Niedenhoff proposed a simple form of truss analogy for the design of reinforced concrete brackets. They considered the bracket as a simple strut-and-tie system acted upon by an external force V, as shown in Figure 1(b). The tensile force, F_t, though slightly inclined, was taken as horizontal for design purposes. The tensile force was then given by

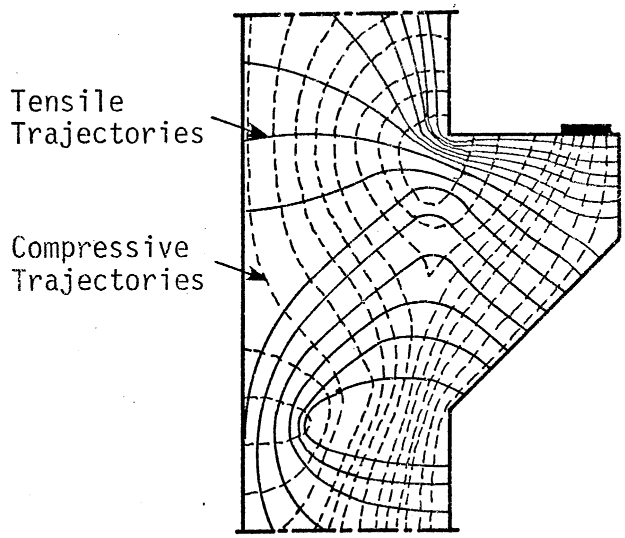

(a) Stress Patterns

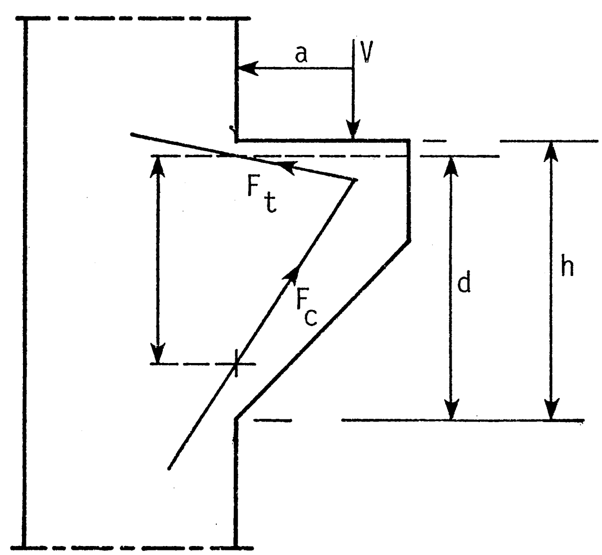

(b) Simple Truss Analogy

Figure 1. Specimen Used by Franz and Niedenhoff (26)

$$F_t = \frac{Va}{z} \tag{2.3}$$

where z = 0.85 d.

The area of the tensile steel required was determined from

$$A_s = \frac{F_t}{f_{s(all)}} \tag{2.4}$$

where $f_{s(all)}$ represents the allowable tensile stress for the reinforcement. The required depth, h, was then determined from flexural considerations of the cross section at the root (column face)--a working stress design approach.

Based on their observations of the stress trajectories, they also suggested some empirical rules for detailing of brackets:

1. The main tension reinforcement should be well anchored at the outside face of the bracket.

2. The column reinforcement at the upper re-entrant angle should be increased locally by 50 percent to accommodate the stress concentrations in that region when low column loads exist.

3. The compression region should be reinforced with at least six 14 mm diameter bars per meter width and these should be secured against buckling with stirrups.

4. The quantity of stirrups should be at least one-quarter of the main reinforcement.

2.1.3 Indeterminate Truss Analogy

Mehmel and Becker (27) also performed photoelastic studies of brackets, and from their results they suggested that a bracket behaved approximately as a statically indeterminate truss, as shown in Figure 2.

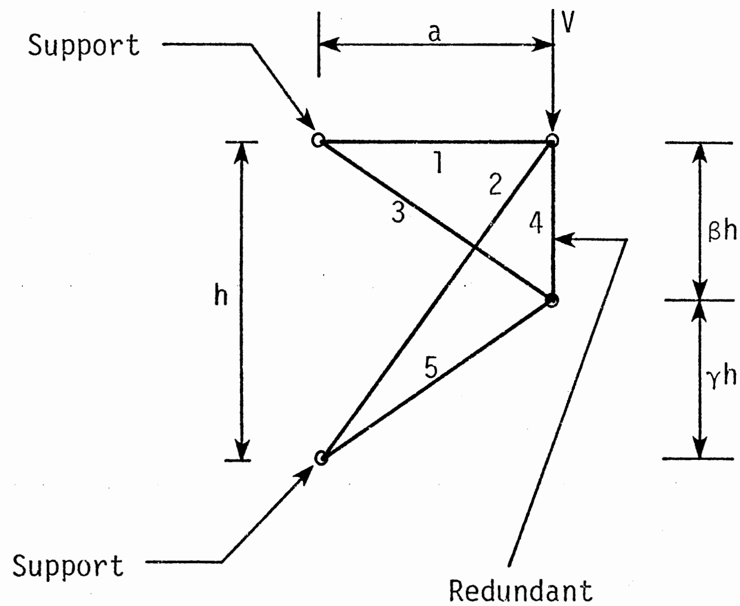

Figure 2. Statically Indeterminate Truss Model of Mehmel and Becker (27)

The behavior of the bracket was divided into two stages: stage 1 was the uncracked condition in which all the truss members were assumed to have the same modulus of elasticity; stage 2 was the cracked condition in which the concrete was assumed to resist only compression and the reinforcement only tension. In both stages they investigated the location of the load (on top, suspended from underneath and in the middle of the depth of the outer face) and the geometric shape of the bracket (rectangular and trapezoidal).

By using equal cross-sectional areas for truss members in stage 1, the redundant shown in Figure 2 together with the forces in the members of the truss were determined. In stage 2 the areas of the truss members were then determined by using the allowable steel and concrete stresses and the magnitudes of the forces obtained from the uncracked condition. The procedure for the uncracked condition was used with modification, taking into account the modular ratio and the allowable stress ratio, to determine the redundant and other member forces.

2.1.4 The Empirical Method

The above methods of truss analogy and of modified flexure are essentially working stress design procedures. To determine the ultimate strength of corbels, Kriz and Raths (4) conducted an in-depth experimental study of the static strength of concrete corbels in 1965. The host of parameters they investigated included the reinforcement ratio (ρ), concrete strength (f'_c), ratio of shear span-to-effective depth (a/d), amount and distribution of stirrups reinforcement, size and shape of corbels and the ratio of the horizontal-to-vertical loads

(H/V). Their study, however, was limited to normal weight concrete specimens.

From tests of 195 specimens they observed that corbels subjected to vertical loads only, i.e., H/V = 0.0, behaved elastically until the first flexural cracks appeared at the junction of the corbel and the column which resulted in an increase in the tensile stresses of the main tension reinforcement. Subsequent development of cracks depended on ρ, a/d, and mode of failure. They observed four principal modes of failure: flexural tension, flexural compression, diagonal splitting, and shear. There were also secondary failures of corbel end splitting and bearing. Stirrups were found to be very effective in resisting the vertical loads.

From a statistical analysis of their data they derived an empirical equation for the ultimate shear stress:

$$v_u = 6.5\,[1 - 0.5^{(a/d)}](1000\,\rho_v)^{1/3}\,\sqrt{f'_c} \tag{2.5}$$

with

$$\rho_v = (A_s + A_h)/bd$$

where

A_s = area of main tension reinforcement; and

A_h = area of the stirrup reinforcement.

Kriz and Raths used load ratios (H/V) of 0.5 and 1.0 during the study of the influence of combined vertical and horizontal static loading on the strength of corbels. They observed that the essential characteristics in the behavior of specimens did not change. A limited number of corbels with stirrups under combined loading were tested; the results from such specimens, although erratic, showed that the stirrups did not increase the resistance of the corbels by as large a proportion as in the case of those under vertical loads only. Hence they suggested that such a contribution should be regarded as a reserved strength. The following empirical equation was then proposed:

$$v_u = 6.5\ [1 - 0.5^{(a/d)}][\frac{(1000\ \rho_s)^{(1/3\ +\ 0.4\ H/V)}}{10^{(0.8\ H/V)}}]\sqrt{f'_c} \qquad (2.6)$$

with

$$\rho_s = A_s/bd$$

where A_s is the area of main tension reinforcement.

Contrary to the suggestions of Franz and Niedenhoff (26), Kriz and Raths observed that:

1. The strength of a corbel was not influenced by an additional load on the column.

2. The amount and arrangement of the column reinforcement had little influence on the strength of a corbel.

3. Compression reinforcement in a corbel contributed very little to the strength of the corbel as a result of low strains recorded in those reinforcements.

2.1.5 Shear Friction Hypothesis

Because of the apparent complexity of the design Equations (2.5) and (2.6) proposed by Kriz and Raths (4), Mast (11) sought to develop a simple but safe design method, and proposed his shear-friction theory. This theory is based on the classical frictional equation of applied mechanics:

$$F = \mu N \tag{2.7}$$

where μ is the coefficient of friction.

In his approach Mast considered a fully cracked concrete specimen subjected to a normal compressive force across the crack and a shearing force along the crack, as shown in Figure 3.

Since a crack is rough and irregular, the coefficient of friction may be quite high. Also, due to the rough and irregular nature of a crack, any slippage that may occur will be accompanied by slight separation of the two concrete pieces. If reinforcement is present and normal to the crack, the subsequent separation along the crack will stress the steel in tension. This in turn will provide a balancing compressive stress across the crack and the shearing stress may be resisted by friction. The ultimate shearing force to be resisted is then obtained when the steel has yielded, and is given by

$$V_u = A_v f_y \tan \alpha \tag{2.8a}$$

or

$$v_u = \frac{V_u}{bd} = \rho_v f_y \tan \alpha \tag{2.8b}$$

where α is the angle of internal friction.

Mast used this theory to design corbels with $a/d \leq 0.7$, because diagonal tension cracks could not be fully developed. If the ratio of $a/d > 0.7$, the main horizontal steel would be controlled by flexure; when $a/d < 0.7$, the problem would be one of shear rather than diagonal tension. Mast compared his results with those obtained by Kriz and Raths (4) for specimens with $a/d \leq 0.7$ and in which yielding occurred in the main tension reinforcement. Using $\tan \alpha$ of 1.4, the shear

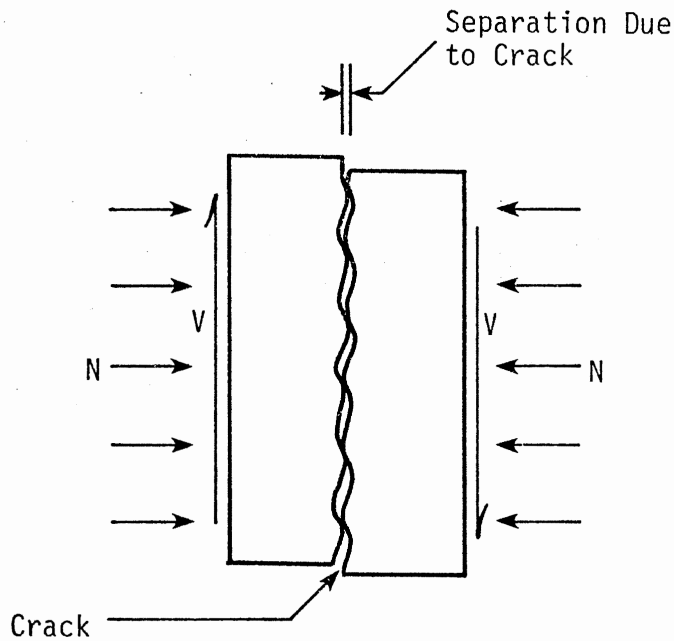

(a) Fully-Cracked Concrete

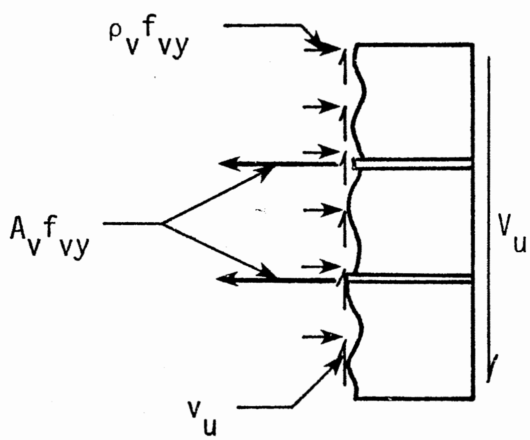

(b) Free-Body Diagram

Figure 3. Basis for Shear-Friction Theory of Mast (11)

friction theory gave a good lower bound for the two cases considered: H/V = 0.0 and H/V = 0.5.

Among the limitations of the shear friction theory are the following:

1. Since the shear friction theory is based on the static ultimate load, it is not applicable to connections in which fatigue is a consideration, or where slip is critical.

2. As a result of different internal structure, the behavior of lightweight concrete may differ from that of normal weight. Hence the theory should not be applied to lightweight concrete without further study and tests.

2.2 Shear Transfer in Concrete

Because of the size of corbels the loads are transferred predominantly through shear. As a result, the proposal of the shear friction theory prompted experimental push-off investigations (2) (3) (7) (8) (29) to understand and evaluate the shear transfer strength of concrete. Earlier push-off tests (13) (24) were performed to study the horizontal shear transfer between precast and cast-in-place concretes. Figure 4 shows some of the typical push-off specimens. Shear transfer in concrete is primarily influenced by (a) nature of shear plane; (b) the reinforcement; (c) the concrete; and (d) the loading.

2.2.1 Nature of Shear Plane

Hanson (13) studied the influence of surface characteristics of the shear plane on the strength and behavior of a shear connection between precast and cast-in-place concretes. The effect of proper bonding

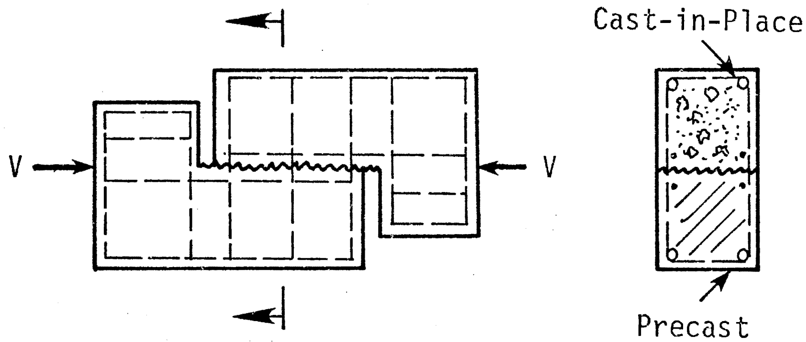

(a) Anderson

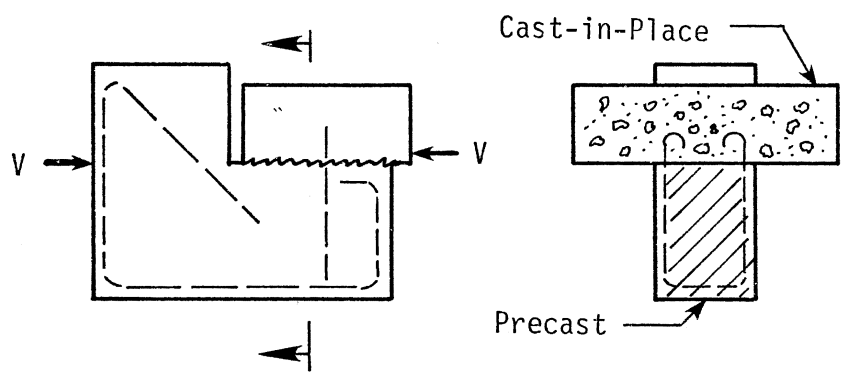

(b) Hanson

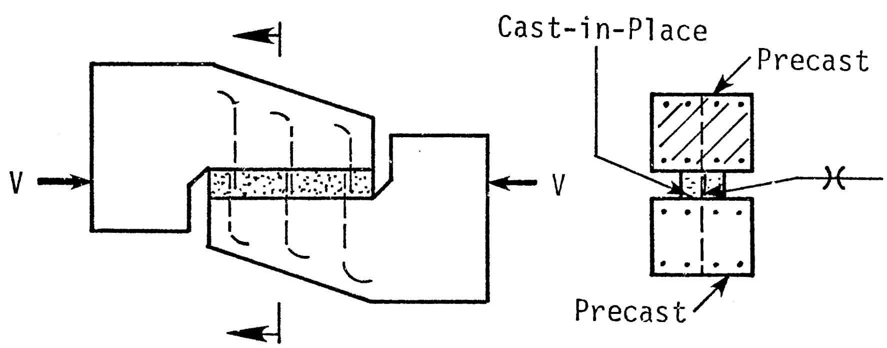

(c) Mast

Figure 4. Push-Off Specimens

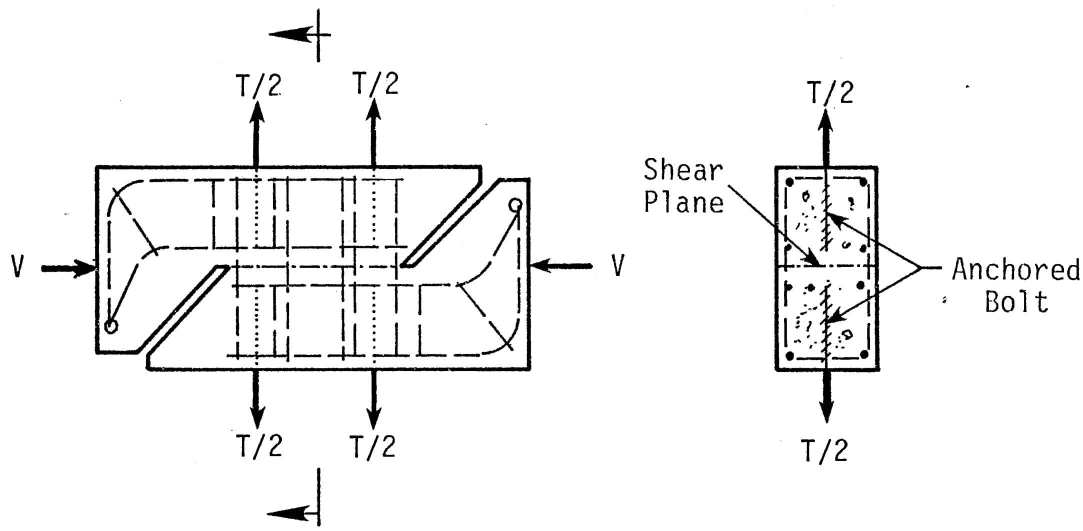

(d) Mattock, Johal and Chow (With Tension Across Shear Plane)

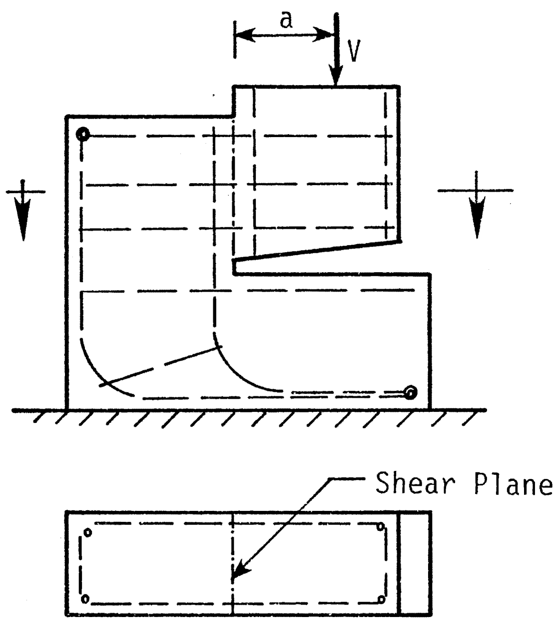

(e) Mattock, Johal and Chow (With Moment Across Shear Plane)

Figure 4. (Continued)

procedure was also considered. The results showed that specimens in which bond was utilized as part of the connection developed high shearing stresses at low joint slip. In contrast, specimens with unbonded joints experienced considerable slip before high shearing stresses were reached. A maximum shearing stress of 500 psi was obtained for specimens with rough bonded surfaces and 300 psi for smooth unbonded surfaces.

The influence of the existence of a crack in the shear plane has been examined by Mattock, Johal and Chow (2); Mattock, Li and Wang (3); Hofbeck, Ibrahim and Mattock (7); and Mattock (29). Their results indicated similar behaviors when cracks pre-existed.

In the case of initially cracked specimens, relative movement was observed from the beginning of the loading. However, for the initially uncracked specimens, no movement was detected until diagonal tension cracks became visible at higher shear stresses. After the formation of the crack there was a relative movement of the two halves in the initially uncracked specimens. This motion was not truly slip but rather resulted from rotation of the short struts formed by the diagonal tension cracks when the stirrups elongated. Similar diagonal cracks were observed in the initially cracked specimens with a high percentage of stirrup reinforcement.

The analysis of their test data indicated that the existence of a crack prior to a shear test produced a slip at all stages of loading greater than that observed when the crack was not present. The existence of a crack also lowered the ultimate shear strength.

2.2.2 The Reinforcement

The investigations of Hofbeck, Ibrahim and Mattock (7) and Anderson (25) showed that the ultimate shear strength of a joint increased as the amount of reinforcement crossing the shear plane increased.

Hofbeck et al. also found that the higher the strength of web reinforcement the greater the shear strength and that the manner in which the reinforcement ratio (ρ) was varied did not affect the relationship between the shear strength and the parameter ρf_y. They also observed that dowel action did not contribute significantly to the shear strength of initially uncracked specimens. On the contrary, for the initially cracked specimens, considerable contribution to shear transfer strength by dowel action was observed. They attributed this difference to the manners of crack formation and failure.

Mattock (29) examined shear transfer in concrete having reinforcement inclined at an arbitrary angle to the shear plane. Both parallel and orthogonally arranged reinforcements were considered. From the analysis of the results Mattock showed that when the reinforcement is normal to the shear plane, the shear strength can be expressed as

$$v_u = 400 + 0.8\ \rho f_y\ \text{(psi)} \tag{2.9}$$

but

$$v_u \not> 0.3\ f'_c$$

The distribution of reinforcement across the shear plane was studied by Mattock, Johal and Chow (2). They observed that for zero eccentricity loading the ultimate slip increased as the distribution of the reinforcement changed from uniform across the depth of the shear plane to concentration at the upper end of the shear plane. In the case of specimens with uniformly distributed reinforcement, the ultimate slip increased as the loading eccentricity increased. However, in the specimens having the reinforcement concentrated near the top of the shear plane there was very little variation in the ultimate slip with eccentricity. If, therefore, both moment and shear are to be transferred across the cracked shear plane, the reinforcement will be more effective when located in the flexural tension zone.

2.2.3 The Concrete

In their investigation Hofbeck, Ibrahim and Mattock (7) found that for reinforcement strength parameter (ρf_y) less than 600 psi, the concrete strength did not affect the shear strength of cracked specimens. However, for higher values of ρf_y, the shear strength was lower for a weaker concrete.

Mattock, Li and Wang (3) studied mainly the influence of the unit weight of concrete on the shear transfer strength of concrete. They observed that as the compressive strength of concrete increased, the specimens exhibited more brittle behavior. In addition, specimens of all-lightweight concrete showed more brittle behavior than those of normal-weight concrete.

The shear transfer strength of normal-weight concrete was found to be consistently greater than that of the lightweight concrete for the same amount of reinforcement and approximately the same compressive strength. Also, sanded-lightweight concrete had a greater shear transfer strength than all-lightweight concrete. These differences in shear transfer capacities, however, did not correlate with the differences in concrete splitting tensile strength. Consequently, they recommended that shear transfer strength of lightweight concrete should not be related to the splitting tensile strength of concrete.

Based on their results, Mattock, Li and Wang determined that Equation (2.8) of the shear-friction theory was unconservative for both sanded-lightweight and all-lightweight concretes. Consequently, they proposed that the coefficient of friction, μ, be modified by a factor of 0.85 for sanded-lightweight concrete and 0.75 for all-lightweight concrete.

In addition, Equation (2.9) proposed by Mattock (29) for shear transfer in normal weight concrete was found to be unconservative for both sanded- and all-lightweight concretes. It was then proposed that for sanded-lightweight concrete, Equation (2.19) should be modified to

$$v_u = 0.8 \rho f_y + 250 \tag{2.10}$$

but not more than 0.2 f'_c or 1000 psi, and for all-lightweight concrete

$$v_u = 0.8 \rho f_y + 200 \tag{2.11}$$

but not more than 0.2 f'_c or 800 psi.

2.2.4 The Loading

In their push-off investigations, Mattock, Johal and Chow (2) examined primarily the influence of the presence of bending moment and tension force across the shear plane on the shear transfer strength of reinforced concrete.

In the case of specimens with tension across the shear plane, their results indicated that it is appropriate to add the normal stress σ_{Nx} to the reinforcement parameter ρf_y when calculating the shear transfer strength by the shear-friction method (σ_{Nx} is taken as positive when compression and negative when tension). Then the shear stress is given by

$$v_u = (\phi\rho f_y + \sigma_{Nx})\,\mu \tag{2.12}$$

In addition, Equation (2.9) for shear transfer strength in concrete proposed by Mattock (29) was also applicable if the above modification was performed, giving

$$v_u = 400 + 0.8\ (\rho f_y + \sigma_{Nx}) \tag{2.13}$$

but not greater than $0.3\ f'_c$.

It appeared that the ultimate shear which can be transferred across the shear plane was not significantly affected by the presence of moment in the plane provided the applied moment was less than or equal to the flexural capacity of the section at the shear plane. They therefore proposed that both flexural and shear capacities of corbels should be checked in accordance with sections 10.2 and 11.5 of the ACI Code (14), respectively.

Paulay and Loeber (8) used both static and cyclic loadings in their investigation of the contribution of aggregate interlock in shear transfer. In the cyclic load tests the load was fluctuated between 0 and 70-80 percent of the ultimate static load. Although failure was similar to that encountered in the static tests, no sudden breakdown of aggregate interlock action was observed. However, there was, with progressive loading, an accumulation of shear displacements which increased proportionally with crack width. They observed after testing that the crack surfaces were heavily striated, the surface irregularities were worn down, and the edges of aggregate indentations were rounded off.

2.3 Recent Investigations--Modified Shear-Friction Method

Results of the push-off experimental studies of shear transfer in concrete indicated that the shear-friction method of corbel design is conservative for lower values of the reinforcement parameter ρf_y and unconservative for higher ρf_y. As a result, recent studies of corbels have been focused on modification of the shear-friction theory.

Hermansen and Cowan (30) sought to improve upon the accuracy of predicting the strength of concrete corbels by the shear-friction method. Their modifications of the method were based on the two main failure modes--shear and flexure; secondary modes were prevented through effective detailing.

Based on the results of the push-off tests by Hofbeck, Ibrahim and Mattock (7), and the results of their experimental tests, Hermansen and Cowan proposed a modified shear-friction method. They found that for the initially uncracked concrete specimens that failed in shear, the ultimate shear stress was given by

$$v_u = 580 + 0.8\ \rho f_y\ \text{(psi)} \tag{2.14}$$

which is similar to Equation (2.9) proposed by Mattock (29).

Hermansen and Cowan also asserted that for $a/d \leq 2.0$, the load to cause yielding in the main reinforcement without yielding the stirrups could be obtained with reasonable accuracy from

$$V_u = A_s f_y\ d/a \tag{2.15}$$

Mattock, Chen and Soongswang (16) sought to extend the shear-friction method of design to corbels with shear span-to-effective depth ratio a/d up to and including 1.0, subjected to combined horizontal and vertical loads, such that $N_u/V_u \leq 1.0$. In their preliminary analyses they considered a free-body diagram of the corbel, as shown in Figure 5. Neglecting the contribution of the stirrups, they determined from equilibrium considerations that the area of the main tension reinforcement could be expressed conservatively as

$$A_s \geq \frac{V_u a + N_u(h-d)}{\phi f_y\, j'd} + \frac{N_u}{\phi f_y} \tag{2.16}$$

that is,

$$A_s \geq A_f + A_n \tag{2.17}$$

where

$j'd$ = internal lever arm if only flexural reinforcement strength of $(A_s f_y - N_u)$ was acting;

A_f = area of reinforcement necessary to resist the applied moment $[V_u a + N_u(h - d]$; and

A_n = area of reinforcement necessary to resist the horizontal force N_u.

Of the 28 specimens tested, 26 had stirrup reinforcement and only 6 of those 26 specimens were of all-lightweight concrete; the remaining 22 specimens were of normal-weight concrete. The experimental results were compared with a number of calculated values of ultimate loads using previously proposed formulas.

The results indicated that in the case of normal-weight concrete specimens, the ultimate load could be predicted from either the smaller of the values obtained from Equations (2.12) and (2.16) or the smaller

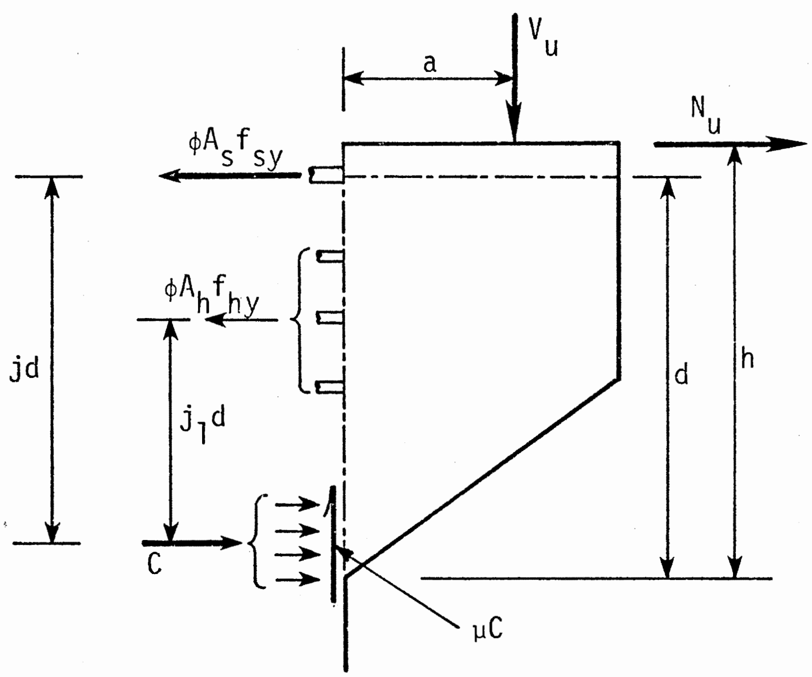

Figure 5. Free-Body Diagram of a Corbel

of the values obtained from Equations (2.13) and (2.16). However, for the all-lightweight specimens the results showed that the maximum shearing stress can be expressed as

$$v_{u(max)} = (0.2 - 0.07\ a/d)\ f'_c \tag{2.18}$$

but not more than (800 - 280 a/d) psi for all-lightweight concrete and not more than (1000 - 350 a/d) for sanded-lightweight concrete.

2.4 Summary

Most of the investigations of corbels and shear transfer in concrete to date have been focused on specimens of normal-weight concrete and subjected to static loadings only.

The limited studies involving lightweight concrete indicated that shear transfer strength and behavior of lightweight concrete specimens differ from those of normal weight concrete specimens. The shear friction theory was found to be unconservative for lightweight concrete and that the coefficient of friction should be modified for lightweight concrete.

In addition, it was found that shear transfer in concrete is influenced by the characteristics of the shear plane--particularly the degree of surface roughness of a cracked plane. The surface roughness was found to be affected by repeated loadings. Hence repeated loading could influence the shear transfer strength of concrete.

The current strength provisions in sections 11.14 and 11.15 of the ACI Code (14) were based on the data obtained from studies of normal weight concrete specimens subjected to static loads (4) (7) (10) (11). Therefore, these provisions should be cautiously applied to the design of corbels made of lightweight concrete which are to be subjected to static or repeated loads. As Mast (11) pointed out, the shear-friction theory is not applicable when fatigue is a consideration and also should not be applied to lightweight concrete without further study because of the different internal structure.

The present design provisions are modifications of Equations (2.5) and (2.6) derived by Kriz and Raths (4) and the shear-friction theory Equation (2.8) by Mast (11). In section 11.14 of the ACI Code (14) the ultimate shear stress is given as:

$$v_u = [6.5 - 5.1 \frac{N_u}{V_u}] [1 - 0.5 \text{ a/d}] \{1 + [64 + 160\sqrt{(\frac{N_u}{V_u})^3}]\rho_s\} \sqrt{f'_c} \tag{2.19a}$$

for $N_u/V_u > 0.0$, where N_u is the design horizontal load; and

$$v_u = 6.5 \ (1 - 0.5 \text{ a/d}) \ (1 + 64 \ \rho_v)\sqrt{f'_c} \tag{2.19b}$$

for $N_u/V_u = 0.0$,

where

$$\rho_s = A_s/bd$$

and

$$\rho_v = (A_s + A_h)/bd$$

The shear-friction provision in section 11.15 of the ACI Code (14) expresses the ultimate shear stress as

$$v_u = \phi\mu(\rho_v f_{vy}) \tag{2.20}$$

but not more than 0.2 f'_c or 800 psi.

Resulting from the above considerations, an investigation into the strength and behavior of lightweight concrete corbels subjected to both static and repeated loadings is deemed necessary.

CHAPTER III

EXPERIMENTAL PROGRAM

3.1 Specimens

A total of 36 corbels were tested. Thirty two specimens were of the same dimensions and consisted of a 6 x 9 in. column 20 in. long with two corbels projecting symmetrically from the column as shown in Figure 6. Four larger specimens also consisted of symmetrically arranged corbels projecting from a 30 in. long, 9 x 12 in. column.

The main tension reinforcement of all specimens was comprised of parallel, straight, deformed bars; they were anchored by short, straight bars of the same diameter, welded across their ends. All corbels had closed horizontal stirrups of No. 3 deformed bars uniformly distributed in the upper two-thirds of the effective depth. Six of the 32 smaller specimens had, in addition, two No. 3 deformed compression reinforcing bars in each corbel.

Corbels to be subjected to combined vertical and horizontal loading were provided with 3/4-in. thick bearing plates welded to the main reinforcement to insure proper load transfer. The dimensions of individual specimens are shown in Table I; Table II gives the pertinent properties of the specimens.

The specimens were divided into five series. Except for series-Y of the larger specimens, each series was cast from the same batch of

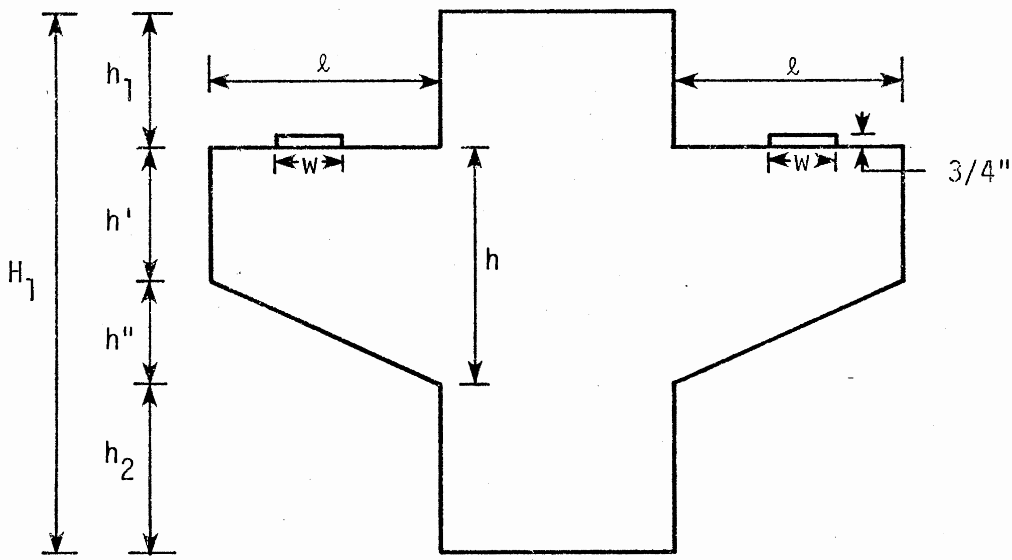

Figure 6. Geometry of Specimens

TABLE I

DIMENSIONS OF SPECIMENS

Specimen	Column (in.)	ℓ (in.)	h (in.)	h' (in.)	h" (in)	h_1 (in.)	h_2 (in.)	H_1 (in.)	w (in.)
Series A-D	9 x 6	10	9	5	4	5	6	20	4.0
Y1	12 x 9	9.5	11.25	6.5	4.75	9.0	9.75	30	5.7
Y2 & Y3	12 x 9	9.5	12.25	7.5	4.75	9.0	8.75	30	5.7
Y4	12 x 9	11.0	12.25	7.0	4.75	9.0	8.75	30	5.7

TABLE II

PROPERTIES OF SPECIMENS

Specimen	Dimensions a, in.	Dimensions d, in.	Dimensions a/d	Main Tension A_s, in.^{2}	Main Tension f_{sy}, ksi	Main Tension ρ_s, %	Stirrup[1] A_h, in.^{2}	$\frac{A_h}{A_s}$
A1	2.5	8.06	0.31	0.22	61.5	0.45	0.22	1.00
A2	2.5	8.06	0.31	0.22	61.5	0.45	0.22	1.00
A3	2.5	8.00	0.31	0.40	57.0	0.83	0.22	0.55
A4	2.5	8.00	0.31	0.40	58.0	0.83	0.22	0.55
A5	2.5	8.00	0.31	0.40	58.0	0.83	0.22	0.55
A6	2.5	7.95	0.31	0.62	70.0	1.30	0.44	0.71
A7	2.5	7.95	0.31	0.62	70.0	1.30	0.44	0.71
A8	2.5	7.95	0.31	0.62	70.0	1.30	0.44	0.71
B1	2.5	8.06	0.31	0.22	57.5	0.45	0.22	1.00
B2	2.5	8.06	0.31	0.22	61.5	0.45	0.22	1.00
B3	2.5	8.00	0.31	0.40	57.0	0.83	0.22	0.55
B4	2.5	8.00	0.31	0.40	57.0	0.83	0.22	0.55
B5	2.5	7.95	0.31	0.62	71.5	1.30	0.44	0.71
B6	2.5	7.95	0.31	0.62	71.5	1.30	0.44	0.71
B7[2]	2.5	7.95	0.31	0.62	68.5	1.30	0.44	0.71
B8[2]	2.5	7.95	0.31	0.62	68.5	1.30	0.44	0.71
C1	4.0	8.00	0.50	0.40	58.5	0.83	0.22	0.55
C2	4.0	8.00	0.50	0.40	58.5	0.83	0.22	0.55
C3	6.0	8.00	0.75	0.40	58.5	0.83	0.22	0.55
C4	6.0	8.00	0.75	0.40	58.5	0.83	0.22	0.55
C5[2]	2.5	8.00	0.31	0.40	59.0	0.83	0.22	0.55
C6[2]	2.5	8.00	0.31	0.40	59.0	0.83	0.22	0.55
C7[2]	6.0	8.00	0.75	0.40	59.0	0.83	0.22	0.55
C8[2]	6.0	8.00	0.75	0.40	59.0	0.83	0.22	0.55

TABLE II (Continued)

Speci-men	Dimensions a, in.	d, in.	a/d	Reinforcement: Main Tension A_s, in.[2]	f_{sy}, ksi	ρ_s, %	Stirrup[1] A_h, in.[2]	$\frac{A_h}{A_s}$
D1	4.0	8.00	0.50	0.40	54.5	0.83	0.22	0.55
D2	4.0	8.00	0.50	0.40	58.5	0.83	0.22	0.55
D3	6.0	8.00	0.75	0.40	58.5	0.83	0.22	0.55
D4	6.0	8.00	0.75	0.40	58.5	0.83	0.22	0.55
D5	4.0	7.95	0.50	0.62	71.5	1.30	0.44	0.71
D6	4.0	8.00	0.50	0.60	59.0	1.25	0.44	0.73
D7	6.0	8.00	0.75	0.60	58.5	1.25	0.44	0.73
D8	6.0	8.00	0.75	0.60	54.5	1.25	0.44	0.73
Y1	3.2	10.25	0.31	0.40	58.0	0.43	0.44	1.10
Y2	3.5	11.13	0.31	0.88	56.0	0.88	0.44	0.50
Y3	3.5	11.13	0.31	0.88	56.0	0.88	0.44	0.50
Y4	5.6	11.13	0.50	0.88	56.0	0.88	0.44	0.50

[1]Average yield strength of stirrups, f_{hy} = 58.5 ksi.

[2]Specimen had two No. 3 compression reinforcing bars in each corbel.

[3]Larger specimens.

concrete. Each series of the smaller specimens consisted of eight specimens of which half were subjected to static loading and the remaining half were subjected to repeated loading.

Series A and B were tested to study the influence of the reinforcement ratio and series C and D were tested to study the influence of the shear span-to-effective depth ratio. In series B and C the effects of compression reinforcement in the corbels were examined. Series Y was tested to determine the influence of the size of the specimens, if any.

3.2 Materials

3.2.1 Concrete

The concrete used in this investigation was obtained from a local precast concrete manufacturing plant and was of the same quality as that used in their manufacturing process. Type III portland cement was used for all concrete. The aggregate consisted of burnt calcined clay conforming to ASTM specification C330 (3/8--No. 8) classification and natural sand. The concrete with a nominal design strength of 6.0 ksi was taken out of the batches during routine operation of the precast plant. The age, strength, air content, and slump of the concrete are given in Table III.

3.2.2 Reinforcement

All specimens were reinforced with deformed bars with deformations in accordance with A615-68 of the ASTM standard specifications. Coupons with 8-in. gage lengths were tested to establish the yield strength and the stress-strain curves of the main reinforcements for all specimens. The average yield strength of the stirrup reinforcement was determined

TABLE III

PROPERTIES OF CONCRETE

Specimen	Unit Weight, pcf	Slump, in.	Air Content, %	Compressive Strength, ksi	Age at Test, Days
Series A and Y4	117	4.0	2	6.80	149
Series B and Y3	120	3.5	2	7.10	147
Series C and Y2	116	3.0	2	6.95	146
Series D and Y1	115	3.0	2	6.45	145

from tests of random samples. Figure 7 gives the stress-strain curve for a typical coupon. Typical reinforcement arrangements are shown in Figure 8.

3.3 Experimental Procedure

3.3.1 Fabrication and Preparation

All corbels and control cylinders were cast in accordance with ASTM specifications at the plant of the precast concrete manufacturer. Corbels were cast in well-oiled plywood forms and the control cylinders were cast in vertical steel molds for each batch of concrete mix. Both the corbels and the control cylinders were initially cured under plastic sheets for 24 hours. After this period the specimens and control cylinders were removed from their forms, transported to the Civil Engineering Laboratory and cured under wet burlap for six days. Thereafter, corbels and control cylinders were stored in the laboratory under ambient conditions until the time of test.

3.3.2 Instrumentation and Measurement

All corbels had an electrical resistance strain gage mounted on one of the main tension reinforcing bars at the column-corbel interface. Each gage had a gage length of 1/4 in. and was mounted in the longitudinal direction of the main tension reinforcement. The strains were monitored with strain indicators to ascertain the level of strain in the main tension reinforcement at failure.

Since none of the specimens was initially cracked, the deformation of each corbel relative to the column was rotational in nature. Both the vertical and the horizontal components of the rotation were monitored

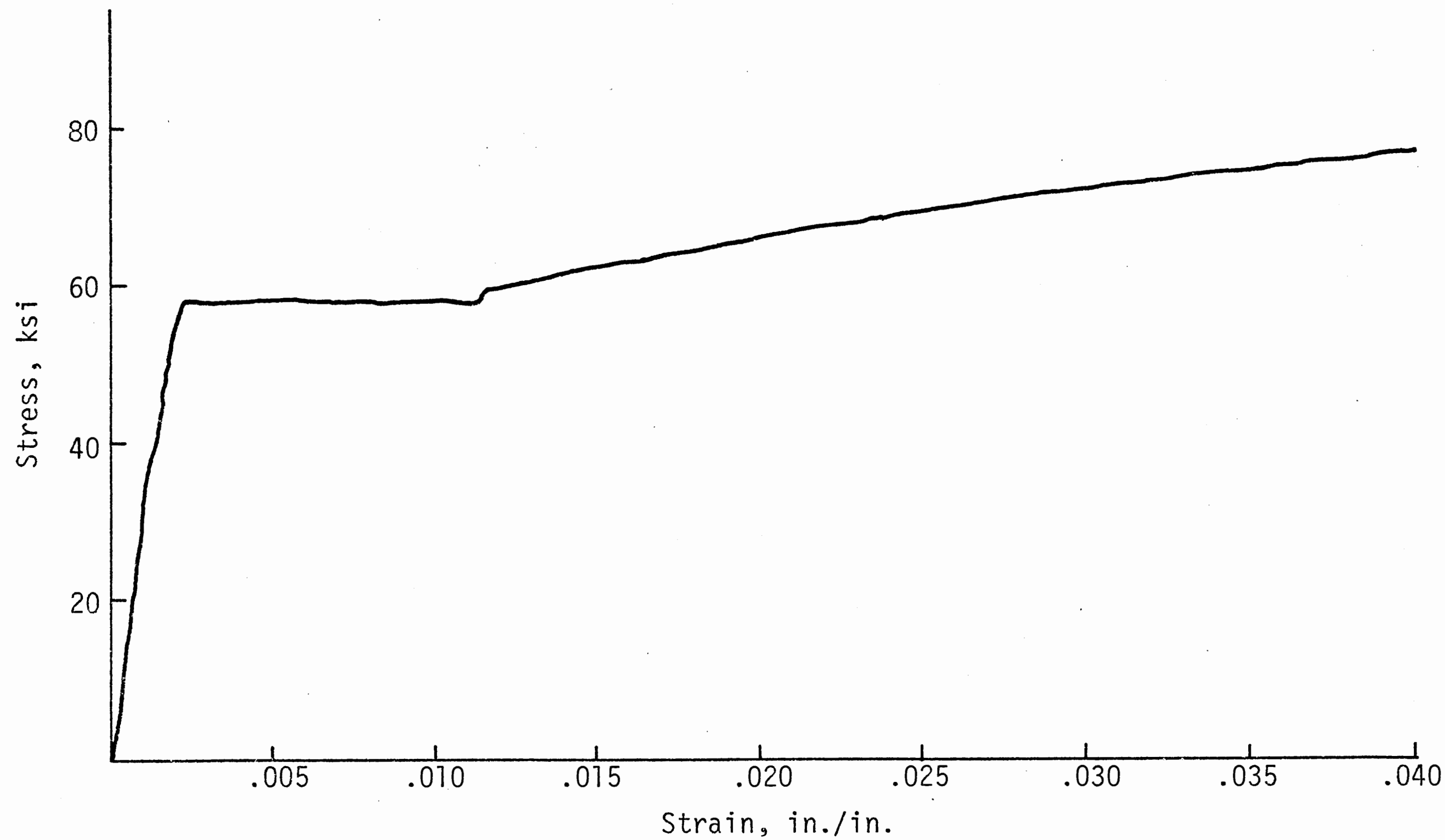

Figure 7. Typical Stress-Strain Curve for Reinforcement

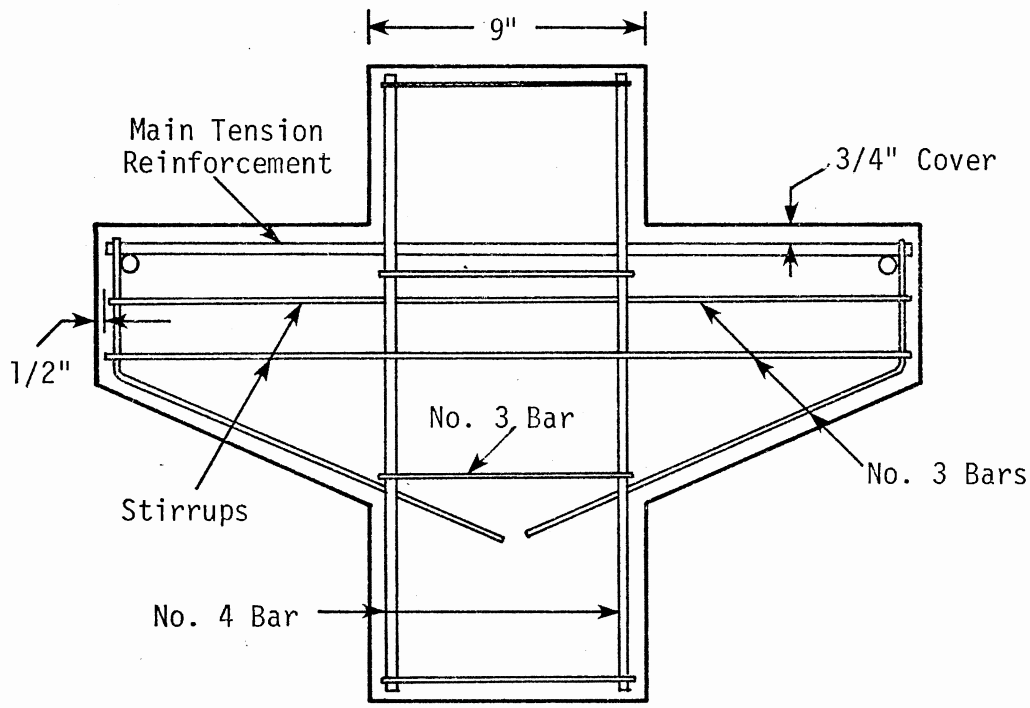

Elevation

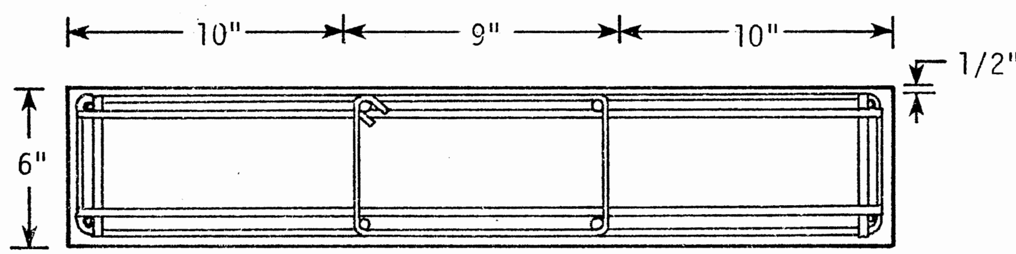

Plan

(a) Specimen Without Compression Bars and Subjected to Vertical Loads Only

Figure 8. Arrangement of Reinforcement

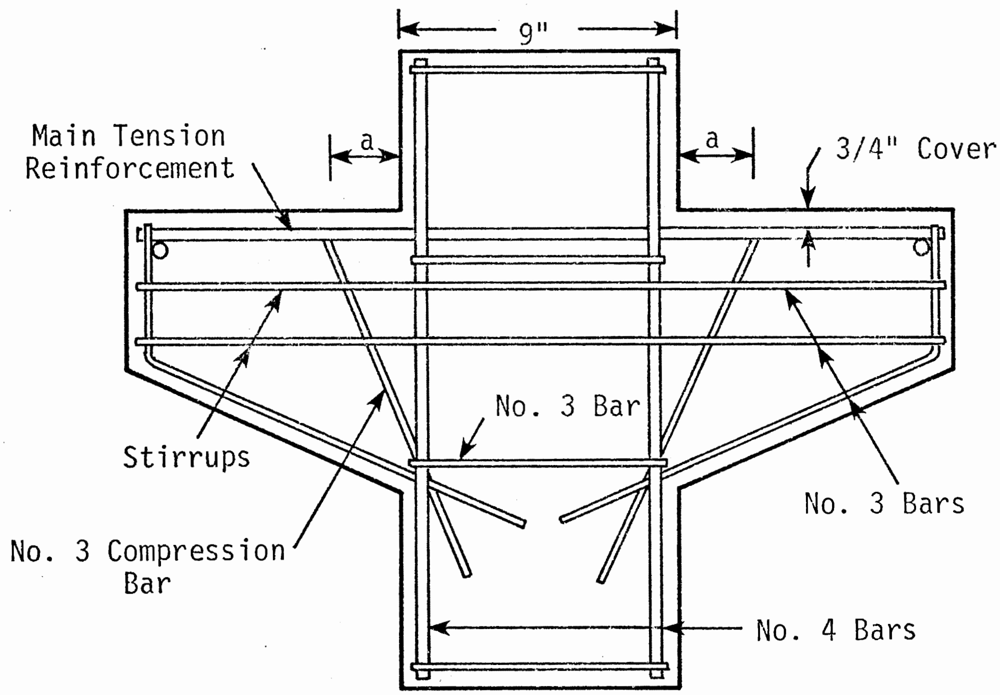

Elevation

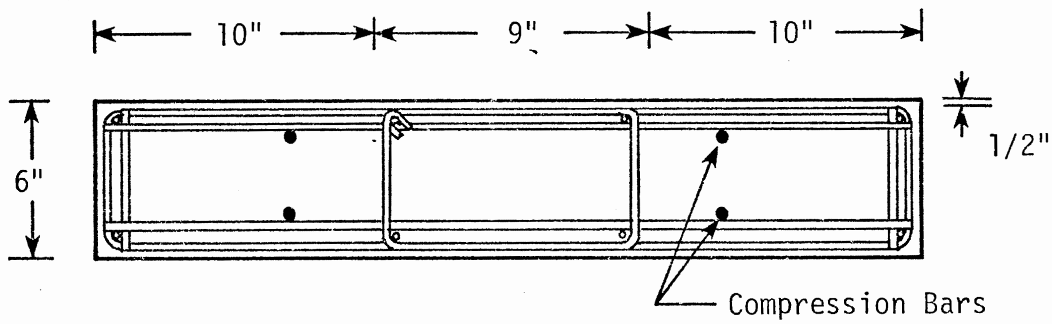

Plan

(b) Specimen With Compression Bars and Subjected to Vertical Loads Only

Figure 8. (Continued)

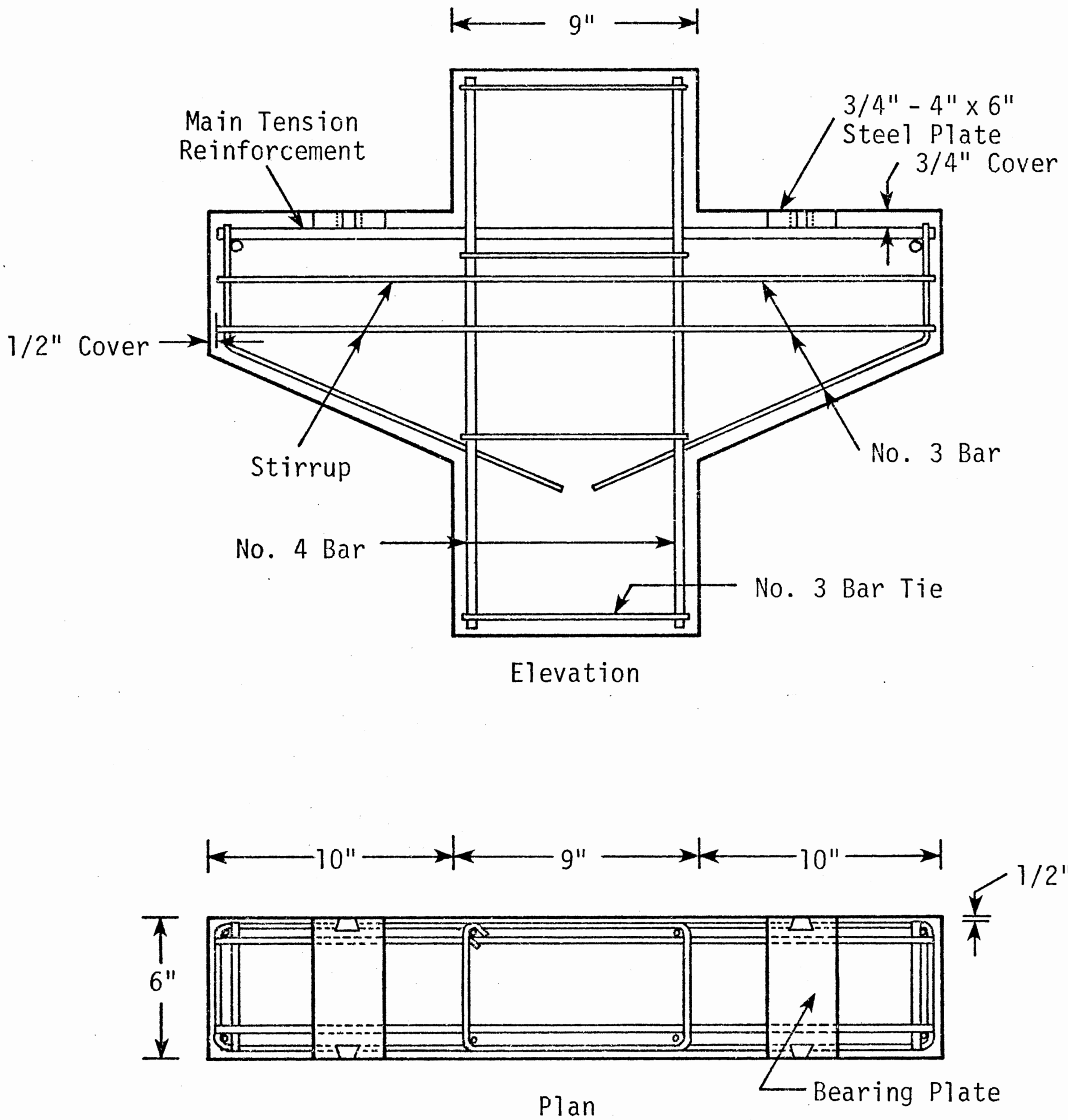

(c) Specimen With Bearing Plates Subjected to Combined Loads

Figure 8. (Continued)

with DCDT-transducers arranged as shown in Figure 9. The arrangement of the transducers was such that the cumulative horizontal deformation and the sum of vertical displacements of both corbels relative to the column were recorded. The load displacement curves were plotted continuously during the test using two x-y plotters.

3.3.3 Testing

For convenience all specimens were tested in an inverted position and the vertical load was applied to the column as shown in Figure 10. To ensure uniform distribution of the load on all bearing areas, new 1/4-in. plywood inserts were placed between the specimen and the bearing plate in each test. All specimens were supported on rollers and the outer edges of all bearing areas were 2 in. or more away from the outer face of the corbel.

In the static loading tests a 400-kip universal testing machine was used; the load was applied in increments of 10 kips for the small specimens and in increments of 20 kips for the larger specimens of series-Y. For specimens subjected to combined loading the horizontal component of the load was applied to the corbel by a 30-ton hydraulic ram and manual pump arrangement, as shown in Figure 11.

Repeated, vertical loads were applied to corbels with a 100-kip servo-controlled hydraulic testing machine. A static horizontal load, if present, was applied in the same fashion as during the static tests. The first cycle of load was applied slowly to a level corresponding to 60 percent of the ultimate load resisted by a companion specimen during the static tests. Thereafter, the corbels were subjected to repeated loads at a frequency of 2 Hz for 100,000 cycles. The repeated loads varied

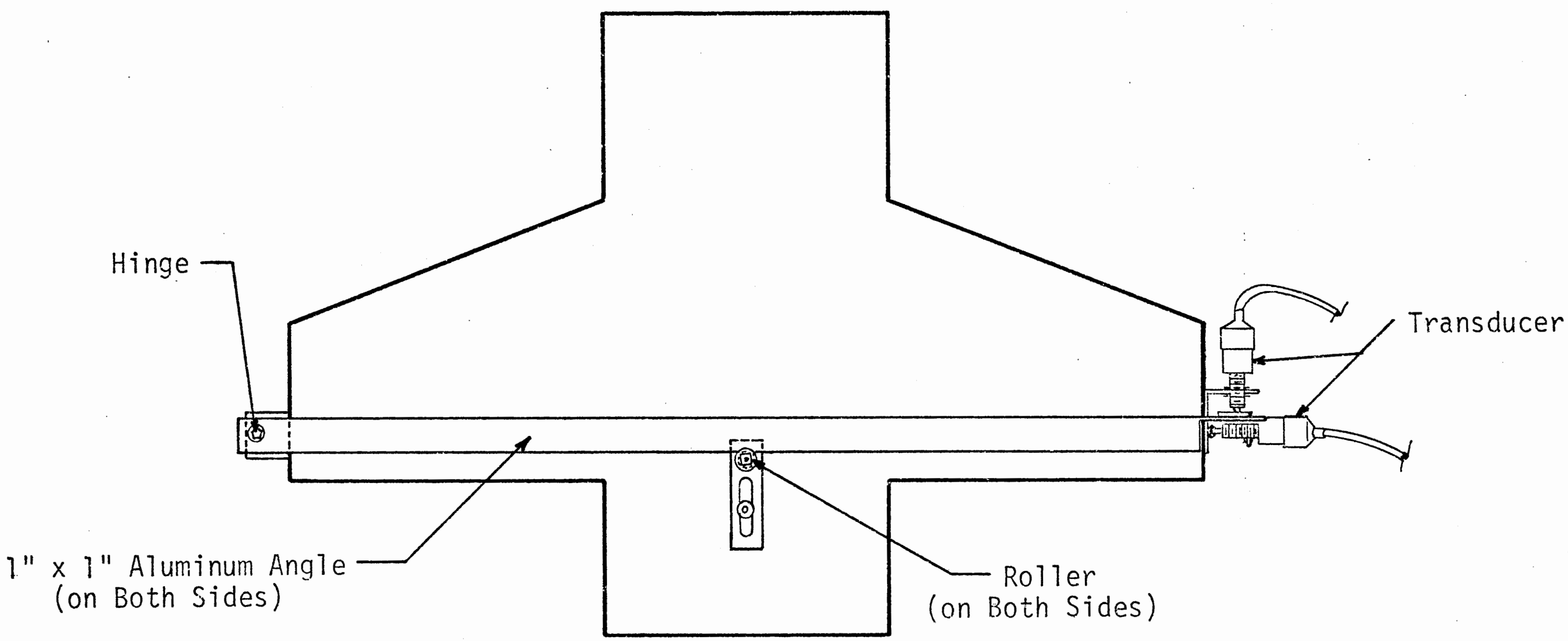

(a) Side View of Specimen

Figure 9. Typical Arrangement of Transducers

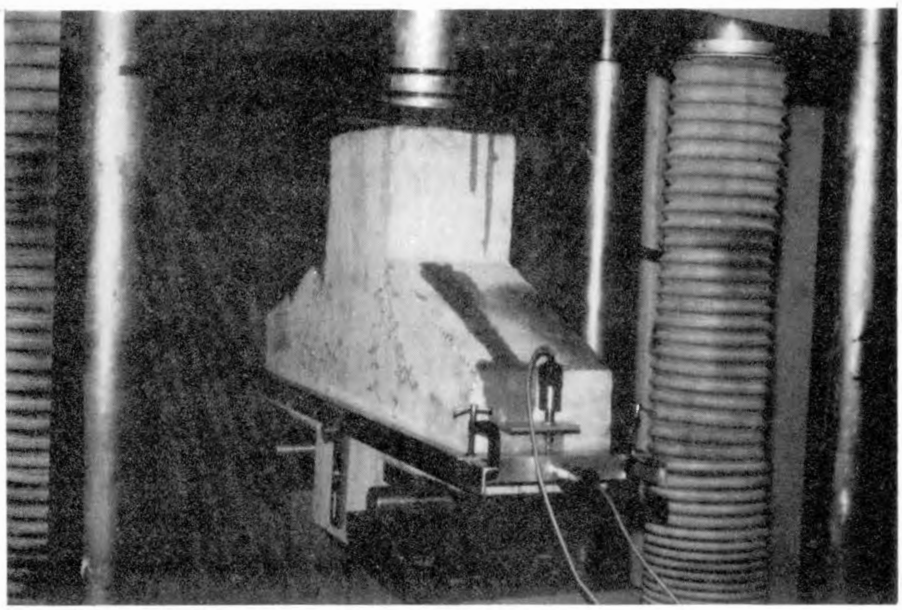

(b) Photograph of Specimen

Figure 9. (Continued)

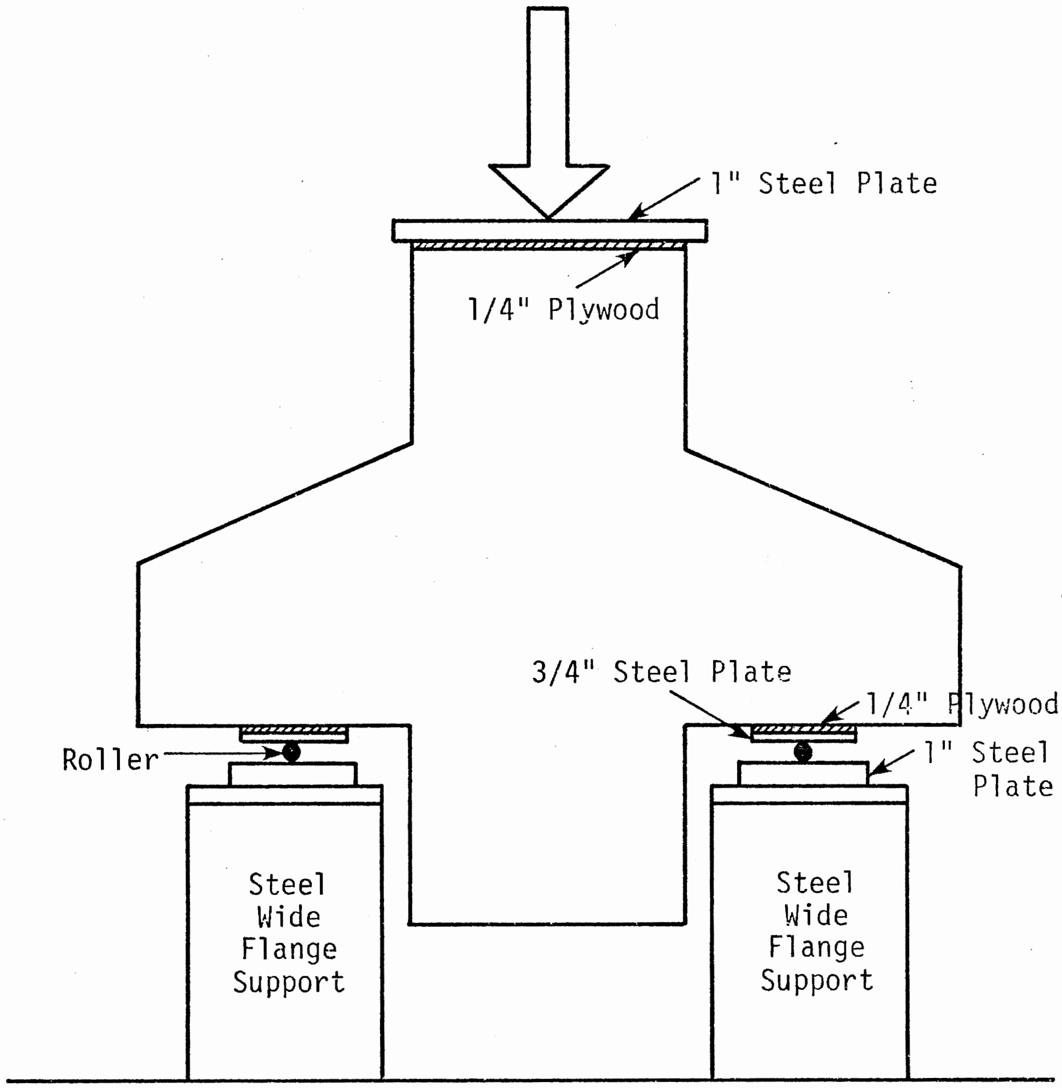

Figure 10. Specimen in Test Position

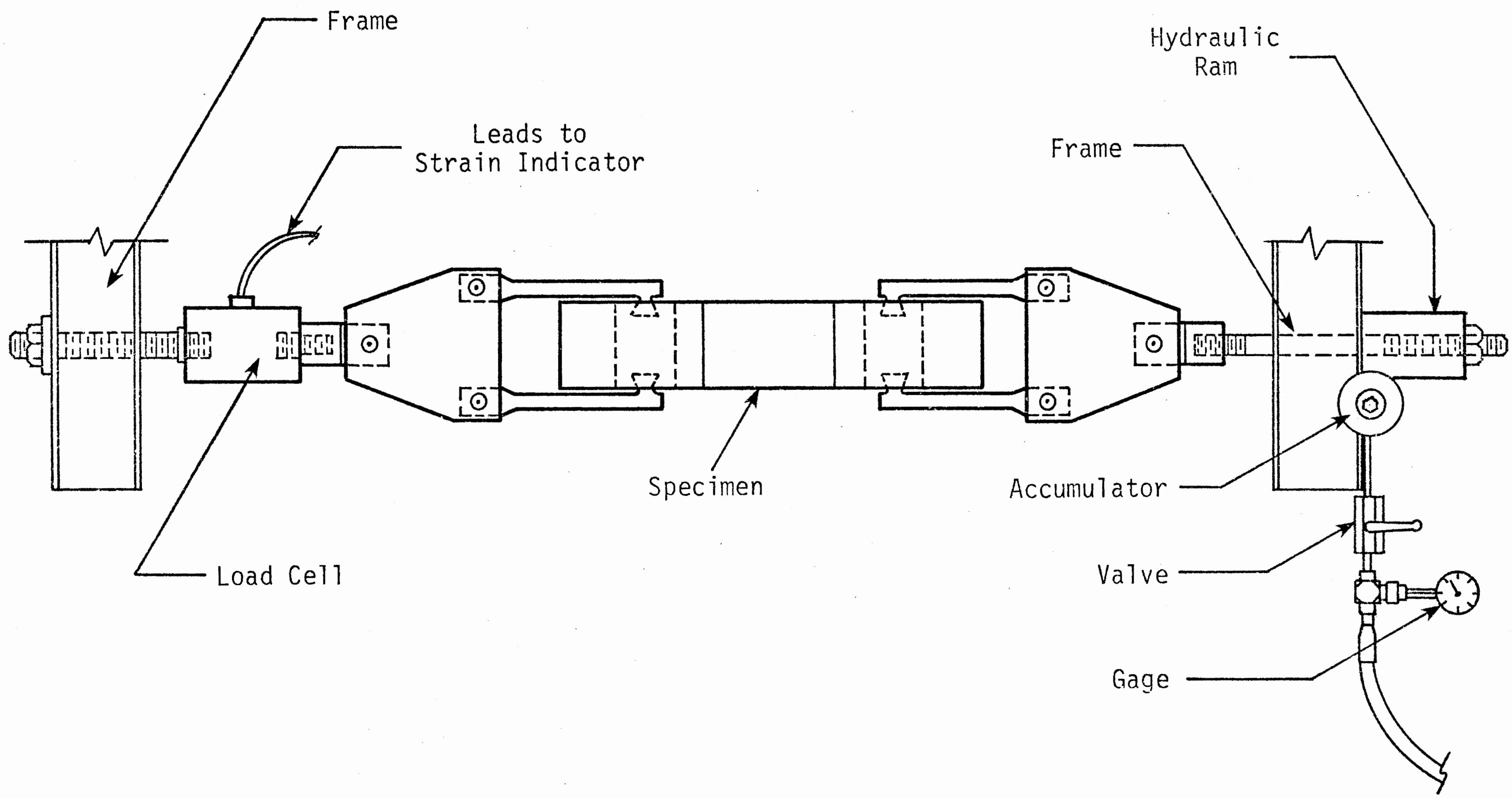

(a) Plan View of Setup

Figure 11. Horizontal Loading System

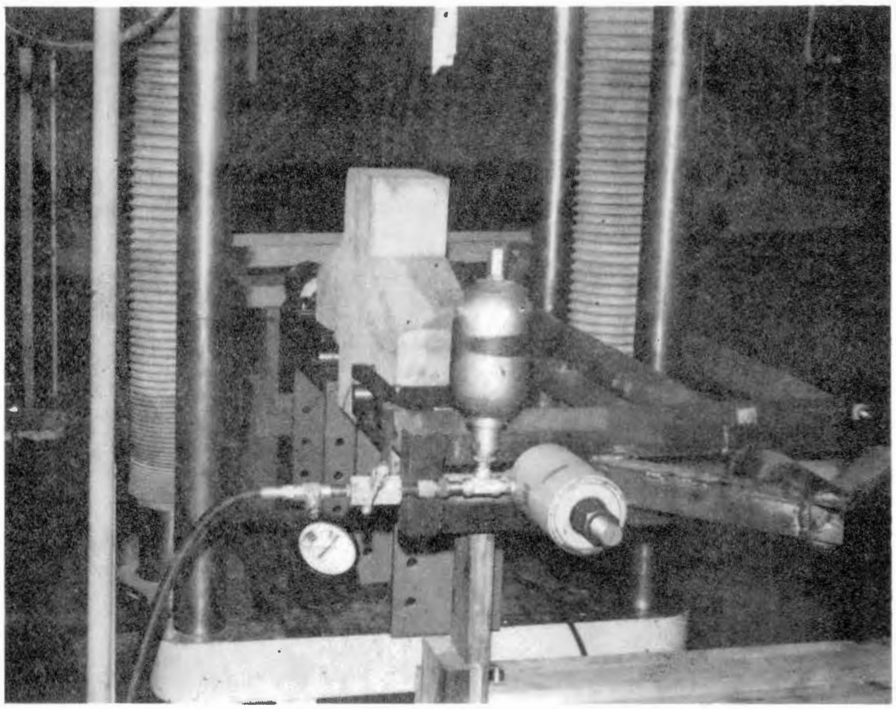

(b) Photograph of Setup

Figure 11. (Continued)

between about 20 and 60 percent of the ultimate loads. The cyclic load was interrupted to permit the plotting of the load-displacement graphs at the end of the 1st, 10th, 100th, 1000th, 10,000th, and 100,000th cycle. After completion of the cyclic loadings the specimens were loaded statically to failure.

CHAPTER IV

RESULTS

4.1 Static Loading

4.1.1 General

The level of strain in the main tension reinforcement was recorded, after each load increment, to ascertain the strain level in the main tension reinforcement at failure. No strain data were available from specimens A1, B7, D5, and D7 because of inoperative strain gages; however, for all other specimens the strain level at failure was found to be at or near yield.

In each test the first cracks to form were flexural cracks which started from the intersection of the horizontal face of the corbel and the column face. These cracks, which were observed at very low loads of between 10 and 40 kips, initially propagated rapidly to about mid-depth of the corbel; the first diagonal tension cracks then became visible.

In the case of corbels with higher a/d ratio, an additional flexural crack formed, at higher loads, at about the middle of the shear span or near the inner edge of the bearing plate. This additional flexural crack propagated rapidly toward the compression zone and appeared to meet the first flexural crack. Some of the crack patterns are shown in Figure 12.

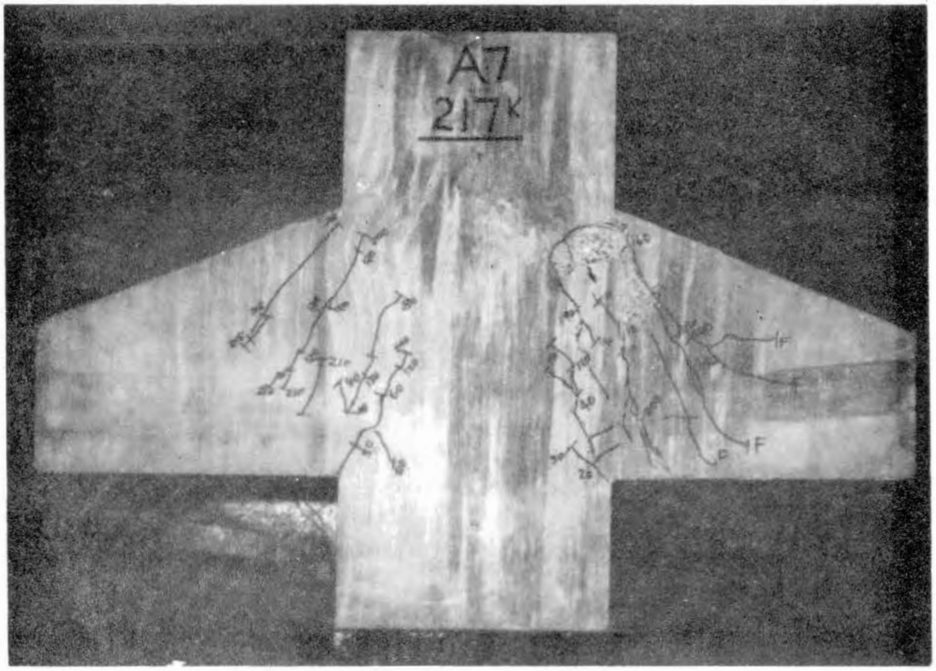

(a) ρ_s = 1.30%; a/d = 0.31; H/V = 0.0

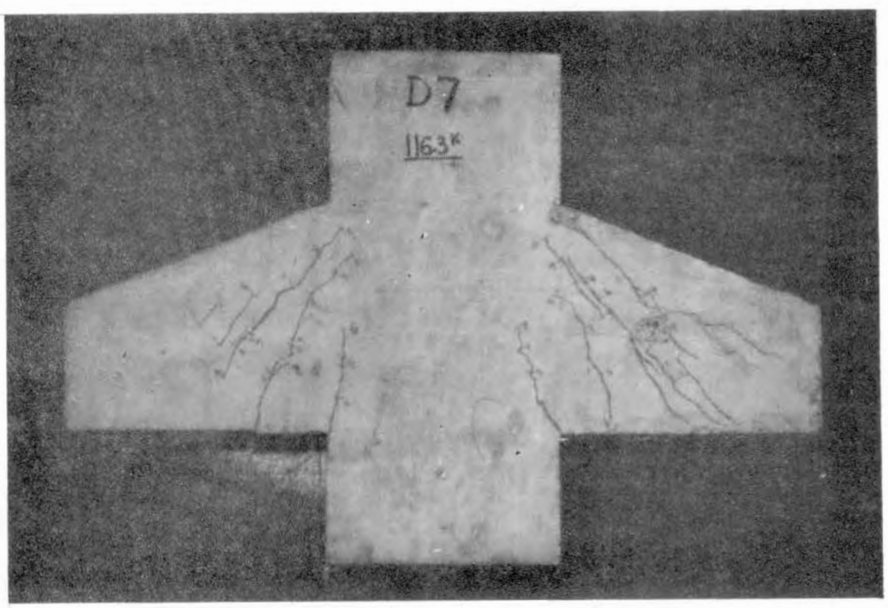

(b) ρ_s = 1.30%; a/d = 0.75; H/V = 0.0

Figure 12. Crack Patterns

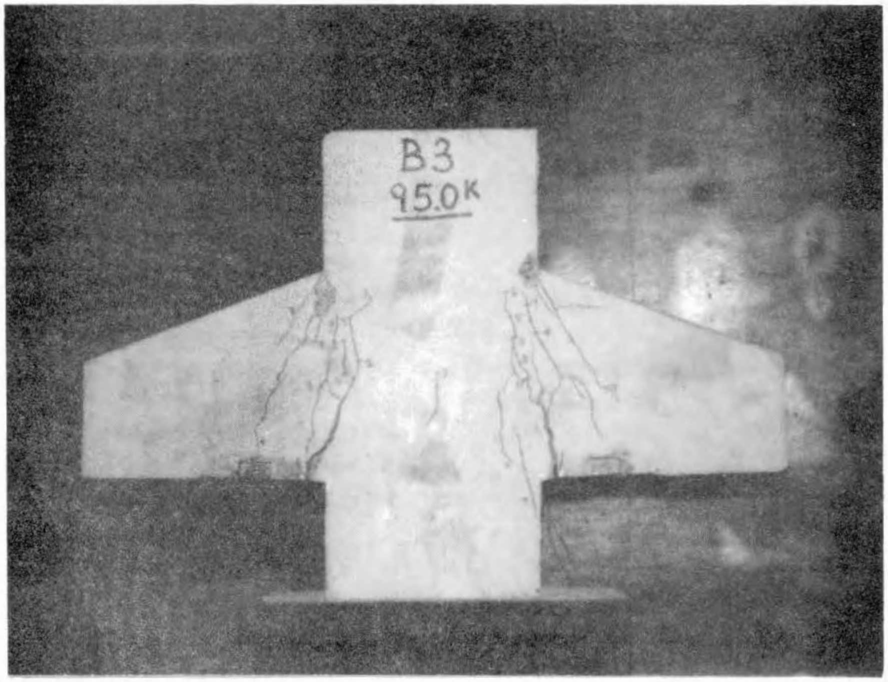

(c) ρ_s = 0.83%; a/d = 0.31; H_u/V_u = 0.47

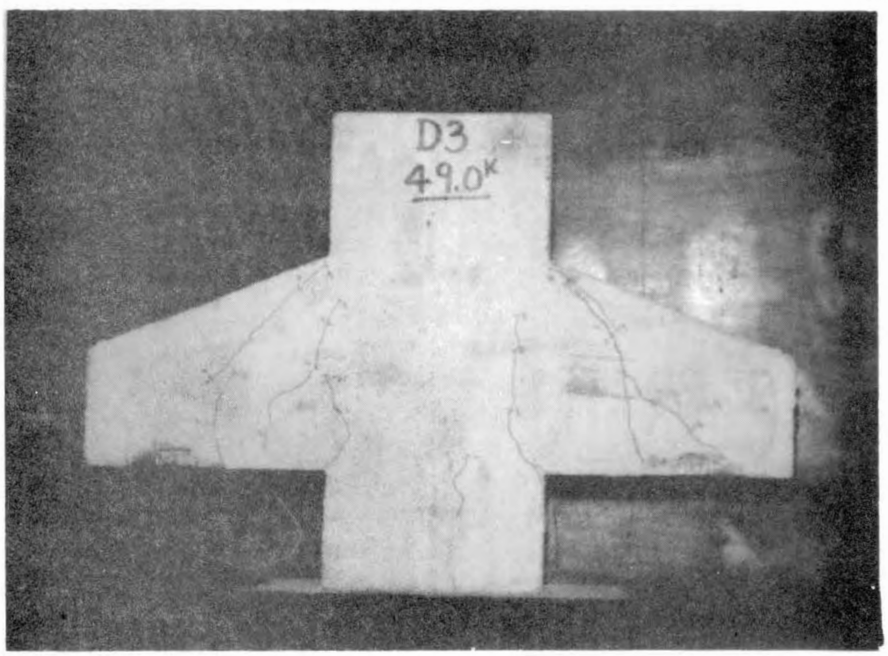

(d) ρ_s = 0.83%; a/d = 0.75; H_u/V_u = 0.40

Figure 12. (Continued)

The first diagonal tension cracks were noticed at loads ranging from about 25 to about 60 percent of the ultimate vertical load and averaged about 2.0 in. in length. The inclinations of these diagonal tension cracks to the vertical was observed to be dependent only on the a/d ratio (i.e., the location of the load). For a/d ratios of about 0.31, 0.50 and 0.75, the angles of the inclinations were observed to be 25-30°, 30-40° and 40-50°, respectively. At lower a/d ratios, these diagonal tension cracks propagated slower than those that occurred at higher a/d ratios. The locations of these first diagonal tension cracks appeared to be influenced by both a/d and H/V ratios.

Additional diagonal tension cracks formed at higher vertical loads; they were 2.0 to 4.0 in. in length and propagated more rapidly than the first diagonal tension cracks. These subsequent diagonal tension cracks were initially spaced about 1.0 to 2.5 in. apart; however, as more diagonal cracks were formed approximately parallel to the first diagonal tension crack, the spacing reduced at or near failure loads.

4.1.2 Vertical Loading Only

For specimens under vertical loading only, the first diagonal tension crack occurred near the mid-depth of the corbel. This crack crossed the column-corbel interface in the case of specimens with a/d of 0.31; for a/d of 0.50, the crack occurred in the corbel but adjacent to the column-corbel interface; for a/d of 0.75, the crack appeared farther from the column-corbel interface and closer to the compression zone.

Typical load-displacement relationships as plotted directly with the x-y recorders are shown in Figure 13. Figure 13(a) gives the load-

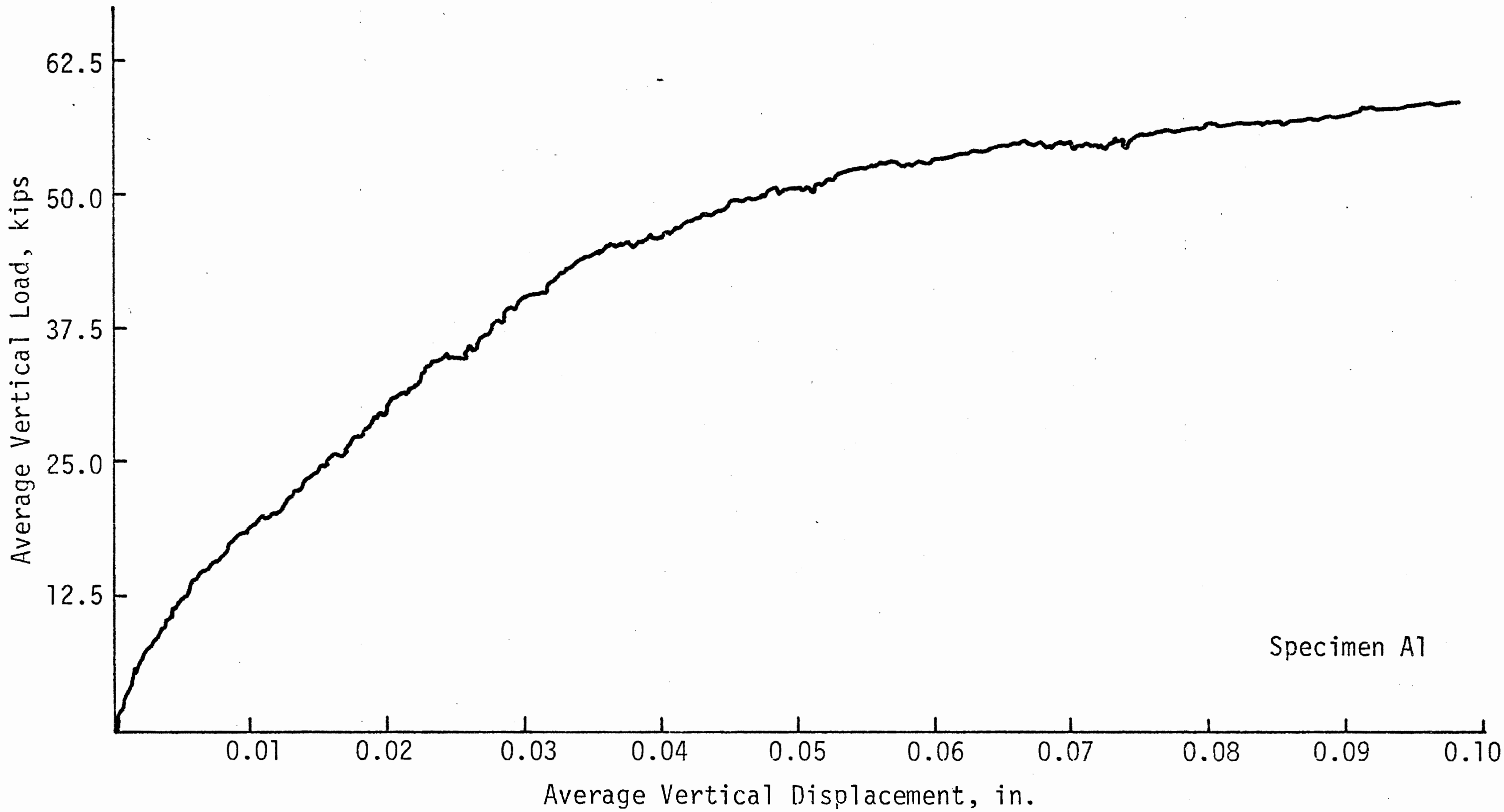

(a) Vertical Load-Vertical Displacement Curve

Figure 13. Load-Displacement Relationship (Vertical Loads Only)

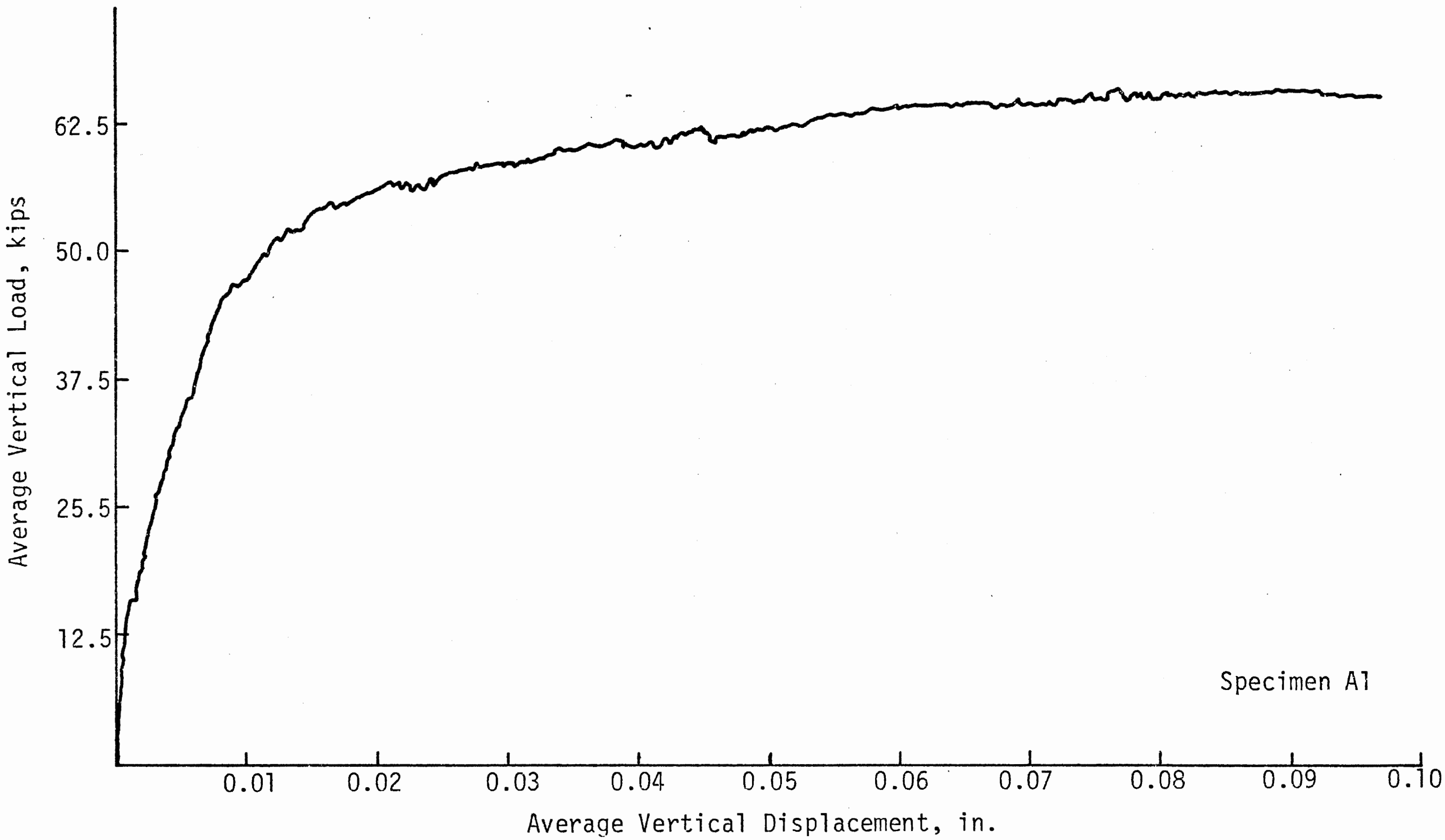

(b) Vertical Load-Horizontal Displacement Curve

Figure 13. (Continued)

vertical displacement curve, while Figure 13(b) shows the load-horizontal displacement.

The test results of all the specimens with vertical loading only are given in Table IV. From these results the graphs illustrating the influence of the reinforcement ratio, (ρ), and shear span-to-effective depth ratio, (a/d), on the ultimate shear stress are shown in Figure 14 and Figure 15. Figure 14 shows a linear relationship between the ultimate shear stress and the reinforcement ratio, while Figure 15 shows a nonlinear relationship between the ultimate shear stress and the shear span-to-effective depth ratio.

Resulting from the inherent properties of the aggregate, light-weight concrete is more compressible than normal weight concrete. Therefore, to determine the influence of compression reinforcement on the strength and behavior, the corbels of specimens B7, C5, and C7 were additionally reinforced with two No. 3 compression bars. In Table V the results of specimens C5, C7 and B7 are compared with their companion specimens A3, C3, A6, and A7 without compression reinforcement. The comparisons indicate that at lower a/d ratios, given the same reinforcement ratio (ρ), the specimen with compression reinforcement resisted higher shear stress. Also, for an a/d ratio of about 0.31 and a given compression reinforcement, the specimen with higher reinforcement ratio (ρ) resisted the higher shear stress. At the higher a/d ratio of 0.75 and a given reinforcement ratio (ρ) the compression reinforcement appeared to have no appreciable influence on the capacity of the corbel.

Table VI summarizes the test results of the four larger specimens, Y1-Y4, and their companion smaller specimens. The comparative ratios of

TABLE IV

TEST RESULTS FOR VERTICAL STATIC LOAD SERIES

Speci-men	a/d	ρ_s, %	V'_y,[1] kip	V'_u,[1] kip	v_y, ksi	v_u, ksi	Type of Failure
A1	0.31	0.45	94.0	127.8	0.97	1.32	Shear
A3	0.31	0.83	107.5	156.3	1.12	1.63	Shear
A6	0.31	1.30	187.5	190.3	1.97	2.00	Shear
A7	0.31	1.30	190.0	217.0	1.99	2.28	Shear
B7[2]	0.31	1.30	192.5	244.0	2.02	2.56	Shear
C1	0.50	0.83	87.5	118.0	0.91	1.23	Shear
C3	0.75	0.83	63.5	88.0	0.66	0.92	Shear
C5[2]	0.31	0.83	119.0	176.0	1.24	1.84	Shear
C7[2]	0.75	0.83	69.5	85.8	0.72	0.89	Shear
D5	0.50	1.30	135.0	146.3	1.42	1.54	Shear
D7	0.75	1.25	110.0	116.3	1.15	1.21	Shear
Y1[3]	0.31	0.43	156.0	243.0	0.85	1.32	Shear
Y2[3]	0.31	0.88	255.0	328.0	1.27	1.64	Shear
Y3[3]	0.31	0.88	255.0	325.0	1.27	1.62	Shear
Y4[3]	0.50	0.88	185.0	244.0	0.92	1.22	Shear

[1]Total load for both corbels in each specimen.

[2]Specimen had two No. 3 bars as compression reinforcement in each corbel.

[3]Larger size specimen.

TABLE V

INFLUENCE OF COMPRESSION REINFORCEMENT

Specimen	a/d	ρ_s, %	v_u,[1] ksi	v_{uc},[2] ksi	$\frac{v_{uc}}{v_u}$[2][1]
C5[3]	0.31	0.83	---	1.84	
A3	0.31	0.83	1.63	---	1.13
C7[3]	0.75	0.83	---	0.89	
C3	0.75	0.83	0.92	---	0.97
B7[3]	0.31	1.30	---	2.56	
A6	0.31	1.30	2.00	---	1.28
A7	0.31	1.30	2.28	---	1.12

[1]Shear stress of specimen without compression reinforcement.

[2]Shear stress of specimen with compression of reinforcement.

[3]Specimen with two No. 3 bars as compression reinforcement in each corbel.

TABLE VI

INFLUENCE OF SIZE

Specimen	a/d	ρ_s, %	v_u,[1] ksi	v_{uL},[2] ksi	$\frac{v_u{}^1}{v_{uL}{}^2}$
A1	0.31	0.45	1.32	---	
Y1[3]	0.31	0.43	---	1.32	1.00
A3	0.31	0.83	1.63	---	
Y2[3]	0.31	0.88	---	1.64	0.99
Y3[3]	0.31	0.88	---	1.62	1.01
C1	0.50	0.83	1.23	---	
Y4[3]	0.50	0.88	---	1.22	1.01

[1]Shear stress of smaller specimen.

[2]Shear stress of larger specimen.

[3]Larger specimen.

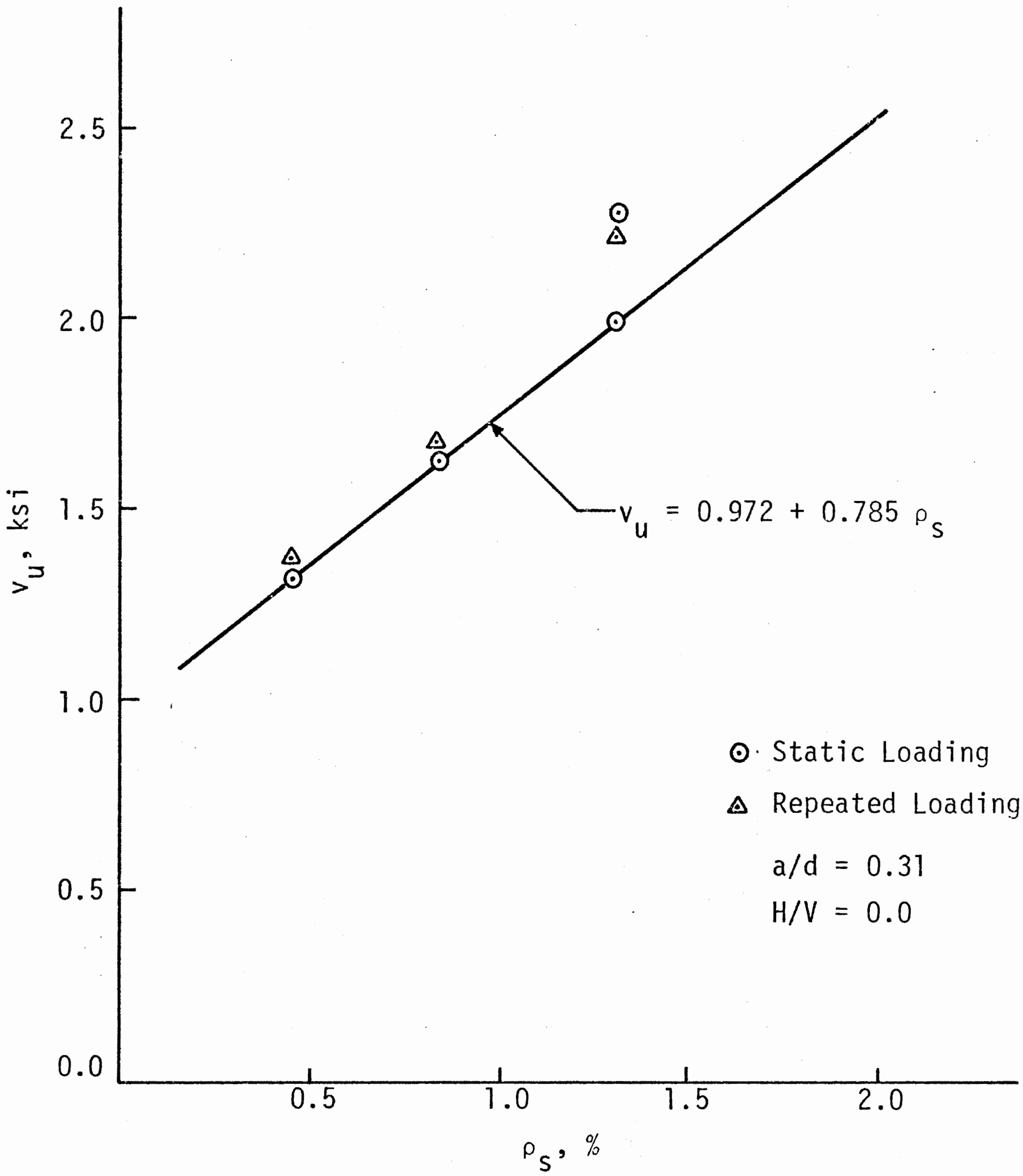

Figure 14. Relationship Between Ultimate Shear Stress and the Reinforcement Ratio

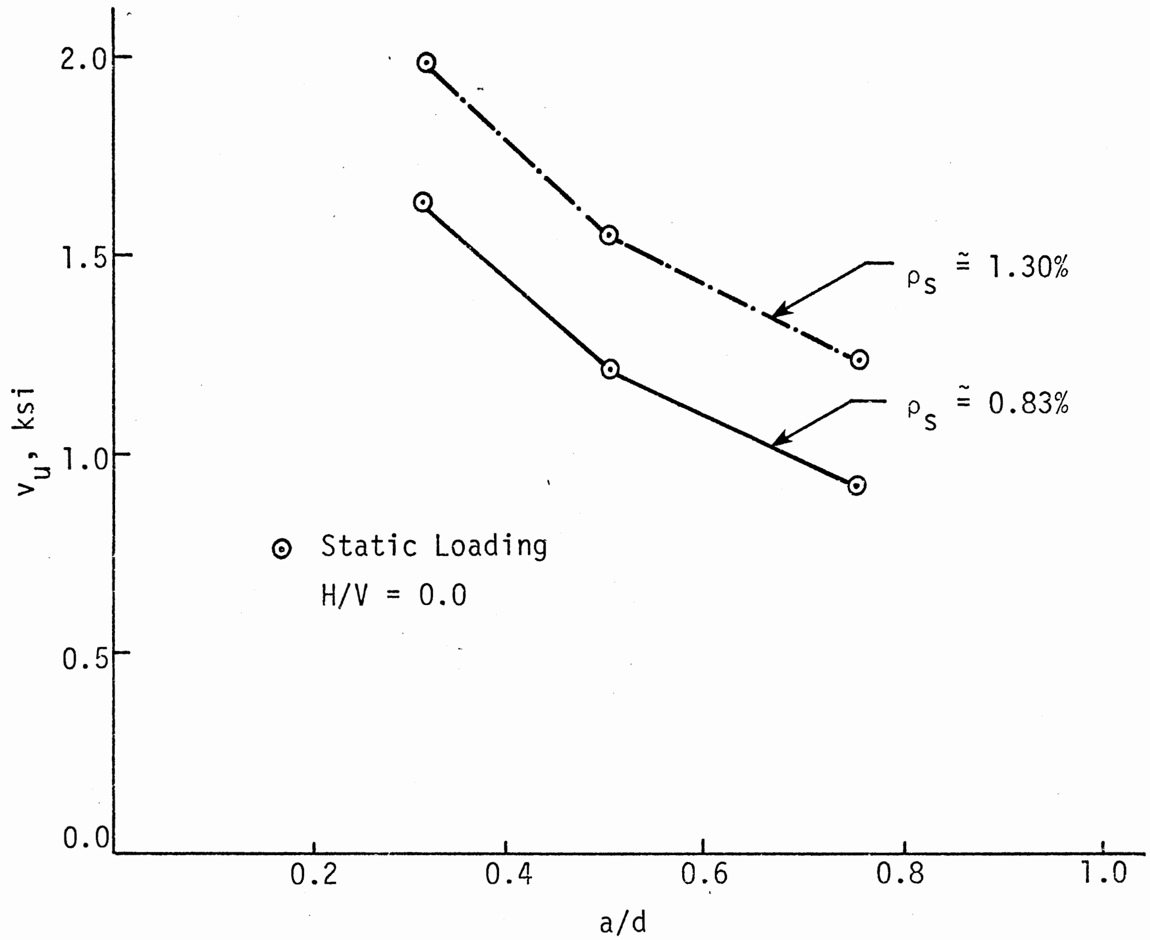

Figure 15. Relationship Between Ultimate Shear Stress and the Shear Span-to-Effective Depth Ratio

their ultimate shear stresses indicate that there was practically no influence of size on the ultimate shear stress.

4.1.3 Combined Loading

In the case of specimens subjected to combined loading, as expected, both the first flexural and diagonal tension cracks were observed at lower vertical loads than those under vertical loading only. The first flexural crack was more nearly vertical and propagated faster than the one in specimens under vertical loading only.

The first diagonal crack appeared within the corbel and about mid-depth adjacent to the column-corbel interface for a/d of 0.31; for a/d of 0.50 or 0.75 the diagonal crack occurred farther from the column-corbel interface and closer to the compression zone.

The vertical and horizontal loads were not simultaneously increased; instead, the vertical load was first increased to the desired value, and then the horizontal load was increased to a predetermined value to obtain a horizontal load-to-vertical load, (H/V), ratio of approximately 0.50. However, because of this alternating manner of loading, failure occurred frequently during the application of increments of vertical loads. Hence at failure loads, the H/V ratios were not exactly 0.50. In the case of specimen B5 the horizontal load was increased in the same manner as the other specimens under combined loads until the maximum value of 20 kips, representing the capacity of the load cell employed, was achieved. Thereafter, the horizontal load was kept constant at 20 kips and the vertical load was increased to failure.

Table VII gives the results of specimens subjected to statically combined loading, while Figure 16 gives the typical vertical load-displacement relationships.

TABLE VII

TEST RESULTS FOR COMBINED STATIC LOAD SERIES

Specimen	a/d	ρ_s, %	V'_y,[1] kips	V'_u,[1] kips	H_u, kips	$\frac{H_u}{V_u}$[2]	v_y, ksi	v_u, ksi	Types of Failure
B1	0.31	0.45	43.8	66.0	16.3	0.49	0.45	0.68	Flexural Tension
B3	0.31	0.83	58.8	95.0	22.5	0.47	0.61	0.99	Flexural Tension
B5	0.31	1.30	147.5	170.0	20.0	0.24	1.54	1.78	Shear
D1	0.50	0.83	48.8	60.0	15.0	0.50	0.51	0.63	Shear
D3	0.75	0.83	40.0	49.0	10.0	0.40	0.42	0.51	Shear

[1]Total load for both corbels in each specimen.

[2]Average load for a corbel in each specimen.

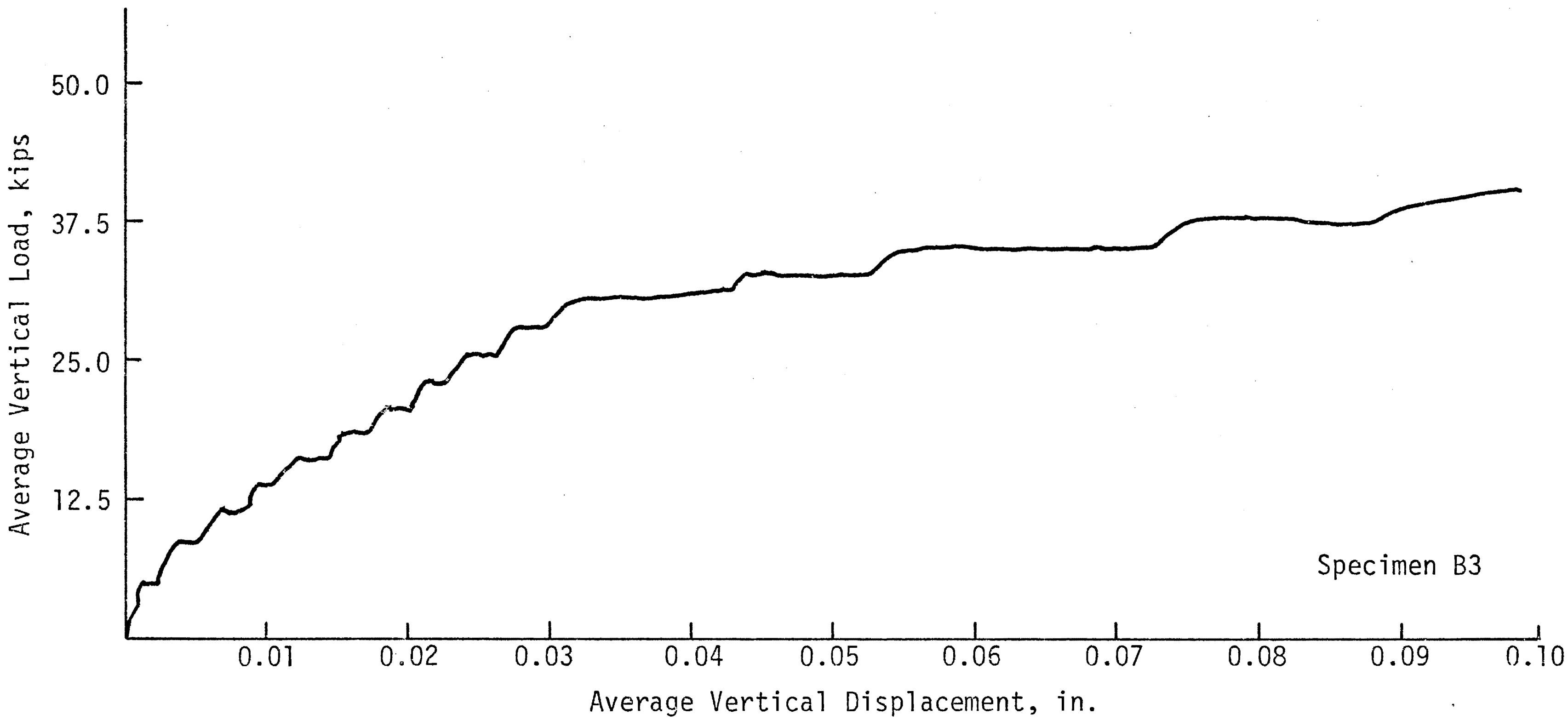

(a) Vertical Load-Vertical Displacement Curve

Figure 16. Load-Displacement Relationship (Combined Loads)

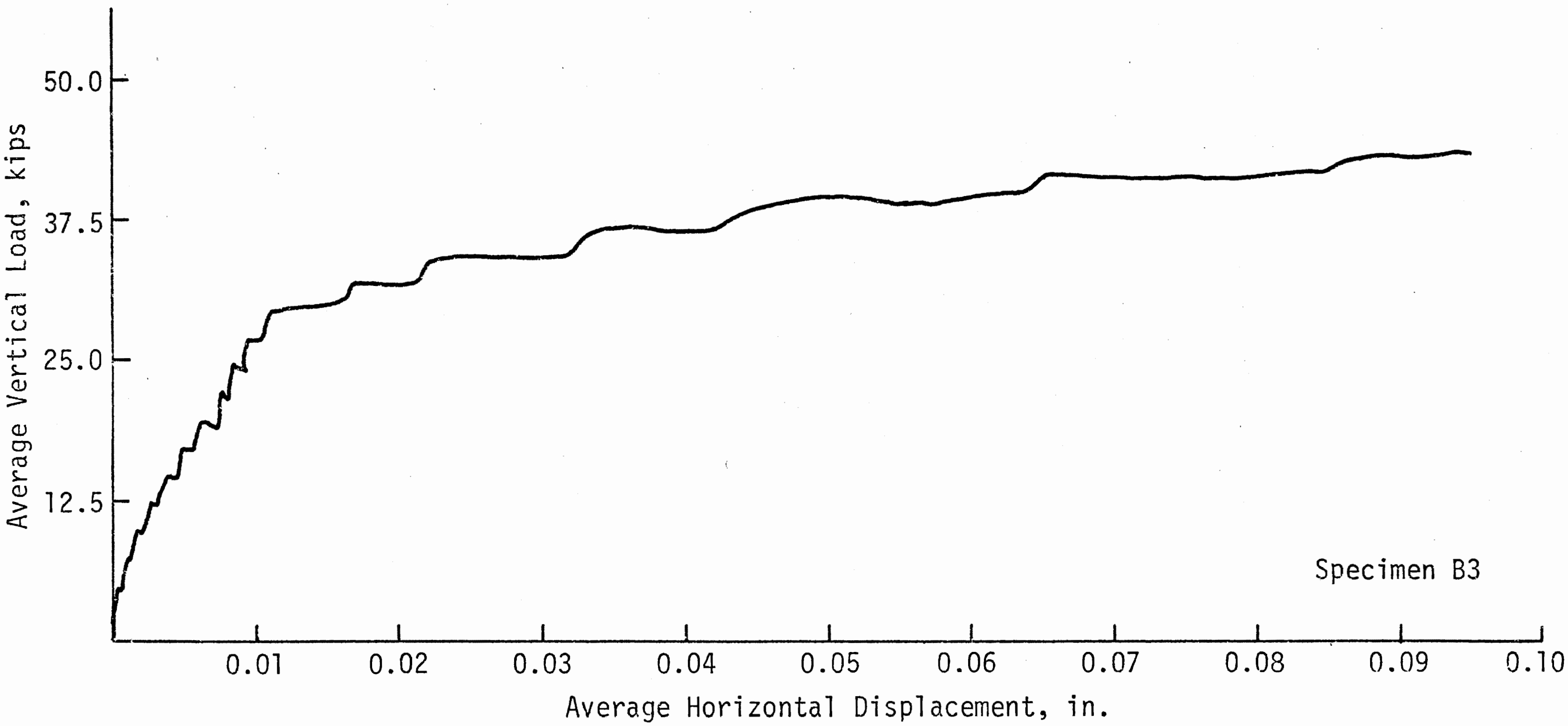

(b) Vertical Load-Horizontal Displacement Curve

Figure 16. (Continued)

4.2 Repeated Loading

4.2.1 General

Each specimen to be subjected to repeated loading was loaded statically to approximately 60 percent of the failure load of the companion specimen in the static test. Thereafter, the specimen was subjected to 100,000 cycles of repeated vertical loading between approximately 0.20 V_u and 0.60 V_u; however, for specimens A8, B8, and C6, the 0.60 V_u could not be achieved because of the high capacities of their companion specimens. Load-displacement curves were plotted at the end of the 1st, 10th, 100th, 1000th, 10,000th, and 100,000th cycle, as shown in Figure 17.

In the case of specimen A5, an attempt was made to increase the cycles from 100,000 to 500,000 cycles. However, the main reinforcement experienced fatigue fracture at the column-corbel interface about 390,000 cycles.

After the completion of the repeated loading, each specimen was loaded statically to failure. The formation and behavior of cracks were similar to those observed in specimens under static loading, except that the length of the cracks appeared to increase during the repeated loading, particularly for specimens having a/d ratios of 0.50 and 0.75.

The results of all the specimens subjected to repeated loading are given in Table VIII and Table IX.

4.2.2 Vertical Loading Only

For specimens without compression reinforcement, Figure 17 shows typical load-displacement curves obtained during the repeated loading at the end of the 1st, 10th, 100th, 1000th, 10,000th, and 100,000th

TABLE VIII

TEST RESULTS FOR REPEATED LOAD SERIES--VERTICAL LOAD ONLY

Speci-men	a/d	ρ_s, %	Loads: Repeated: $V'_{(min)}$,[1] kips	$V'_{(max)}$,[1] kips	Static: V'_y,[1] kips	V'_u,[1] kips	v_y, ksi	v_u, ksi	Type of Failure
A2	0.31	0.45	25.0	75.0	82.5	132.5	0.85	1.37	Shear
A4	0.31	0.83	30.0	90.0	107.5	161.5	1.20	1.68	Shear
A5	0.31	0.83	30.0	90.0	---[2]	---[2]	---[2]	---[2]	Fatigue
A8	0.31	1.30	32.0	96.0	160.0	211.5	1.68	2.22	Shear
B8[3]	0.31	1.30	32.0	96.0	207.5	236.0	2.18	2.48	Shear
C2	0.50	0.83	23.0	69.0	87.5	119.5	0.91	1.25	Shear
C4	0.75	0.83	17.0	51.0	66.5	83.0	0.69	0.87	Shear
C6[3]	0.31	0.83	32.0	96.0	110.0	171.0	1.15	1.78	Shear
C8[3]	0.75	0.83	17.0	51.0	62.5	79.0	0.65	0.82	Shear
D6	0.50	1.25	29.0	87.0	137.5	155.5	1.43	1.62	Shear
D8	0.75	1.25	23.0	69.0	90.0	99.5	0.94	1.04	Shear

[1]Total load for both corbels in each specimen.

[2]Main reinforcement of specimen fractured during repeated loading at about 390,000 cycles.

[3]Specimen had two No. 3 compression reinforcement in each corbel.

TABLE IX

TEST RESULTS FOR REPEATED LOADS--COMBINED LOADS

			Loads									
			Repeated			Static						
Specimen	a/d	ρ_s, %	$V'_{(min)}$,[1] kips	$V'_{(max)}$,[1] kips	H_R,[2] kips	V'_y,[1] kips	V'_u,[1] kips	H_u, kips	$\frac{H_u}{V_u}$[3]	v_y, ksi	v_u, ksi	Type of Failure
B2	0.31	0.45	13.0	40.0	9.75	45.0	70.0	16.3	0.46	0.47	0.72	F.T.[4]
B4	0.31	0.83	19.0	57.0	14.25	58.8	97.0	22.5	0.46	0.61	1.01	F.T.[4]
B6	0.31	1.30	32.0	96.0	20.00	146.3	175.0	20.0	0.23	1.52	1.84	Shear
D2	0.50	0.83	12.0	36.0	9.00	53.0	70.0	17.5	0.50	0.55	0.73	Shear
D4	0.75	0.83	10.0	30.0	7.50	34.0	38.0	9.0	0.47	0.35	0.40	Shear

[1]Total load for both corbels in each specimen.

[2]H_R represents horizontal tensile force during its repeated loading.

[3]F.T. represents flexural tension.

[4]Average load for a corbel in each specimen.

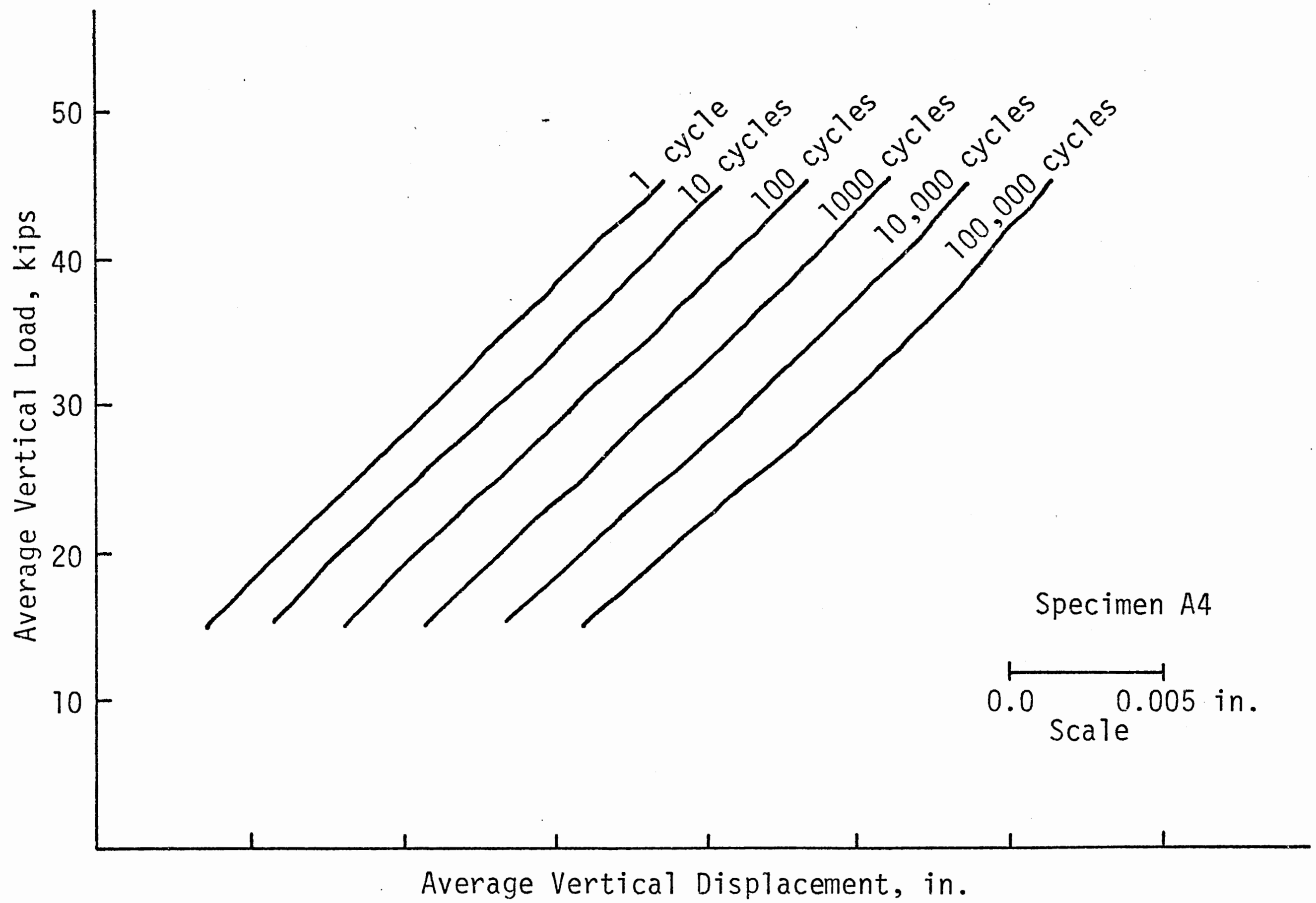

(a) Vertical Load-Vertical Displacement Curve

Figure 17. Load-Displacement Relationship During Repeated Loading (Vertical Loads Only)

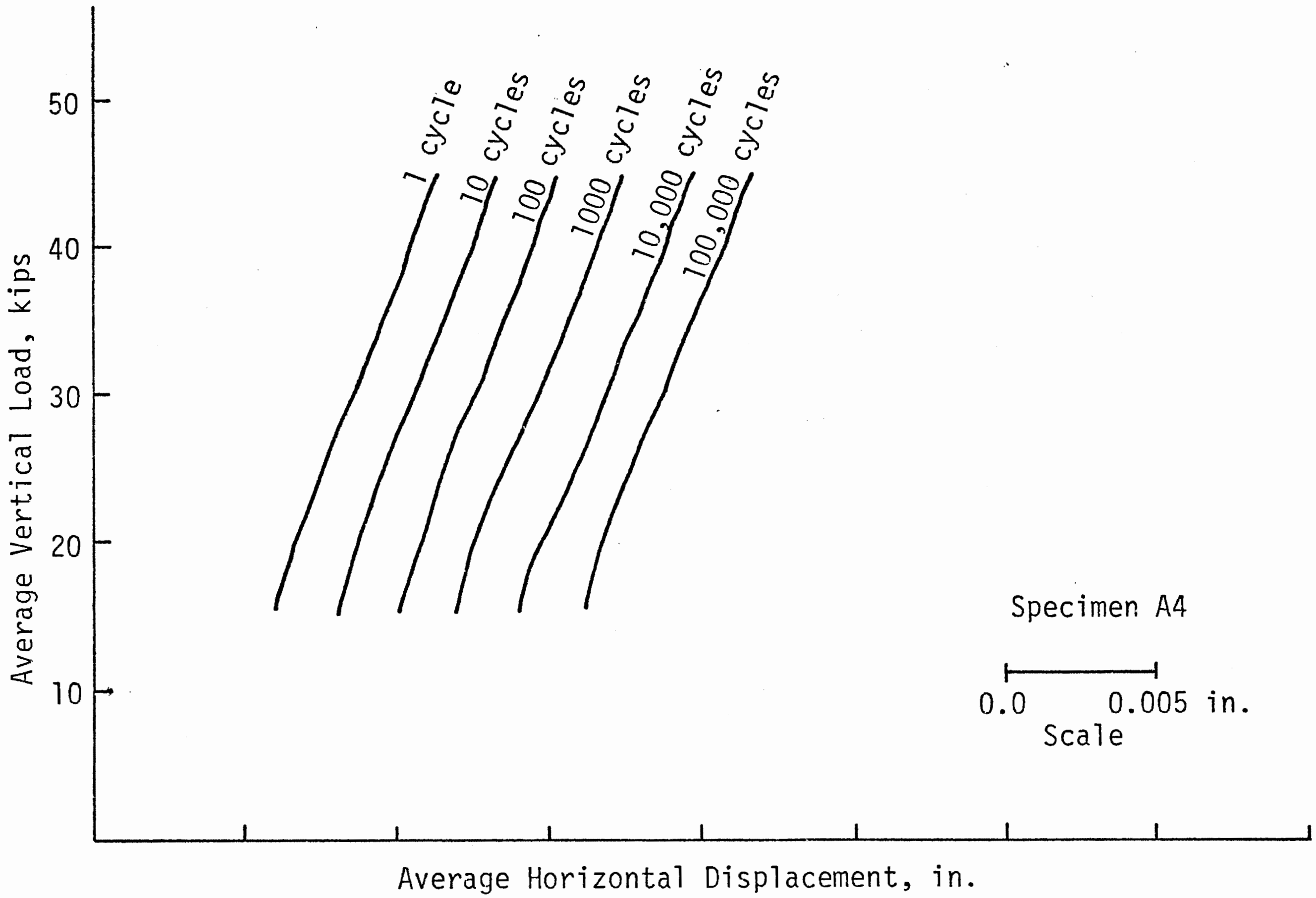

(b) Vertical Load-Horizontal Displacement Curve

Figure 17. (Continued)

cycle. A study of the slopes of the curves indicate that there was negligible change in the shear stiffness.

The vertical load-vertical displacement curves obtained for specimens with compression reinforcement were different from those for specimens without compression reinforcement. There was a crimp in each vertical load-vertical displacement curve, as depicted in Figure 18; it resulted from the presence of the compression reinforcement. However, the crimp seemed to be less pronounced as the number of load cycles was increased.

In Tables X and XI the results of specimens subjected to repeated loading are compared with those of their companion specimens subjected to static loading only. A study of Table X and Figure 19 shows that for specimens with a/d ratios of 0.31 and 0.50, there was a slight increase in the ultimate shear strength after the repeated loading. However, for those with a/d ratio of 0.75, there was a reduction in strength after the repeated loading.

In the case of specimens with compression reinforcement, Table XI shows that the repeated loading had a slightly adverse effect on the ultimate shear strength of all the specimens. The largest reduction in shear capacity occurred in specimen C8 with a/d ratio of 0.75.

4.2.3 Combined Loading

With the exception of specimen B6, the horizontal load was maintained fairly constant at approximately 60 percent of the ultimate horizontal tensile force obtained from companion specimens, while the vertical load was repeated. In the case of specimen B6, the horizontal load was maintained at 20 kips.

TABLE X

INFLUENCE OF REPEATED LOADS--VERTICAL LOADING ONLY
(SPECIMENS WITHOUT COMPRESSION REINFORCEMENT)

Speci-men	a/d	ρ_s, %	v_{us},[1] ksi	v_{ur},[2] ksi	$\frac{v_{ur}^{2}}{v_{us}^{1}}$
A2	0.31	0.45	---	1.37	
A1	0.31	0.45	1.32	---	1.04
A4	0.31	0.83	---	1.68	
A3	0.31	0.83	1.63	---	1.03
A8	0.31	1.30	---	2.22	
A6	0.31	1.30	2.00	---	1.11
A7	0.31	1.30	2.28	---	0.97
C2	0.50	0.83	---	1.25	
C1	0.50	0.83	1.23	---	1.02
C4	0.75	0.83	---	0.87	
C3	0.75	0.83	0.92	---	0.94
D6	0.50	1.25	---	1.62	
D5	0.50	1.30	1.54	---	1.05
D8	0.75	1.25	---	1.04	
D7	0.75	1.25	1.21	---	0.86

[1]Shear stress of specimen subjected to static loading only.

[2]Shear stress of specimen subjected to repeated loading.

TABLE XI

INFLUENCE OF REPEATED LOADS--VERTICAL LOADING ONLY
(SPECIMENS WITH COMPRESSION REINFORCEMENT)

Specimen	a/d	ρ_s, %	v_{us},[1] ksi	v_{ur},[2] ksi	$\frac{v_{ur}^{2}}{v_{us}^{1}}$
B8	0.31	1.30	---	2.48	
B7	0.31	1.30	2.56	---	0.97
C6	0.31	0.83	---	1.78	
C5	0.31	0.83	1.84	---	0.97
C8	0.75	0.83	---	0.82	
C7	0.75	0.83	0.89	---	0.92

[1]Shear stress of specimen subjected to static loading only.

[2]Shear stress of specimen subjected to repeated loading.

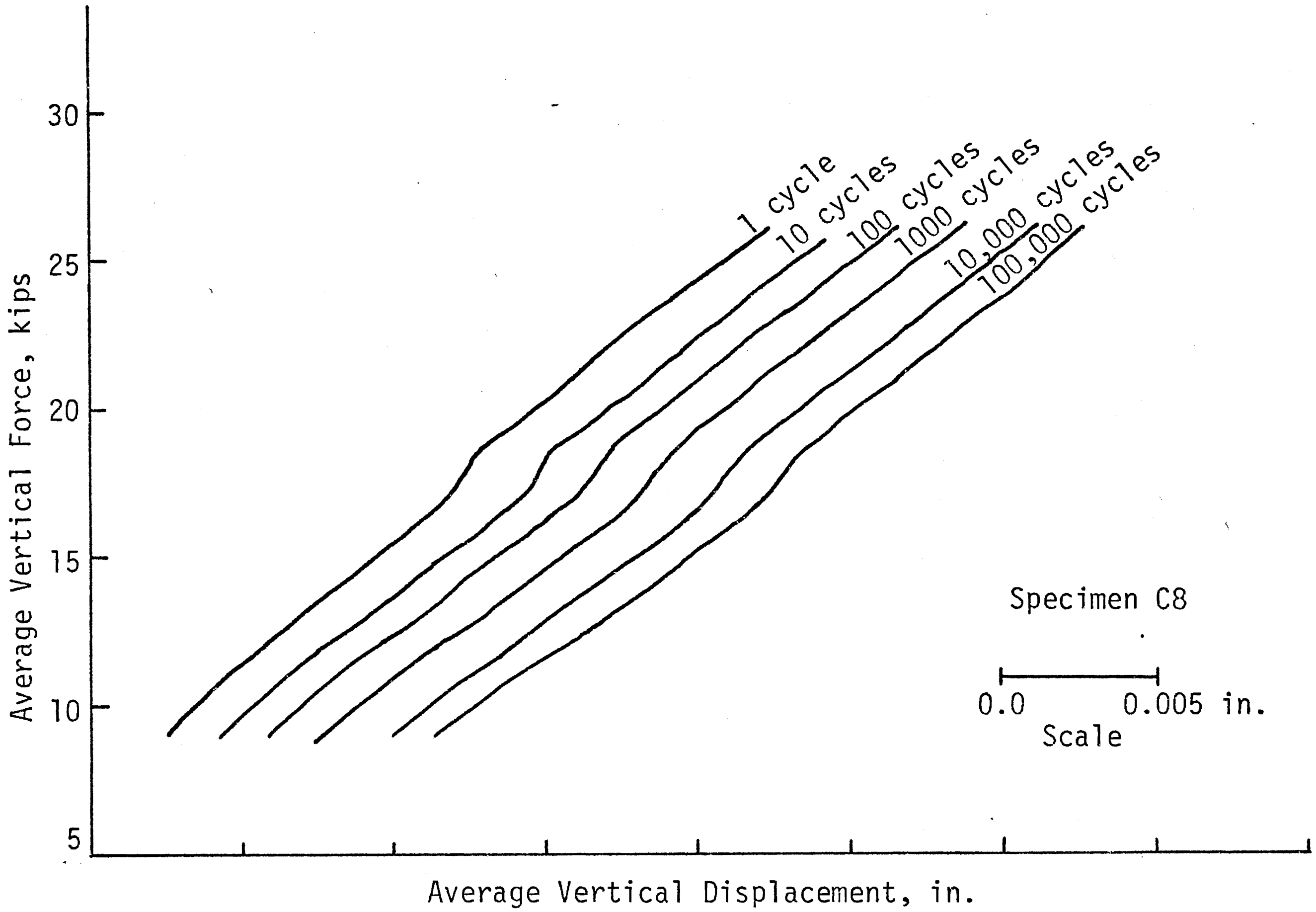

Figure 18. Vertical Load-Vertical Displacement Relationship During Repeated Loading of Specimen With Compression Reinforcement (Vertical Loads Only)

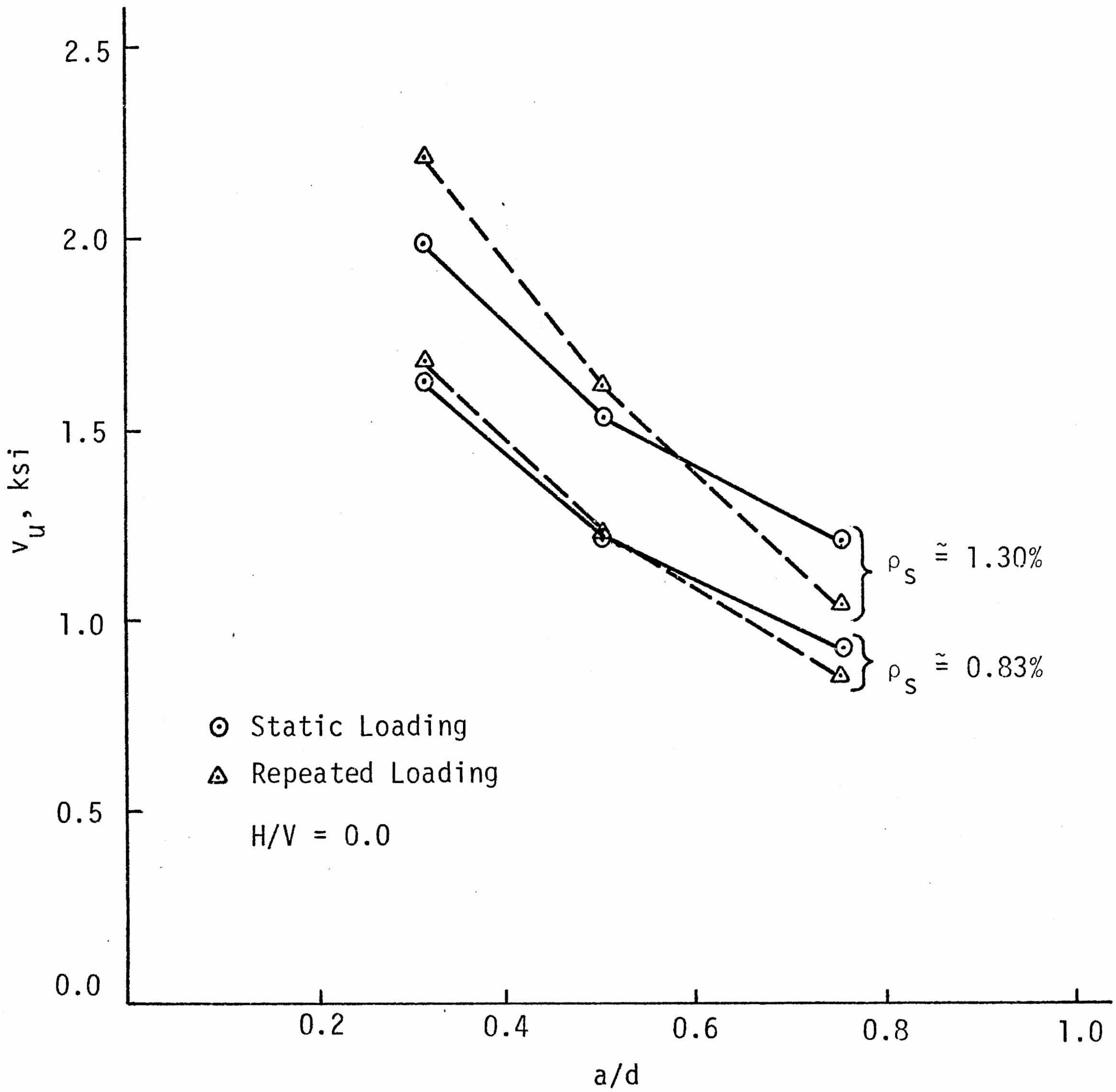

(a) Vertical Loads Only

Figure 19. Influence of Repeated Loading

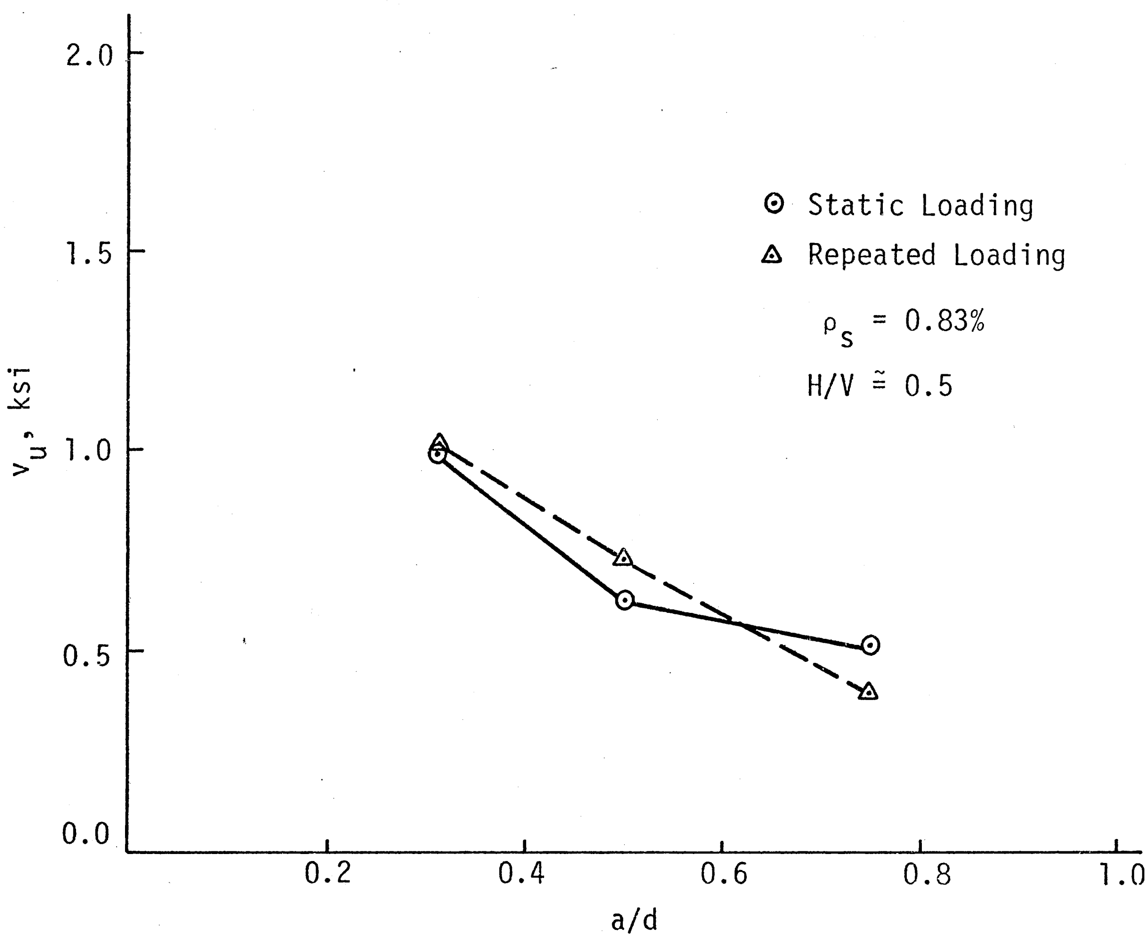

(b) Combined Loads

Figure 19. (Continued)

During the repeated loading the horizontal load in each specimen except B6 showed a slight increase during the unloading stage. The average of the maximum increases in the horizontal loads was found to be approximately 350 lbs and occurred at the beginning of the load stage; this increase was caused by the system of horizontal loading.

Figure 20 shows typical load-displacement curves. A study of the slopes of the curves indicates again that there was very little or no change between the shear stiffness at the end of the first cycle and that at the end of 100,000 cycles.

In Table XII the results of specimens subjected to combined repeated loading are compared with those of specimens subjected to combined static loading. Table XII and Figure 19(b) show that again the specimens with a/d ratios of about 0.31 and 0.50 resisted higher shear loads after the application of repeated loads. Also, the capacity of specimen D4 with a/d ratio of 0.75 was lower than that of the companion specimen D3 which was subjected to combined loading only. The higher H/V ratio for specimen D4 could have contributed to its lower shear strength.

TABLE XII

INFLUENCE OF REPEATED LOADS--COMBINED LOADING

Speci-men	a/d	ρ_s, %	H/V	v_{us},[1] ksi	v_{ur},[2] ksi	$\frac{v_{ur}^{2}}{v_{us}^{1}}$
B2	0.31	0.45	0.46	---	0.72	
B1	0.31	0.45	0.49	0.68	---	1.06
B4	0.31	0.83	0.46	---	1.01	
B3	0.31	0.83	0.47	0.99	---	1.02
B6	0.31	1.30	0.23	---	1.84	
B5	0.31	1.30	0.24	1.78	---	1.03
D2	0.50	0.83	0.50	---	0.73	
D1	0.50	0.83	0.50	0.63	---	1.17
D4[3]	0.75	0.83	0.47	---	0.40	
D3	0.75	0.83	0.40	0.51	---	0.78

[1]Shear stress of specimen subjected to static loading only.

[2]Shear stress of specimen subjected to repeated loading.

[3]Specimen appeared to be damaged slightly during repeated loading test When a temporary power failure occurred.

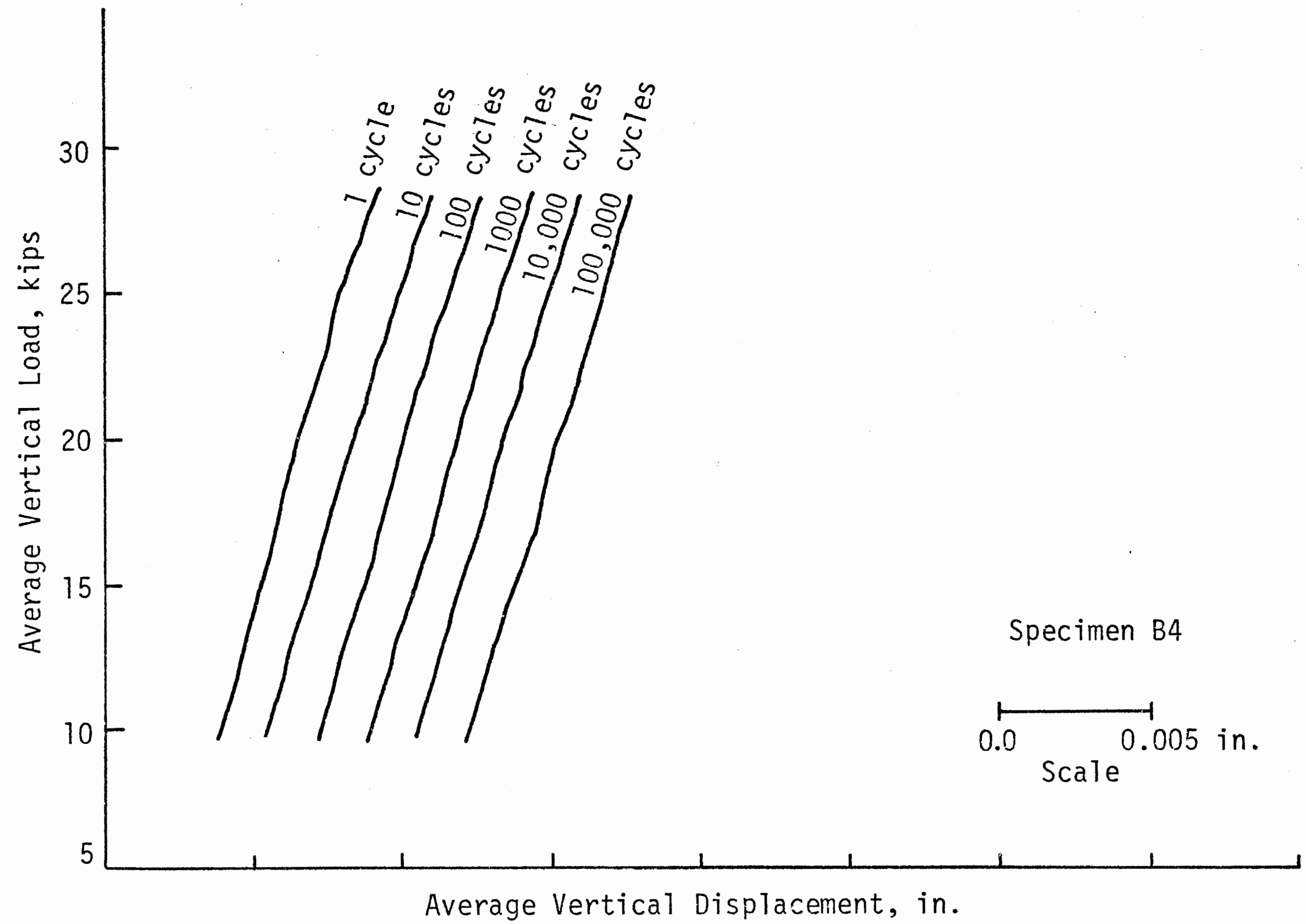

(a) Vertical Load-Vertical Displacement Curve

Figure 20. Load-Displacement Relationship During Repeated Loading (Combined Loads)

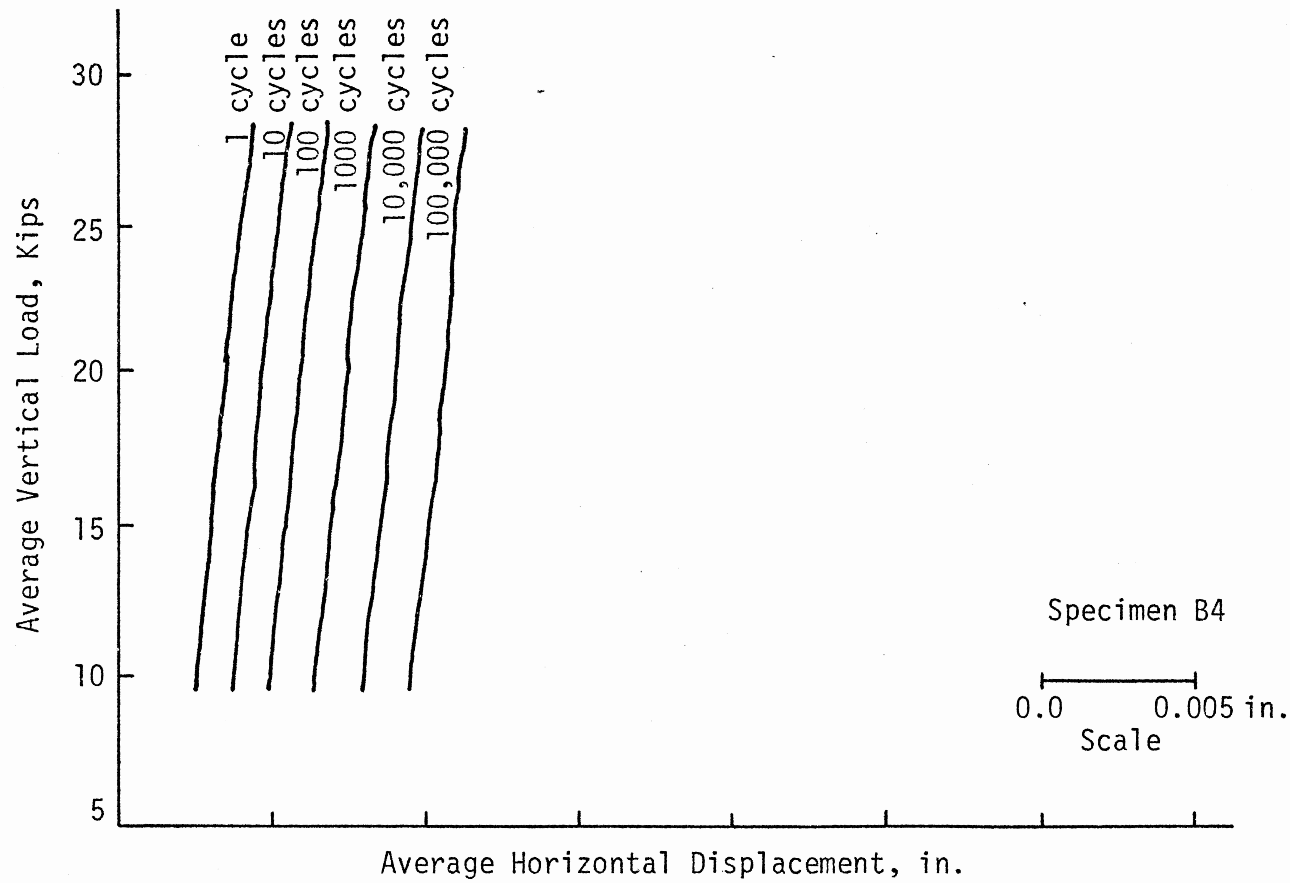

(b) Vertical Load-Horizontal Displacement Curve

Figure 20. (Continued)

CHAPTER V

ANALYSIS AND DISCUSSION OF RESULTS

5.1 Behavior

The load-displacement curves obtained in this study clearly indicated that during the loading each specimen behaved linearly until the strain in the main tension reinforcement was at or near the yield strain, at which time nonlinear behavior began and continued until failure.

The shear stress (v_y) at which nonlinear behavior of a corbel began appeared to be influenced by the main tension reinforcement ratio (ρ_s). The ratios of yield stress-to-ultimate stress (v_y/v_u) were then scrutinized. The mean and standard deviations were determined for each of the reinforcement ratios investigated. For main tension reinforcement ratios of 0.43-0.45, 0.83-0.88, and 1.25-1.30 percent, the means of the v_y/v_u ratios were 0.66, 0.74 and 0.88, respectively, with their corresponding standard deviations being 0.044, 0.076 and 0.067. Therefore, at higher values of ρ_s, the yield stress approached the ultimate stress and a more sudden and explosive failure was observed; the higher the reinforcement ratios, then, the more brittle was the behavior of the corbel.

As shown in Tables IV, VII, VIII, and IX, there were two primary failures--shear and flexural tension; secondary failures (bearing and corbel-end failures) were prevented by complying with the requirements of the ACI Code (14).

Shear failure was characterized, in most cases, by the formation of a series of short diagonal tension cracks and concrete struts between the cracks in the vicinity of the column-corbel interface. The final failure was by shearing along the weakened plane. For specimens with a/d of 0.31 and 0.50 the plane of failure was formed by a crack from either the inside edge or the middle of the bearing plate to the intersection of the column and the sloping face of the corbel. For specimens with a/d of 0.75 the plane of failure was formed by the crack from the inside edge of the bearing plate to the intersection of the column and the sloping face of the corbel. In a few cases of specimens with low a/d ratio, an increase in the flexural crack width accompanied the shear failure.

Flexural tension failure resulted from excessive yielding of the main tension reinforcement and was followed by crushing of the concrete at the intersection of the column and the sloping face of the corbel. This type of failure occurred only in specimens subjected to combined loading, and was characterized by very wide flexural cracks.

5.2 Compression Reinforcement

In their study of normal weight concrete corbels, Kriz and Raths (4) determined that compression reinforcement had no influence on the ultimate strength of corbels. This result was due, to a very large extent, to the type of aggregate used in the concrete mix because the compressibility of concrete is influenced by that of the aggregate.

The internal structure of lightweight aggregate makes lightweight concrete more compressible than normal weight concrete made with gravel. Hence the existence of compression reinforcement in a corbel was expected to improve the compression resistance of the lightweight concrete. Consequently, the ultimate strength of the corbel with compression reinforcement was expected to be increased, particularly those with high reinforcement ratios, by prevention of premature compression failure.

As expected, the specimens with compression reinforcement and low shear span-to-effective depth ratios (a/d) exhibited increases in shear strength of between 10 and 30 percent, as shown in Table V. However, for higher a/d ratios the compression reinforcement had no influence on the shear capacity of the corbel because of the large angle of inclination of the compression steel to the vertical.

In Figure 21 the load-displacement curves for specimen B7 with compression reinforcement are compared with those of companion specimen A7 without compression reinforcement. A study of Figure 21 shows that the slope of the vertical load-horizontal displacement curve is not affected by the presence of the compression reinforcement. On the contrary, the slope of the vertical load-vertical displacement curve as depicted in Figure 21(b) is affected by the presence of compression reinforcement. Also, the presence of the compression reinforcement appeared to increase the ductility of the corbel, as shown in Figure 21(a).

The results of this portion of the investigation suggest that compression reinforcement in corbels made of lightweight concrete has beneficial effect on the shear strength of corbels, particularly with small a/d ratios.

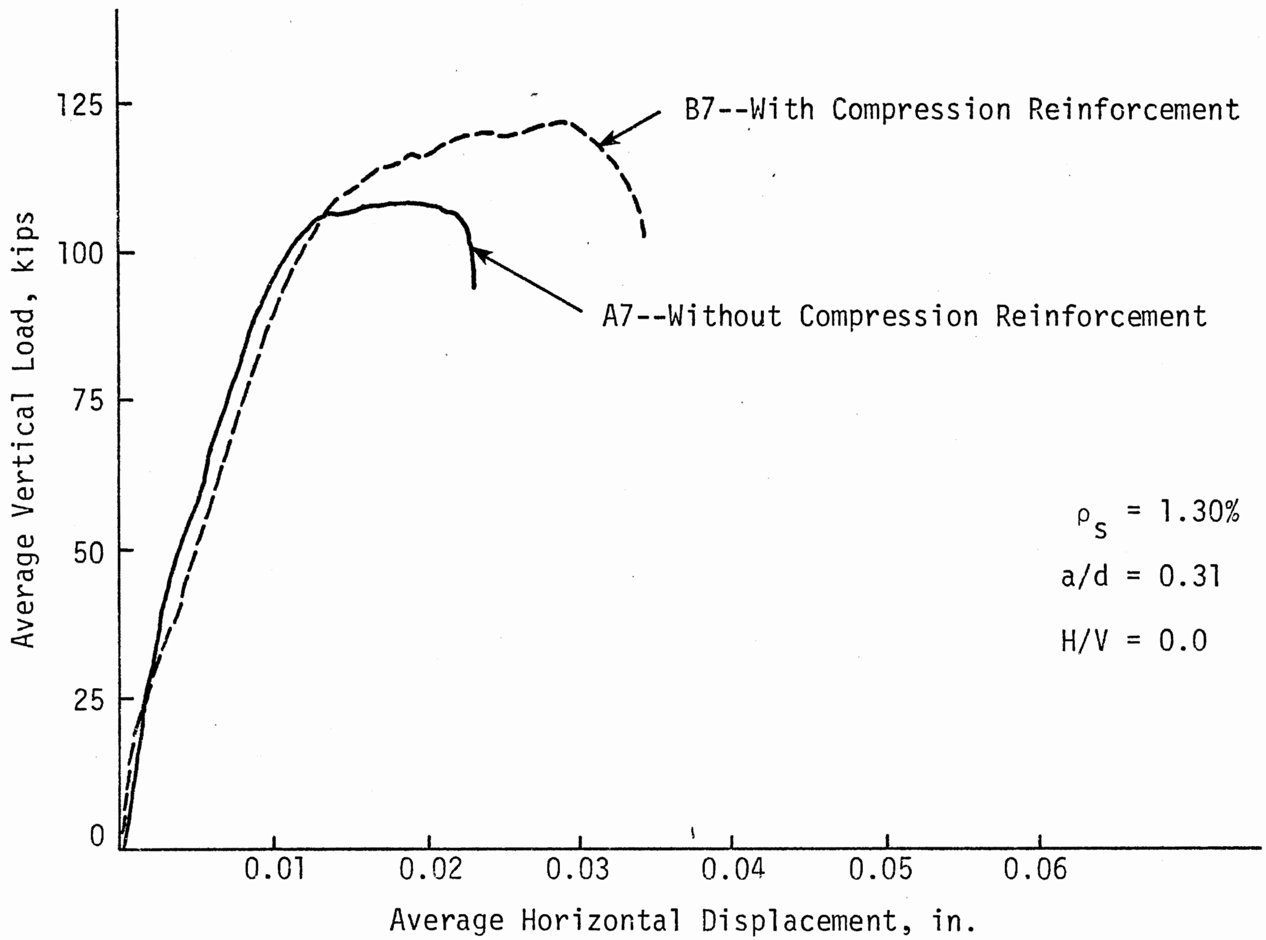

(a) Vertical Load-Horizontal Displacement Curve

Figure 21. Influence of Compression Reinforcement

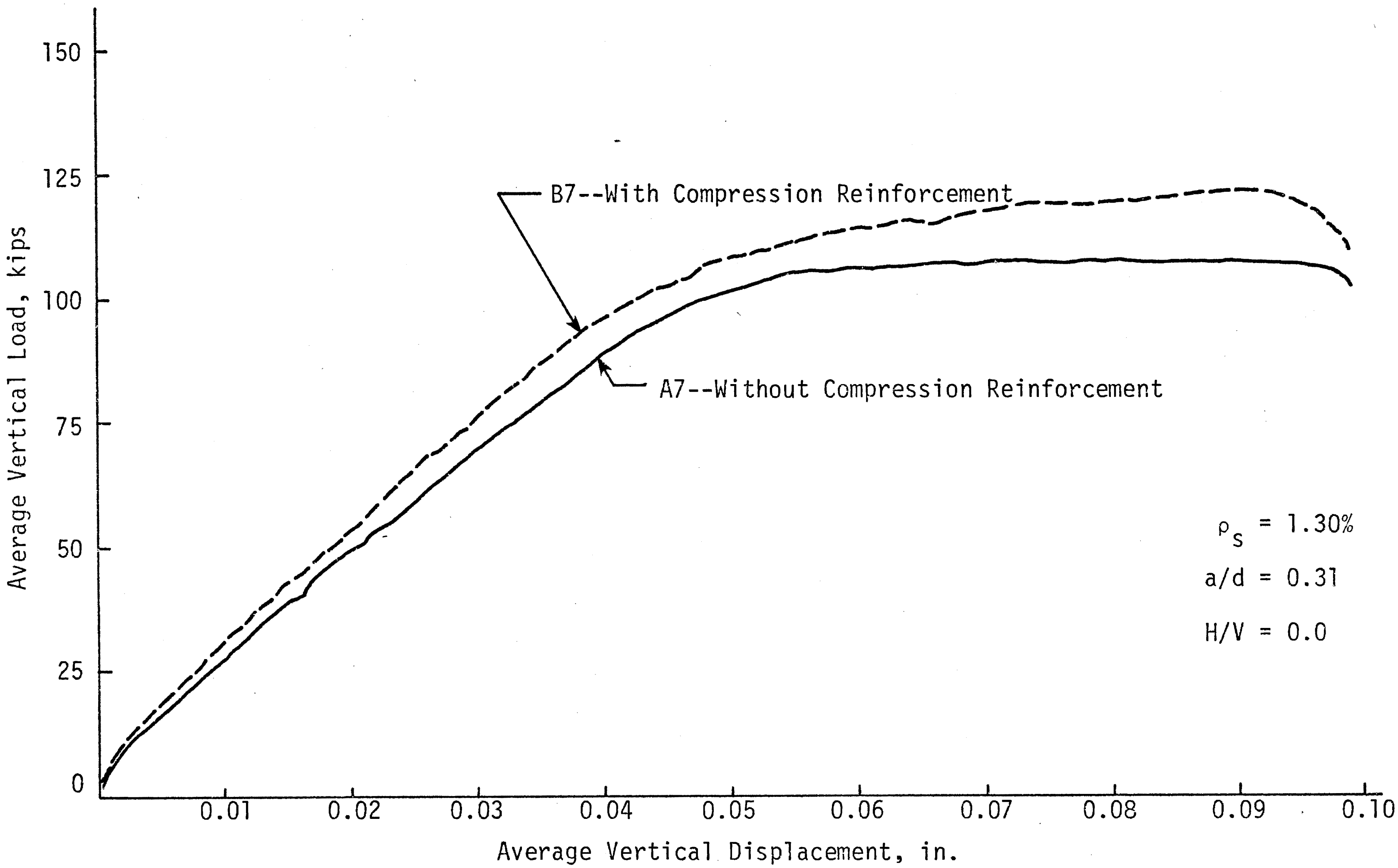

(b) Vertical Load-Vertical Displacement Curve

Figure 21. (Continued)

5.3 Size of Specimens

In most investigations in which smaller scale specimens have been studied, the results of the smaller specimens frequently differed from those of larger specimens. As a result, four larger specimens were tested to determine the influence of size on the results. In Table VI the ultimate shear stresses of companion specimens are compared in terms of the ratios of the shear stress of the smaller specimens to those of their companion larger specimens. The mean of these ratios was found to be 1.003 with a standard deviation of 0.010.

The results of the above comparisons indicated that size did not have any influence on the results and that a size factor of 1.0 is appropriate in this study. Hence any design equations and suggestions obtained from the analyses of the data from the smaller specimens should be applicable to larger specimens without any modification.

5.4 Reinforcement Ratio

The main tension reinforcement ratios considered in this investigation were within the limits required by the ACI Code (14). Furthermore, the area of the horizontal stirrups in each corbel was at least one-half that of the main tension steel. Figure 14 shows that within the limits of reinforcement ratios considered, an approximately linear relationship exists between the shear stress and the main tension reinforcement ratio. However, it is possible to have a nonlinear relationship at higher reinforcement ratios. Hence the results from this investigation should be applied with caution when the main reinforcement ratio is outside the present range of consideration.

5.5 Shear Span--Effective Depth Ratio

The shear transfer mechanism in concrete (2), in concrete brackets (4) (16) (25) (26) (27), and in composite and deep beams (22) (33) is influenced by the shear span-to-effective depth ratio (a/d). In their investigation of all-lightweight concrete corbels, Mattock, Chen and Soongswang (16) derived the linear Equation (2.18) to represent the relationship between the ultimate shear stress and the a/d ratio for all-lightweight concrete corbels. Equation (2.18) was based on the results of push-off studies (3) and those of all-lightweight concrete corbels subjected to equal, combined static loading (i.e., H/V = 1.0). In addition, four of the six specimens used in the study (16) did not experience yielding of their main tension reinforcement. However, the linear Equation (2.18) was also proposed for the design of sanded-lightweight concrete corbels.

Figure 22 indicates that the relationship between ultimate shear stress and a/d ratio is more of a nonlinear curve instead of a straight line. A study of Figure 22 reveals that any slight increase in the a/d ratio substantially reduces the ultimate shear strength of the corbel at lower a/d ratios. At higher a/d ratios the amount of reduction, as a result of an increase in a/d ratio, decreases. This suggests that corbels with small a/d ratios should be used to take advantage of the high shear capacities at low a/d ratios.

5.6 Repeated Loading

In almost all applications of a concrete corbel the loading does not remain constant but instead fluctuates between dead load and service load. The intensity and duration of the repeated loads depend on the

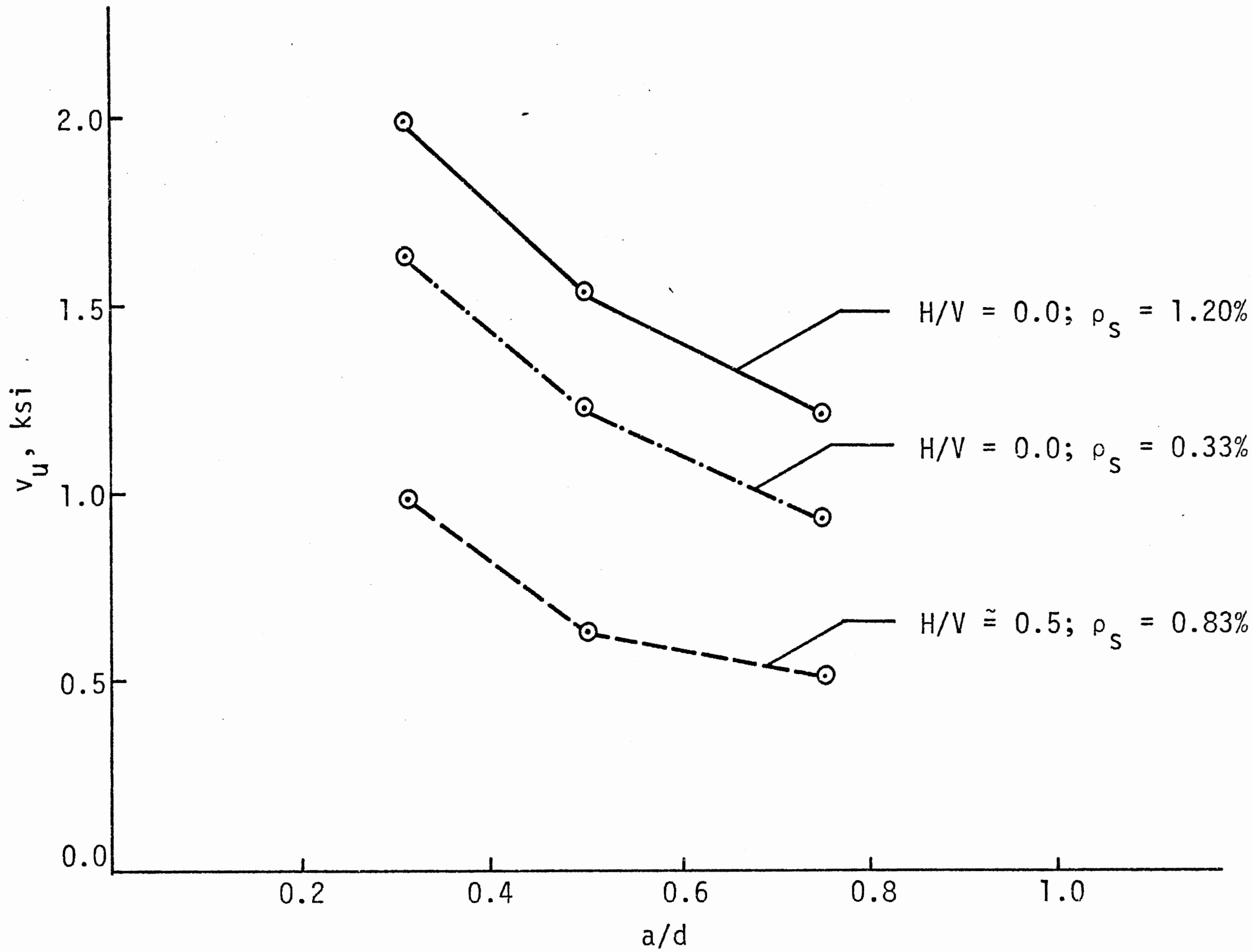

Figure 22. Influence of Shear Span-to-Effective Depth Ratio (Static Loading)

type or place of application: during an earthquake a corbel might experience high intensity but short duration repeated loads.

The shear capacity of fully cracked concrete through aggregate interlock is substantially influenced by the characteristics of the cracked surfaces. Under repeated loading the degree of cracked surface roughness is reduced, resulting in a partial or complete destruction of the load transfer mechanism. Although the corbels used in this study were not fully cracked prior to the repeated loading, it was expected that the application of repeated loads would reduce the shear capacity of all corbels regardless of other test parameters.

The results show that all specimens with compression reinforcement, as expected, experienced a slight reduction in strength after the repeated loading regardless of ρ_s and a/d ratios. The biggest reduction in strength occurred in the specimen with a/d ratio of 0.75, as shown in Table XI. In spite of this reduction in shear capacity after the repeated loading, the specimens with compression reinforcement showed higher ultimate strength than any of their companion specimens without compression reinforcement, except when the a/d ratio was 0.75. Hence for lower a/d ratios, compression reinforcement could be very beneficial to the load transfer capacity of the corbel under either static or repeated loading.

In the case of specimens without compression reinforcement the results indicated, contrary to expectations, that when subjected to either vertical loading only or combined loading, there was a slight increase in the shear strength after the repeated loading for a/d of 0.31 and 0.50; there was a decrease in strength for a/d ratios of 0.75 (Figure 19). The capacities of specimens with a/d of 0.75 that were subjected to repeated load were reduced, on the average, by approximately 12.8 percent after the application of the repeated loads.

An examination of the crack patterns showed that for specimens with a/d of 0.31 and 0.50 a considerable number of diagonal tension cracks formed before the failure load was achieved. As a result, the plane of failure was not well defined. However, for specimens with a/d of 0.75, fewer diagonal tension cracks formed in addition to the first one that was observed closer to the compression zone of the corbel. The additional flexural crack which started at the inside edge of the bearing plate propagated rapidly into the compression zone and, at failure, linked with the first diagonal tension crack to establish the plane of failure more distinctly. It is therefore possible that the repeated loads might have had a more damaging effect on the plane of failure for the specimens with a/d of 0.75.

However, there appeared to be no lucid explanation for the increase in shear strength observed after the repeated loading in corbels with low a/d ratios.

A close study of Figure 19(a) shows that the critical value of the a/d ratio beyond which the repeated loading adversely affects the shear strength of the corbel is influenced by the reinforcement ratio: the higher the reinforcement ratio, the higher the critical a/d ratio. Figure 19(b) shows that the critical value of the a/d ratio is higher for specimens under combined loading. As a result, the safe critical value of a/d appears to be approximately 0.50. Hence when a corbel is used in places where repeated loadings are inevitable, the a/d ratio should be limited to 0.50.

The performance of a structural member is not only influenced by the range and the mean value of the repeated loading, but also by the maximum value of the repeated loads. In this study the repeated loading was varied between 0.20 V_u and 0.60 V_u in most cases. Also, an examination of Tables VIII and IX shows that in each specimen the maximum value of the repeated load did not exceed the load at which the nonlinear behavior of the specimen started. This indicates that the repeated load occurred within the elastic range of each specimen. The results of this study therefore exhibit the performance of the specimens when subjected to repeated service loads. If, however, the maximum value of the repeated loads had exceeded the yield loads, different strength and behavior might have resulted.

5.7 Existing Design Methods

From a design standpoint it is necessary to determine how well the present design provisions predict the strength of the corbels in this study. For purposes of comparison, the shear-friction Equation (2.20) has to be modified to account for the type of concrete. When the reduction capacity ϕ is taken as unity, the coefficient of friction μ is multiplied by 0.85 as proposed by Mattock (17), and the term $\rho_v f_{vy}$ is replaced by $[(\rho_s f_{sy} - N_u/bd) + \rho_h f_{hy}]$ to account for the horizontal force N_u; Equation (2.20) thus becomes

$$v_u = (0.85\ \mu)[(\rho_s f_{sy} - N_u/bd) + \rho_h f_{hy}]. \tag{5.1}$$

The test results were compared with the ultimate strengths predicted by Equation (2.19) and (5.1) which represent the current design expressions of section 11.14 and the modified form of section 11.15 of the ACI

Code (14). By using Equations (2.19) and (5.1) the two different values of the ultimate shear stresses $(v_u)_1$ and $(v_u)_2$ were respectively calculated. In Table XIII these calculated values are compared with the test results. A study of the ratios $v_{u(test)}/(v_u)_1$ indicates that Equation (2.19) can be applied to the design of sanded-lightweight corbels.

It is of interest to note that Equation (2.19) is a conservative modification of Equations (2.5) and (2.6) proposed by Kriz and Raths (4), whose investigation involved a majority of corbel specimens without stirrups. However, for specimens with stirrups, Kriz and Raths found that by using Equations (2.5) and (2.6) the mean and standard deviation of $v_{u(test)}/v_{u(calc)}$ were 1.11 and 0.08, respectively, when H/V = 0.0; when H/V = 0.5, the mean and standard deviation were 1.42 and 0.32.

The shear-friction Equation (5.1) with a modified coefficient of friction appears to be useful, particularly for low a/d and reinforcement ratios. The $v_{u(test)}/(v_u)_2$ ratios in Table XII indicate that at higher reinforcement ratios and also at higher a/d ratios the shear-friction theory becomes unconservative.

Recently, Mattock, Chen and Soongswang (16) and Mattock (17) proposed the use of the modified shear-friction expression for the design of lightweight concrete corbels. For sanded-lightweight concrete the shear stress was expressed as

$$v_u = 0.8\, \rho_v f_{vy} + 250 \text{ psi} \tag{5.2}$$

but not greater than (0.2 - 0.07 a/d) f'_c, nor (1000 - 350 a/d). For the purpose of analysis the term $\rho_v f_{vy}$ will be replaced by $[(\rho_s f_{sy} - N_u/bd) + \rho_h f_{hy}]$ to account for the horizontal tensile force N_u. The design shear stress then becomes the smallest of the following:

TABLE XIII

COMPARISON OF TEST RESULTS WITH CALCULATED VALUES USING EXISTING AND PROPOSED DESIGN EQUATIONS

Specimen	a/d	ρ_v[1]	ρ_s,[2] %	$v_{u(test)}$, ksi	$(v_u)_1$, ksi	$(v_u)_2$, ksi	$(v_u)_3$, ksi	$\frac{v_{u(test)}}{(v_u)_1}$	$\frac{v_{u(test)}}{(v_u)_2}$	$\frac{v_{u(test)}}{(v_u)_3}$
Static Loading With H/V = 0										
A1	0.31	0.0091	0.45	1.32	0.72	0.65	0.69	1.83	2.03	1.91
A3	0.31	0.0129	0.83	1.63	0.83	0.89	0.85	1.96	1.83	1.92
A6	0.31	0.0223	1.30	1.99	1.10	1.73	0.89	1.81	1.15	2.24
A7	0.31	0.0223	1.30	2.28	1.10	1.73	0.89	2.07	1.32	2.56
B7[3]	0.31	0.0223	1.30	2.56	1.12	1.71	0.89	2.29	1.50	2.88
C1	0.50	0.0129	0.83	1.23	0.74	0.90	0.83	1.66	1.24	1.48
C3	0.75	0.0129	0.83	0.92	0.62	0.90	0.74	1.48	1.02	1.24
C5[3]	0.31	0.0129	0.83	1.84	0.84	0.90	0.86	2.19	2.04	2.14
C7[3]	0.75	0.0129	0.83	0.89	0.62	0.90	0.74	1.44	0.99	1.20
D5	0.50	0.0223	1.30	1.54	0.95	1.75	0.83	1.62	0.88	1.86
D7	0.75	0.0217	1.25	1.21	0.78	1.51	0.74	1.55	0.82	1.64
Y1[4]	0.31	0.0910	0.43	1.32	0.70	0.63	0.68	1.89	2.09	1.94
Y2[4]	0.31	0.0132	0.88	1.64	0.84	0.89	0.85	1.95	1.84	1.93
Y3[4]	0.31	0.0132	0.88	1.62	0.85	0.89	0.85	1.90	1.83	1.91
Y4[4]	0.50	0.0132	0.88	1.22	0.74	0.89	0.82	1.65	1.37	1.49

TABLE XIII (Continued)

Specimen	a/d	ρ_v	ρ_s,[2] %	$v_{u(test)}$, ksi	$(v_u)_1$, ksi	$(v_u)_2$, ksi	$(v_u)_3$, ksi	$\frac{v_{u(test)}}{(v_u)_1}$	$\frac{v_{u(test)}}{(v_u)_2}$	$\frac{v_{u(test)}}{(v_u)_3}$
Repeated Loading With H/V = 0										
A2	0.31	0.0091	0.45	1.37	0.72	0.65	0.69	1.90	2.11	1.99
A4	0.31	0.0129	0.83	1.68	0.83	0.89	0.85	2.02	1.89	1.98
A5	0.31	0.0129	0.83	---[5]	0.83	0.89	0.85	---	---	---
A8	0.31	0.0223	1.30	2.20	1.10	1.73	0.89	2.00	1.28	2.50
B8[3]	0.31	0.0223	1.30	2.48	1.12	1.71	0.89	2.21	1.45	2.79
C2	0.50	0.0129	0.83	1.24	0.74	0.90	0.83	1.68	1.38	1.49
C4	0.75	0.0129	0.83	0.86	0.62	0.90	0.74	1.39	0.96	1.16
C6[3]	0.31	0.0129	0.83	1.78	0.84	0.90	0.86	2.12	1.97	2.07
C8[3]	0.75	0.0129	0.83	0.82	0.62	0.90	0.74	1.32	0.91	1.11
D6	0.50	0.0217	1.25	1.62	0.94	1.52	0.83	1.72	1.07	1.95
D8	0.75	0.0217	1.25	1.04	0.78	1.45	0.74	1.33	0.72	1.41

TABLE XIII (Continued)

Speci- men	a/d	ρ_s,[2] %	H/V	$v_{u(test)}$, ksi	$(v_u)_1$, ksi	$(v_u)_2$, ksi	$(v_u)_3$, ksi	$\frac{v_{u(test)}}{(v_u)_1}$	$\frac{v_{u(test)}}{(v_u)_2}$	$\frac{v_{u(test)}}{(v_u)_3}$
Static Loading With H/V > 0.0										
B1	0.41	0.45	0.49	0.68	0.32	0.32	0.46	2.13	2.13	1.48
B3	0.31	0.83	0.47	0.99	0.42	0.33	0.47	2.36	3.00	2.11
B5	0.31	1.30	0.24	1.78	0.59	1.25	0.89	3.02	1.42	2.00
D1	0.50	0.83	0.50	0.63	0.35	0.49	0.58	1.80	1.28	1.09
D3	0.75	0.83	0.40	0.51	0.31	0.65	0.69	1.66	0.78	0.74
Repeated Loading With H/V > 0.0										
B2	0.31	0.45	0.46	0.72	0.33	0.32	0.46	2.18	2.25	1.56
B4	0.31	0.83	0.46	1.01	0.42	0.33	0.47	2.40	3.06	2.15
B6	0.31	1.30	0.23	1.84	0.59	1.25	0.89	3.12	1.47	2.07
D2	0.50	0.83	0.50	0.73	0.35	0.46	0.56	2.09	1.59	1.30
D4	0.75	0.83	0.47	0.40	0.30	0.68	0.70	1.33	0.59	0.57

[1] $\rho_v = (A_s + A_h)/bd$.

[2] $\rho_s = 100\ A_s/bd$.

[3] Specimen had two No. 3 bars as compression reinforcement in each corbel.

[4] Larger specimen.

[5] Main tension reinforcement fractured during repeated loading at approximately 390,000 cycles.

$$v_u = 0.8\ [(\rho_s f_{sy} - N_u/bd) + \rho_h f_{hy}] + 250\ \text{psi} \tag{5.3a}$$

or

$$v_u = (0.2 - 0.07\ a/d)\cdot f'_c \tag{5.3b}$$

or

$$v_u = (1000 - 350\ a/d) \tag{5.4c}$$

By using Equation (5.3) the design shear stress $(v_u)_3$ was calculated and compared with the test results. Again, a study of $v_{u(test)}/(v_u)_3$ in Table XIII shows that Equation (5.3) produced conservative results for all specimens, except D3 and D4, subjected to combined loading and with an a/d ratio of 0.75; less conservative results were obtained for specimens under vertical loads only and with an a/d ratio of 0.75. Equation (5.3), however, was obtained from test results of all-lightweight concrete corbels for which the mean and standard deviation of $v_{u(test)}/v_{u(calc)}$ were 1.08 and 0.12, respectively.

5.8 Design Proposal

Based on the relationship between the shear stress and the a/d and ρ_s ratios, and using the data from the static tests with vertical loading only, the ultimate shear stress can be expressed as

$$v_u = e^{(0.96 - 3.11\ a/d)} + 0.78\ \rho_s \tag{5.4}$$

where a/d is the shear span-to-evvective depth ratio, and ρ_s is the percentage of the main tension reinforcement. To provide a lower bound on all data points, Equation (5.4) was modified to

$$v_u = (1 - a/d)[e^{(1 - 3a/d)}] + 0.75\ \rho_s \tag{5.5}$$

In the case of specimens subjected to combined loading, it was difficult to attain a constant H/V ratio of 0.5 for all specimens. Therefore, an average percentage reduction of approximately 45% in shear capacity for H/V of nearly 0.5 was computed. Also, an average percentage reduction of approximately 57% in shear strength for H/V of 1.0 was determined from the results of specimens with stirrup reinforcement from the study of Kriz and Raths (4). Based on these reduction averages in shear capacity, a modification to account for the combined loading could be expressed as

$$\lambda = [1 - H/V\ (1 - 0.4\ H/V)] \tag{5.6}$$

In addition, for a concrete strength different from the average strength of 6.80 ksi used in this investigation, a concrete strength modification factor should be applied. Hence, Equations (5.4) and (5.5) become

$$v_u = \lambda\{e^{(0.96 - 3.11\ a/d)} + 0.78\ \rho_s\}\psi \tag{5.7}$$

$$v_u = \lambda\{(1 - a/d)[e^{(1 - 3a/d)}] + 0.75\ \rho_s\}\psi \tag{5.8}$$

where

$$\psi = \frac{f'_c}{6.80}\ .$$

In Figure 23, Equations (5.7) and (5.8) together with the data from the specimens with vertical loading only have been plotted to depict how conservative Equation (5.8) is.

As stated earlier, the current design provision of section 11.14 of the ACI Code (14) was based on the results from the investigation of Kriz and Raths (4). In Figure 24, therefore, Equations (5.7) and (5.8)

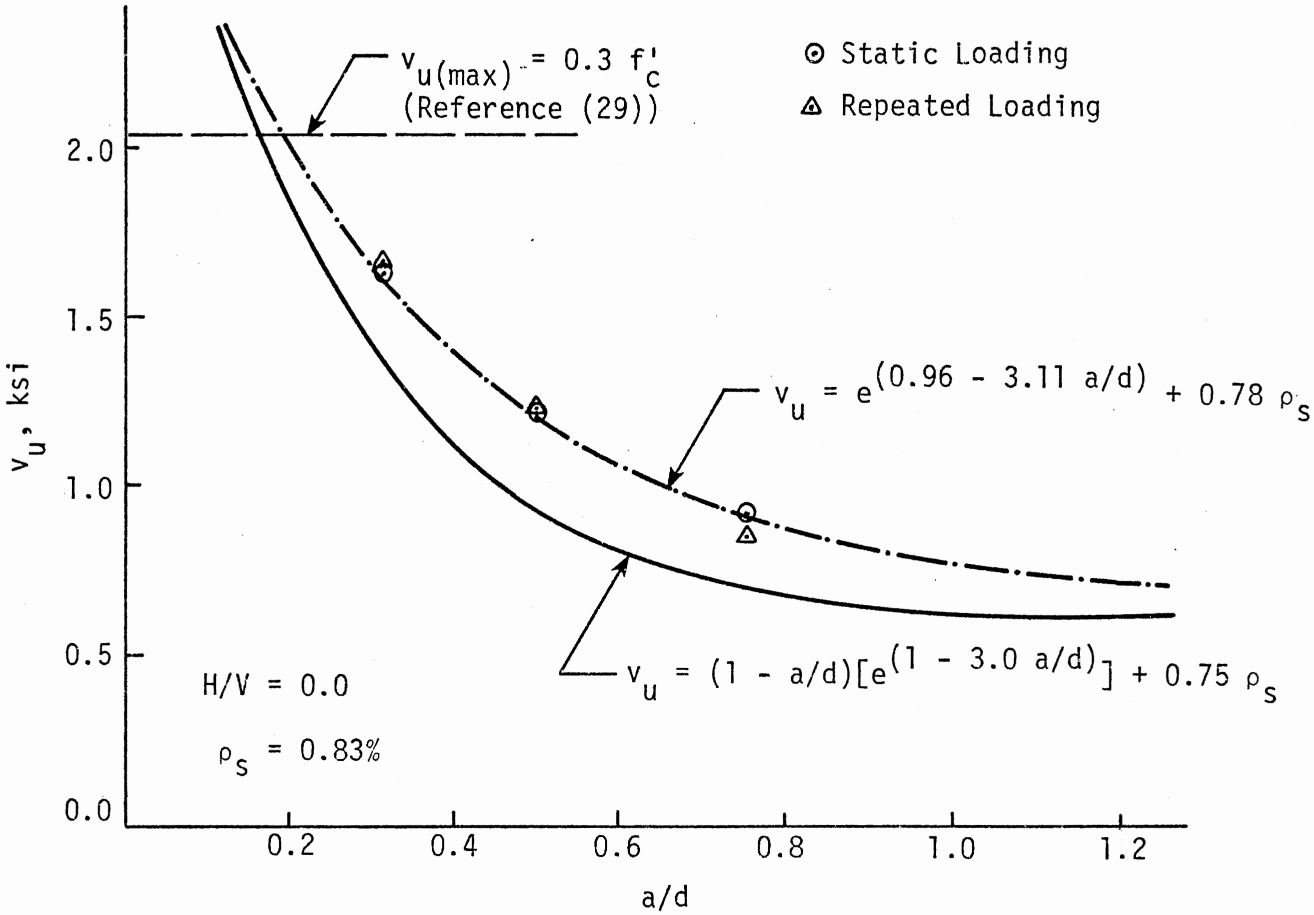

(a) ρ_s = 0.83%, H/V = 0.0

Figure 23. Comparison of Proposed Equations With Test Results

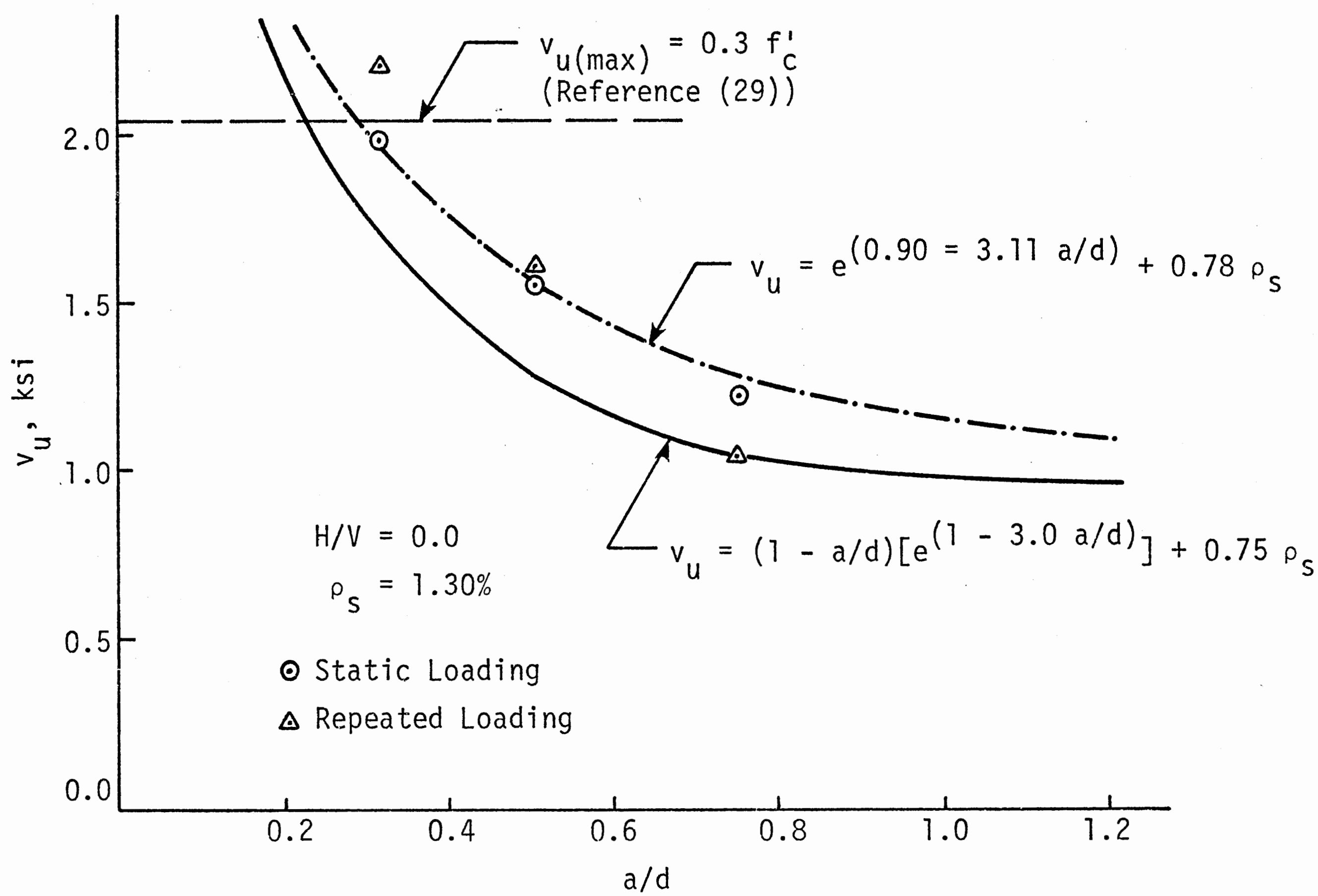

(b) ρ_s = 1.30%; H/V = 0.0

Figure 23. (Continued)

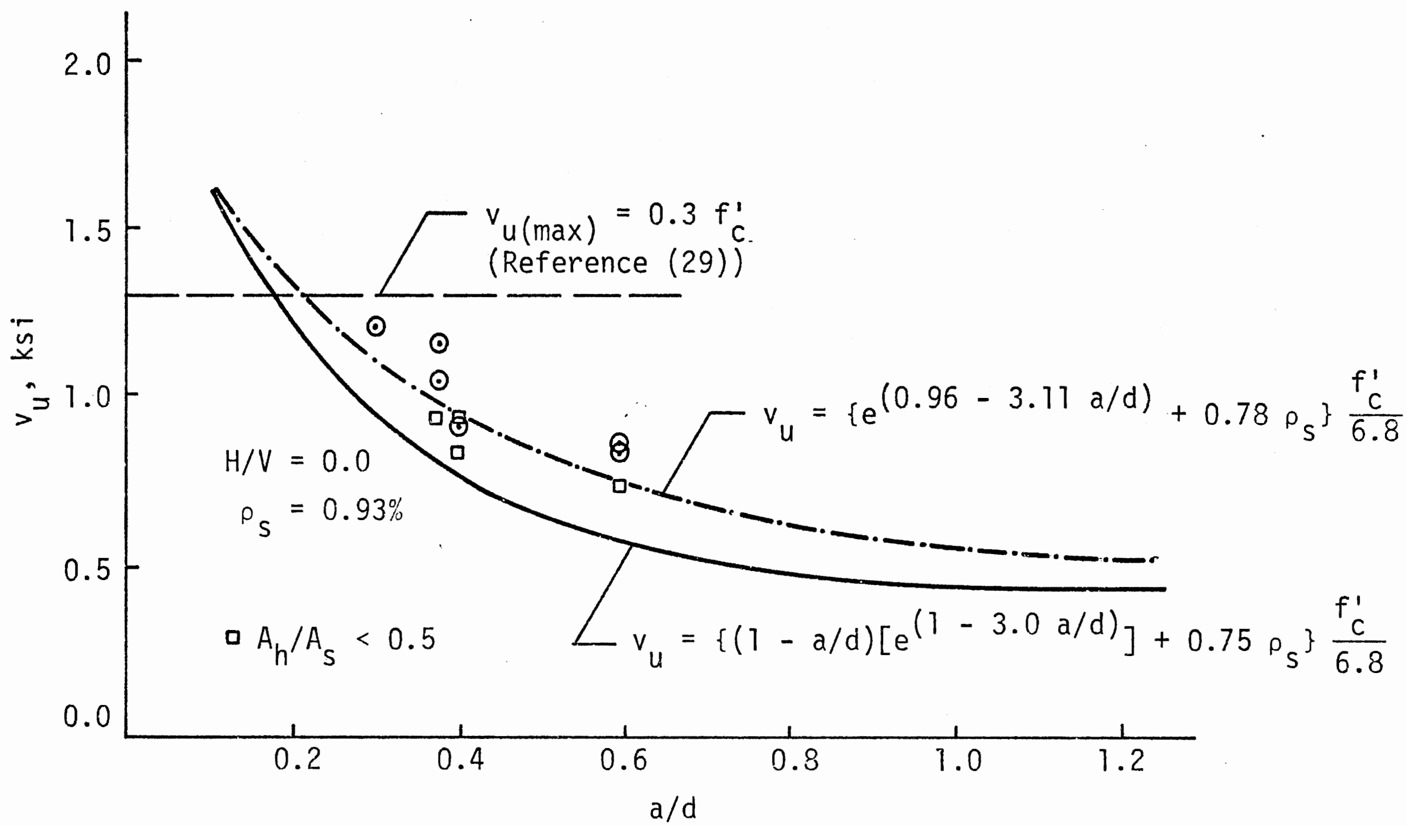

Figure 24. Comparison of Proposed Equations With Results of Kriz and Raths (4) (Specimens With Stirrups)

are compared with the results of specimens with stirrups and subjected to vertical loads only from the study of Kriz and Raths (4). Again, Equation (5.8) proved to be a good lower bound.

From a design standpoint it is necessary to determine how well Equation (5.8) can predict the ultimate shear strength of corbels. Therefore, Equation (5.8) was used to calculate the ultimate shear stress of each corbel in this study. In Table XIV the calculated shear stresses $v_{u(calc)}$ are compared with the corresponding test results $v_{u(test)}$ in the form of ratios. A study of Table XIV indicates that except for specimen D4, the ratio of $v_{u(test)}/v_{u(calc)}$ in each case is greater than unity. The mean of these ratios varies between 1.10 for specimens under combined repeated loading and 1.34 for specimens with compression reinforcement under static loading.

Equation (5.8) was also used to predict the ultimate shear strength of specimens with stirrups used by previous investigators (4) (16). In Table XV the calculated values are compared with the results of Kriz and Raths (4). Table XV shows that for specimens under vertical loads only, the mean and standard deviation of $v_{u(test)}/v_{u(calc)}$ are 1.30 and 0.11, respectively; for H/V of 1.0 they are 1.33 and 0.11, respectively.

Specimens used by Mattock et al. (16) had very high main reinforcement ratios. Twenty-five of the twenty-six specimens with stirrups were reinforced with quantities of main tension steel that were on the average of 2.62 times the maximum limit recommended by the ACI Code (14). In spite of high reinforcement ratios, Equation (5.8) was used to predict the ultimate strength of the specimens. Table XVI shows that for all-lightweight concrete specimens with H/V of 1.0, the mean and standard

TABLE XIV

COMPARISON OF PROPOSED EQUATION (5.8) WITH TEST RESULTS

Specimen	a/d	ρ_s, %	f'_c, ksi	$v_{u(test)}$, ksi	$v_{u(calc)}$, ksi	$\frac{v_{u(test)}}{v_{u(calc)}}$
Static Loading With H/V = 0.0						
Specimens Without Compression Reinforcement						
A1	0.31	0.45	6.80	1.32	1.08	1.22
A3	0.31	0.83	6.80	1.63	1.35	1.21
A6	0.31	1.30	6.80	1.99	1.70	1.17
A7	0.31	1.30	6.80	2.28	1.70	1.34
C1	0.50	0.83	6.96	1.23	0.95	1.29
C3	0.75	0.83	6.96	0.92	0.71	1.30
D5	0.50	1.30	6.45	1.54	1.21	1.27
D7	0.75	1.25	6.45	1.21	0.96	1.26
					Mean, $\bar{x}$ =	1.26
					Standard Deviation, s =	0.06
Specimens With Compression Reinforcement						
B7	0.31	1.30	7.10	2.56	1.77	1.45
C5	0.31	0.83	6.96	1.84	1.39	1.32
C7	0.75	0.83	6.96	0.89	0.71	1.25
					Mean, $\bar{x}$ =	1.34
					Standard Deviation, s =	0.10
Large Specimens						
Y1	0.31	0.43	6.45	1.32	0.99	1.33
Y2	0.31	0.88	6.96	1.64	1.42	1.15
Y3	0.31	0.88	7.10	1.62	1.45	1.12
Y4	0.50	0.88	6.80	1.22	0.96	1.27
					Mean, $\bar{x}$ =	1.22
					Standard Deviation, s =	0.10

TABLE XIV (Continued)

Speci-men	a/d	ρ_s, %	f'_c, ksi	$v_{u(test)}$, ksi	$v_{u(calc)}$, ksi	$\frac{v_{u(test)}}{v_{u(calc)}}$
			Repeated Loading With H/V = 0.0			
Specimens Without Compression Reinforcement						
A2	0.31	0.45	6.80	1.37	1.08	1.27
A4	0.31	0.83	6.80	1.68	1.35	1.24
A5	0.31	0.83	6.80	---[1]	---	---
A8	0.31	1.30	6.80	2.22	1.70	1.31
C2	0.50	0.83	6.96	1.24	0.95	1.31
C4	0.75	0.83	6.96	0.86	0.71	1.21
D6	0.50	1.25	6.45	1.62	1.18	1.37
D8	0.75	1.25	6.45	1.04	0.96	1.08
					Mean, $\bar{x}$ =	1.26
					Standard Deviation, s =	0.09
Specimens With Compression Reinforcement						
B8	0.31	1.30	7.10	2.48	1.77	1.40
C6	0.31	0.83	6.96	1.78	1.39	1.28
C8	0.75	0.83	6.96	0.82	0.71	1.15
					Mean, $\bar{x}$ =	1.28
					Standard Deviation, s =	0.13

TABLE XIV (Continued)

Speci-men	a/d	ρ_s, %	f'_c, ksi	H/V	$v_{u(test)}$, ksi	$v_{u(calc)}$, ksi	$\frac{v_{u(test)}}{v_{u(calc)}}$
			Static Loading With H/V > 0.0				
Specimens Without Compression Reinforcement							
B1	0.31	0.45	7.10	0.49	0.68	0.68	1.00
B3	0.31	0.83	7.10	0.47	0.99	0.87	1.14
B5	0.31	1.30	7.10	0.23	1.78	1.40	1.27
D1	0.50	0.83	6.45	0.50	0.63	0.53	1.19
D3	0.75	0.83	6.45	0.40	0.51	0.44	1.16
						Mean, $\bar{x}$ =	1.15
						Standard Deviation, s =	0.10
			Repeated Loading With H/V > 0.0				
Specimens Without Compression Reinforcement							
B2	0.31	0.45	7.10	0.46	0.72	0.70	1.03
B4	0.31	0.83	7.10	0.46	1.01	0.88	1.15
B6	0.31	1.30	7.10	0.23	1.84	1.41	1.31
D2	0.50	0.83	0.83	0.50	0.73	0.70	1.04
D4	0.75	0.83	0.83	0.47	0.40	0.41	0.98
						Mean, $\bar{x}$ =	1.10
						Standard Deviation, s =	0.13

[1]Main tension reinforcement fractured at about 390,000 cycles.

TABLE XV

COMPARISON OF PROPOSED EQUATION (5.8) WITH PREVIOUS RESULTS OF KRIZ AND RATHS[1] (NORMAL WEIGHT CONCRETE WITH STIRRUPS)

Speci-men	a/d	ρ_s, %	f_c', ksi	$v_{u(test)}$, ksi	$v_{u(calc)}$, ksi	$\frac{v_{u(test)}}{v_{u(calc)}}$
Static Loading With H/V = 0.0						
1S[2]	0.59	0.93	4.34	0.74	0.57	1.30
2S	0.59	0.93	4.59	0.84	0.60	1.40
3S	0.59	0.93	4.43	0.85	0.58	1.47
4S[2]	0.37	0.93	4.33	0.93	0.80	1.16
5S	0.37	0.93	4.34	1.05	0.80	1.30
6S	0.37	0.93	4.48	1.16	0.83	1.40
7S[2]	0.39	0.93	4.11	0.83	0.73	1.14
8S	0.39	0.93	4.30	0.94	0.76	1.24
9S	0.39	0.93	4.23	0.91	0.75	1.21
10S	0.30	0.93	4.15	1.21	0.90	1.34
11S	0.20	0.93	4.28	---[3]	1.20	---
					Mean, $\bar{x}$ =	1.30
					Standard Deviation, s =	0.11
Static Loading With H/V = 0.5						
12S	0.62	0.93	6.12	0.54	0.46	1.17
Static Loading With H/V = 1.0						
13S	0.62	0.93	3.90	0.26	0.20	1.32
14S	0.62	0.93	4.35	0.27	0.22	1.23
15S	0.40	0.93	4.11	0.43	0.29	1.48
16S	0.20	0.93	4.10	0.59	0.46	1.28
					Mean, $\bar{x}$ =	1.33
					Standard Deviation, s =	0.11

[1] Data from Reference (4).

[2] $A_h/A_s < 0.5$.

[3] Test stopped at v = 1.19 ksi.

TABLE XVI

COMPARISON OF PROPOSED EQUATION (5.8) WITH PREVIOUS RESULTS OF MATTOCK ET AL.[1] (STATIC TESTS OF ALL-LIGHTWEIGHT CONCRETE CORBELS WITH STIRRUPS)

Speci- men	a/d	ρ_s, %	f'_c ksi	H/V	Design v_u, ksi	$v_{u(test)}$, ksi	$v_{u(calc)}$, ksi	$\frac{v_{u(test)}}{v_{u(calc)}}$
G4[2]	0.99	1.47	3.75	0.0	0.80	0.53	0.61	0.87
F2	0.45	2.10	3.72	1.0	0.80	0.82	0.43	1.91
F3[2]	0.68	2.43	3.73	1.0	0.80	0.54	0.43	1.26
F4[2]	1.01	2.97	4.04	1.0	0.80	0.54	0.53	1.02
F4A[2]	1.01	2.97	3.72	1.0	0.80	0.53	0.49	1.08
J4	1.01	1.98	3.65	1.0	0.56	0.49	0.32	1.53

Mean, $\overline{x}$ = 1.36

Standard Deviation, s = 0.37

For H/V = 1.0

[1]Data from Reference (16).

[2]Main tension reinforcement did not yield.

deviation of the $v_{u(test)}/v_{u(calc)}$ are 1.36 and 0.37, respectively.

Table XVII shows Equation (5.8) results in very conservative predictions for specimens of normal weight concrete that are over-reinforced. Based on the above analysis, it is evident that Equation (5.8) could be used to predict the ultimate strength of concrete corbels with a reasonable margin of safety. The ultimate shear stress may therefore be expressed as

$$v_u = \lambda\{(1 - a/d)[e^{(1 - 3a/d)}] + 0.75\ \rho_s\}\psi$$

where

$$\lambda = [1 - H/V\ (1 - 0.4\ H/V)];$$

and

$$\psi = \frac{f'_c}{6.80}\ .$$

TABLE XVII

COMPARISON OF PROPOSED EQUATION (5.8) WITH PREVIOUS RESULTS OF MATTOCK ET AL.[1] (STATIC TESTS OF NORMAL WEIGHT CONCRETE CORBELS WITH STIRRUPS)

Speci-men	a/d	ρ_s, %	f_c' ksi	H/V	Design v_u, ksi	$v_{u(test)}$, ksi	$v_{u(calc)}$, ksi	$\frac{v_{u(test)}}{v_{u(calc)}}$
B1[2]	0.44	0.75	3.63	0.00	0.80	0.87	0.52	1.67
B2	0.67	1.16	3.45	0.00	0.80	0.73	0.50	1.46
B3A	1.01	1.86	4.17	0.00	0.80	0.79	0.85	0.93
C1	0.45	2.03	4.01	0.75	0.80	0.83	0.54	1.54
C2	0.68	2.48	3.72	0.75	0.80	0.75	0.51	1.47
C2A	0.68	2.23	3.71	0.75	0.80	0.76	0.46	1.65
C3	1.02	3.10	4.39	0.75	0.80	0.71	0.71	1.00
D1	0.45	1.65	3.91	1.00	0.57	0.53	0.28	1.89
D2	0.68	2.03	3.81	1.00	0.57	0.64	0.37	1.73
D3	1.01	2.48	3.70	1.00	0.56	0.62	0.41	1.51
E1	0.22	1.89	4.03	1.00	0.80	1.24	0.64	1.94
E2	0.45	2.10	4.45	1.00	0.80	1.04	0.51	2.04
E3	0.68	2.43	4.22	1.00	0.80	1.10	0.48	2.29
E4	1.01	2.97	4.06	1.00	0.80	0.80	0.53	1.51
H1	0.23	2.10	3.92	1.00	1.20	1.51	0.61	2.48
H2	0.45	2.43	3.92	1.00	1.20	1.13	0.51	2.22
H3	0.68	2.97	3.86	1.00	1.20	1.07	0.58	1.84
H3A	0.68	2.97	3.96	1.00	1.20	0.89	0.55	1.62
H3B	0.68	2.97	3.82	1.00	1.20	1.04	0.53	1.96

Mean, $\bar{x}$ = 1.92

Standard Deviation, s = 0.31

For H/V = 1.0 only

[1]Data from Reference (16).

[2]Only specimen in the investigation of Mattock et al. (16) in which ρ_s (%) < 0.13 f_c'/f_{sy} (%), a requirement of ACI Code (14).

CHAPTER VI

SUMMARY AND CONCLUSIONS

6.1 Summary

The study reported herein was conducted to obtain information about the strength and behavior of lightweight concrete corbels, particularly when subjected to repeated loads.

Thirty-six reinforced sanded-lightweight concrete specimens were tested: four larger specimens with 9 x 12 in. columns and thirty-two smaller specimens with 6 x 8 in. columns. Each specimen had two corbels arranged symmetrically about the column, and reinforced with quantities of steel as per the ACI Code (14) limitations. Six of the smaller specimens had additional compression reinforcement. All of the larger specimens and half of the smaller specimens were subjected to static loading only, while the remaining half of the smaller specimens were subjected to vertically repeated loading prior to their static tests. Five specimens of each group of sixteen smaller specimens were subjected to combined loading.

Each specimen was tested in an inverted position and the load-displacement curves were directly plotted by means of transducer-plotter arrangements. In the case of specimens subjected to repeated loading the load-deformation curves were also plotted at the end of 1st, 10th, 100th, 1000th, 10,000th, and 100,000th cycle. The repeated loading was applied at 120 cycles per minute and varied between approximately $0.2V_u$ and $0.6V_u$ for most specimens. The static horizontal load, if present, was maintained constant during the repeated loading. Each specimen was then statically loaded to failure.

Strength predictions from current design Equations (2.19) and (2.20), and proposed Equation (5.2) were compared with test results. Based on data from the tests the expression (5.8) was developed to predict the ultimate strength of sanded-lightweight concrete corbels.

6.2 Conclusions

The strength and behavior of reinforced sanded-lightweight concrete corbels are affected by both the shear span-to-effective depth ration (a/d) and the reinforcement ratio (ρ) as well as the presence of compression reinforcement. The results showed that there is an exponential relationship between the shear strength of the corbel and the a/d ratio; at lower a/d ratios, the shear capacity of a corbel is rapidly increased. Therefore, from the stand-point of strength it is advantageous to use low a/d ratios.

It was also observed that in corbels with high reinforcement ratio, the yield strength approached the ultimate strength resulting in a more brittle behavior and a more abrupt failure. Such sudden failure could be prevented by the use of compression reinforcement since specimens with compression reinforcement exhibited more ductility. In addition, specimens with compression reinforcement experienced higher ultimate shear loads at low a/d ratios; no influence was observed at higher a/d ratios.

It was expected that a repeated loading history will reduce the shear capacity of each corbel regardless of ρ or a/d ratios. Contrary to expectations, at low a/d ratios of 0.31 and 0.50 the repeated loading history consistently produced slight increases in the ultimate strength of corbels without compression reinforcement; for those with higher a/d ratio of 0.75, the repeated loading history consistently reduced the shear capacity. In the case of specimens with compression reinforcement, however, the repeated loading produced a slight decrease in the shear capacity at both low and high a/d ratios; the largest reduction in strength occurred at a/d ratio of 0.75.

Current design Equations (2.19) and (2.20) from sections 11.14 and 11.15 of the ACI Code (14) predicted the ultimate strength of the sanded-lightweight concrete corbels more conservatively at low a/d ratios but less conservatively at higher a/d ratios. In fact, Equation (2.20) was unconservative at all a/d ratios of 0.75. The expression (5.2) proposed recently by Mattlock (17) also produced conservative predictions of the shear strength but less conservative at higher a/d ratios and yielded unconservative results for combined loading and high a/d ratios. The derived expression (5.8) predicted the ultimate strength of the sanded-lightweight concrete corbels with a fairly constant margin of safety. Equation (5.8) was also used to predict conservatively the strengths of corbels of normal weight concrete and all-lightweight concrete from previous investigations (4) (16).

From the results of this study of 36 sanded-lightweight concrete specimens, it may be concluded that:

1. At low shear span-to-effective depth ratios the presence of compression reinforcement in a lightweight concrete corbel appears to be beneficial to its behavior and its load-carrying capacity.

2. To take advantage of shear strength, corbels should be limited to low shear span-to-effective depth ratios.

3. Repeated loading history has a detrimental effect on the shear strength of corbels with high shear span-to-effective depth ratio. In places of possible load repetitions, the shear span-to-effective depth should be limited to 0.50.

4. The design provisions of sections 11.14 and 11.15 of the ACI Code (14) with modified coefficient of friction could be used for satisfactory design of sanded-lightweight concrete corbels with low shear span-to-effective depth ratios.

5. Data indicate that the following expression can be used to design reinforced concrete corbel.

$$v_u = \lambda\{(1-a/d)[e^{(1 - 3\,a/d)}] + 0.75\,\rho_s\}\,\psi$$

where

$$\lambda = [1 - H/V(1 - 0.4H/V)]$$

$$\psi = f_c'/6.80.$$

6.3 Suggestions for Future Work

Presently there is a limited amount of information on the behavior and strength of reinforced concrete corbels, particularly those of lightweight concrete. Excluding this study there is no known investigation of concrete corbels subject to repeated loading. It is therefore evident that more research is needed to thoroughly investigate the strength and behavior of concrete corbels under repeated loading. The following are some suggestions for further research work that were noted during this study:

1. Examination of strength and performance of corbels under low intensity-long duration, and high intensity-short duration repeated loads.

2. A study of the effects of variations in compression reinforcement.

3. Determination of the effects of simultaneous repetitions of combined loads.

4. Comparision of the effects of different frequencies of repeated loads.

A SELECTED BIBLIOGRAPHY

(1) Kunze, W. E., J. A. Sbarounis, and J. E. Amrhen. "The March 27 Alaskan Earthquake--Effects on Structures in Anchorage." Proceedings, Journal of the American Concrete Institute, Vol. 62, No. 6 (June, 1965), pp. 635-649.

(2) Mattock, A. H., L. Johal, and C. H. Chow. "Shear Transfer in Reinforced Concrete with Moment and Tension Acting Across the Shear Plane." Proceedings, Journal of the Prestressed Concrete Institute, Vol. 20, No. 4 (July-August, 1975), pp. 76-93.

(3) Mattock, A. H., W. K. Li, and T. C. Wang. "Shear Transfer in Lightweight Reinforced Concrete." Journal of the Prestressed Concrete Institute, Vol. 21, No. 1 (January-February, 1976), pp. 20-39.

(4) Kriz, L. B., and C. H. Raths. "Connections in Precast Concrete Structures--Strength of Corbels." Journal of the Prestressed Concrete Institute, Vol. 10, No. 1 (January-February, 1965), pp. 16-61.

(5) The Joint ASCE-ACI Task Committee 426. "The Shear Strength of Reinforced Concrete Members." Journal of the Structural Division, ASCE, Vol. 99, No. ST6 (June, 1973), pp. 1091-1187.

(6) Swamy, R. N., and A. D. Andriopoulos. "Contribution of Aggregate Interlock and Dowel Forces to the Shear Resistance of Reinforced Beams with Web Reinforcement." Shear in Reinforced Concrete, Publication SP-42, Vol. 1. Detroit: American Concrete Institute, 1974, pp. 129-166.

(7) Hofbeck, J. A., I. O. Ibrahim, and A. H. Mattock. "Shear Transfer in Reinforced Concrete." Proceedings, Journal of the American Concrete Institute, Vol. 66, No. 2 (February, 1969), pp. 119-128.

(8) Paulay, T., and P. J. Loeber. "Shear Transfer by Aggregate Interlock." Shear in Reinforced Concrete, Publication SP-42, Vol. 1. Detroit: American Concrete Institute, 1974, pp. 1-16.

(9) Loeber, P. J. "Shear Transfer by Aggregate Interlock." (Unpub. Master of Engineering thesis, University of Canterbury, Christchurch, New Zealand, 1970.)

(10) Birkland, P. W., and H. W. Birkland. "Connections in Precast Concrete Construction." Proceedings, Journal of the American Concrete Institute, Vol. 63, No. 3 (March, 1966), pp. 345-367.

(11) Mast, R. F. "Auxiliary Reinforcement in Concrete Connections." Journal of the Structural Division, ASCE, Vol. 94, No. ST6 (June, 1968), pp. 1485-1504.

(12) Perry, E. S., and N. Jundi. "Pullout Bond Stress Distribution Under Static and Dynamic Loadings." Proceedings, Journal of the American Concrete Institute, Vol. 66, No. 5 (May, 1969), pp. 377-380.

(13) Hanson, N. W. "Precast-Prestressed Concrete Bridges, 2-Horizontal Shear Connections." Journal of the Portland Cement Association Research and Development Laboratories, Vol. 2, No. 2 (May, 1960), pp. 38-58.

(14) ACI Committee 318. Building Code Requirements for Reinforced Concrete (ACI 318-71). Detroit: American Concrete Institute, 1971.

(15) PCI Design Handbook. Chicago: Prestressed Concrete Institute, 1972.

(16) Mattock, A. H., K. C. Chen, and K. Soongswang. "The Behavior of Reinforced Concrete Corbels." Journal of the Prestressed Concrete Institute, Vol. 21, No. 2 (March-April, 1976), pp. 53-77.

(17) Mattock, A. H. "Design Proposals for Reinforced Concrete Corbels." Journal of the Prestressed Concrete Institute, Vol. 21, No. 3 (May-June, 1976), pp. 17-42.

(18) Report of ACI Ad Hoc Board Committee on Concrete. "Concrete--Year 2000." Proceedings, Journal of the American Concrete Institute, Vol. 68, No. 8 (August, 1971), pp. 581-589.

(19) ACI Committee 213. "Guide for Structural Lightweight Aggregate Concrete." Proceedings, Journal of the American Concrete Institute, Vol. 64, No. 8 (August, 1967), pp. 433-470.

(20) Kong, F. K., and P. J. Robins. "Web Reinforcement Effects on Lightweight Concrete Deep Beams." Proceedings, Journal of the American Concrete Institute, Vol. 68, No. 7 (July, 1971), pp. 514-520.

(21) Kong, F. K., and A. Singh. "Diagonal Cracking and Ultimate Loads on Lightweight Concrete Deep Beams." Proceedings, Journal of the American Concrete Institute, Vol. 69, No. 8 (August, 1972), pp. 513-521.

(22) Kong, F. K., and A. Singh. "Shear Strength of Lightweight Concrete Deep Beams Subjected to Repeated Loads." Shear in Reinforced Concrete, Publication SP-42, Vol. 2. Detroit: American Concrete Institute, 1974, pp. 461-476.

(23) Nichols, G. W., and W. B. Ledbetter. "Bond and Tensile Capacity of Lightweight Aggregates." Proceedings, Journal of the American Concrete Institute, Vol. 67, No. 12 (December, 1970), pp. 959-962.

(24) Anderson, A. R. "Composite Design in Precast and Cast-In-Place Concrete." Progressive Architecture, Vol. 41, No. 9 (September, 1960), pp. 172-179.

(25) Rausch, E. "Berechnung der Abbiegungen gegen Abcheren." Der Bauingenieur, Heft 7 (1922), pp. 211-212.

(26) Franz, G., and H. Niedenhoff. "The Reinforcement of Brackets and Short Deep Beams." (A translation of an article in German that appeared in Beton-und Stahlbetonbau, Vol. 58, No. 5 (1963), pp. 112-120.) Translation N. 114, Cement and Concrete Association, London, 1964.

(27) Mehmel, A., and G. Becker. "Zur Schubbemessung des kurzen Kragarmes." Der Bauingenieur, Heft 6 (1965), pp. 224-231.

(28) Mehmel, A., and W. Freitag. "Tragfahigkeitsversuche an Stahlbetonkonsolen." Der Bauingenieur, Heft 10 (1967), pp. 362-369.

(29) Mattock, A. H. "Shear Transfer in Concrete Having Reinforcement at an Angle to the Shear Plane." Shear in Reinforced Concrete, Publication SP-42, Vol. 1. Detroit: American Concrete Institute, 1974, pp. 17-42

(30) Hermansen, B. R., and J. Cowan. "Modified Shear-Friction Theory for Bracket Design." Proceedings, Journal of the American Concrete Institute, Vol. 71, No. 2 (February, 1974), pp. 55-60.

(31) Sommerville, G. "The Behavior and Design of Reinforced Concrete Corbels." Shear in Reinforced Concrete, Publication SP-42, Vol. 2. Detroit: American Concrete Institute, 1972, pp. 477-502.

(32) Council for Codes of Practice, CP110. The Structural Use of Concrete, Part 1. London: British Standards Institution, November, 1972

(33) Badoux, J. C., and C. L. Hulsbos. "Horizontal Shear Connection in Composite Concrete Beams Under Repeated Loads." Proceedings, Journal of the American Concrete Institute, Vol. 64, No. 12 (December, 1967), pp. 811-819.

(34) Bresler, B., and V. Bertero. "Behavior of Reinforced Concrete Under Repeated Loads." Journal of the Structural Division, ASCE, Vol. 94, No. ST6 (June, 1968), pp. 1567-1590.

(35) Winter, G., and A. H. Nilson. Design of Concrete Structures. 8th ed. New York: McGraw-Hill Book Company, 1972.

(36) Clarke, J. L. "Behavior and Design of Small Continuous Corbels." Technical report, Cement and Concrete Association, 1976.

VITA

Clifford Nii-Ayi Clottey

Candidate for the Degree of

Doctor of Philosophy

Thesis: PERFORMANCE OF LIGHTWEIGHT CONCRETE CORBELS SUBJECTED TO STATIC AND REPEATED LOADS

Major Field: Civil Engineering

Biographical:

Personal Data: Born March 7, 1942, in Accra, Ghana, the son of Mr. Alfred Clottey and Ms. Beatrice Adjei.

Education: Graduated from Odorgonno Secondary School, Accra, Ghana, in June, 1962; received Advanced Level G.C.E. (University of London), from Adisadel College, June, 1964; received the Bachelor of Science degree in Building Technology in June, 1969, from the University of Science and Technology, Kumasi, Ghana; received the Master of Science in Civil Engineering degree in May, 1972, from the University of Cincinnati, Cincinnati, Ohio; completed requirements for the Doctor of Philosophy degree at Oklahoma State University in December, 1977.

Professional Experience: Quantity Surveying Assistant, Rowland and Partners, Ghana, summer, 1966; Engineering Assistant (Quantities), Ghana Housing Corporation, Ghana, summer, 1967; Quantity Surveying Assistant, Rowland and Partners, Ghana, summer, 1968; Assistant Quantity Surveyor, Public Works Department, Ghana, 1969-1970; Research Assistant, School of Civil Engineering, Oklahoma State University, August to December, 1972; Teaching Assistant, School of Civil Engineering, Oklahoma State University, January, 1973, to December, 1977.

Professional Organizations: Associate Member, American Society of Civil Engineers; Member, American Concrete Institute; Member, Chi Epsilon.